LTI@UniTO
LONG·TERM INVESTORS

Dynamic ESG Equilibrium

Doron Avramov
Abraham Lioui
Yang Liu
Andrea Tarelli

No. 17
September 2023

LTI WORKING PAPERS

www.carloalberto.org/lti/working-papers

Dynamic ESG Equilibrium*

Doron Avramov† Abraham Lioui‡ Yang Liu§ Andrea Tarelli¶

August 27, 2023

Abstract

This paper proposes a conditional asset pricing model that integrates ESG demand and supply dynamics. Shocks in the demand for sustainable investing represent a novel risk source, characterized by diminishing marginal utility and positive premium. Green assets exhibit positive exposure to ESG demand shocks, hence commanding higher premia. Conversely, time-varying convenience yield leads to lower expected returns for green assets. Moreover, ESG demand shocks have positive contemporaneous effects on unexpected returns, contributing to large positive payoffs in the green-minus-brown portfolio over extended horizons. The model predictions align closely with evidence on return spreads between green and brown assets, further reinforcing the apparent gap between realized and expected spreads.

Keywords: ESG, Dynamic equilibrium, Asset pricing, Preference shock.
JEL classification: G12, G19, J71.

1 Introduction

In 2021, as reported by Morningstar, the collective assets under the management of sustainable funds surged to $2.74 trillion, a remarkable increase from approximately $700 billion in 2018. While the pace of expansion moderated in 2022 due to widespread fund outflows globally, sustainable funds exhibited greater resilience compared to the broader market, reaching a total of $2.83 trillion by June 2023. The consistent growth of sustainable investing in recent years has been further propelled by the profound impact of significant events, including the coronavirus pandemic and the energy crisis that followed the war in Ukraine. These events have heightened discussions surrounding the intricate interplay between sustainability and the capital markets.

*We thank Will Cong (Editor), the Associate Editor, and three anonymous referees for insightful feedback. We also thank Robert Engle, Stefano Giglio, Fabio Girardi, Frank de Jong, Paul Karehnke, Elisa Luciano, Alessandro Melone, Valeria Nale, Jean-Paul Renne, Pablo Ruiz-Verdu, Peter Norman Sørensen, Marco Taboga, Claudio Tebaldi, the seminar participants at the Catholic University of Milan and EDHEC Business School, as well as the conference attendants at the 2022 Financial Risks International Forum, 2022 Econometric Society Australasia Meeting, 2022 European Summer Meetings of the Econometric Society, 2022 Research in Behavioral Finance Conference, 2022 CREDIT Long Run Risks Conference, 2022 SAFE Asset Pricing Workshop, and 2023 LTI/Bank of Italy Workshop for useful comments and discussions. Part of this research was developed when Andrea Tarelli was visiting Collegio Carlo Alberto, whose hospitality is gratefully acknowledged. We are solely responsible for any remaining errors.

†Arison School of Business, Reichman University (IDC Herzliya), Herzliya, Israel. doron.avramov@runi.ac.il
‡EDHEC Business School, Nice, France. abraham.lioui@edhec.edu
§The University of Hong Kong, Hong Kong, China. yangliu5@hku.hk
¶Catholic University, Milan, Italy. andrea.tarelli@unicatt.it

The literature on asset pricing has reacted to the upsurge in sustainable investing. Pástor et al. (2021) consider an agent who derives nonpecuniary benefits from holding green stocks. They derive a CAPM representation for the cross section of expected returns, where the alpha is inversely related to the firm's ESG score. An ESG objective in a mean-variance setting has also been proposed by Pedersen et al. (2021). Avramov et al. (2022) account for uncertainty about the correct firm's ESG profile and explore its effects on aggregate and individual average returns. Berk and van Binsbergen (2022) investigate how ESG divestitures impact the cost of capital. Notably, all these studies establish their analyses within a single-period, unconditional, equilibrium context.

This paper develops and estimates a conditional asset pricing model that effectively captures the dynamics of ESG demand and supply factors. The model's framework is grounded in four primary rationales.

To begin, the model incorporates the temporal dynamics of ESG demand, specifically representing the fluctuations in preferences for holding sustainable assets. While Albuquerque et al. (2016) address shocks to preferences for physical consumption, our focus remains on shocks to preferences for ESG externalities. This is in line with the evidence presented in Figure 1, which illustrates press attention towards ESG issues using data from Factiva records. The reported metric demonstrates a remarkable increase from the initial period of the dataset until 2002, followed by a decline after the dot-com bubble burst and the 2008 financial crisis. However, a substantial upward trend emerges thereafter, leading up to 2022, where a slight downturn follows. In a related context, Engle et al. (2020) recognize the dynamic nature of climate risks. Thus, they construct mimicking portfolios that are tailored to hedge climate change news. In our pursuit to push this research forward, we expand upon the dynamic aspects of ESG concerns, thereby extending the analysis into the domain of asset pricing equilibrium.

Second, the model also accounts for ESG supply shocks. The expansion of sustainable products and services, alongside breakthroughs in technology (e.g., innovations supporting sustainable urban infrastructure, eco-friendly vehicles, and renewable energy plants), is incorporated into the dynamics of ESG supply.

Third, dynamic models have yielded valuable insights into asset pricing regularities, including the high equity premium, the low risk-free rate, and the excess volatility, while also shedding light on anomalies within the cross-section of asset returns (e.g., Campbell and Cochrane, 1999; Gomes et al., 2003). As we develop the model, we clarify how the proposed equilibrium offers supplementary insights into the asset pricing implications associated with sustainable investing.

Fourth, expanding beyond theoretical insights, the dynamic model can be easily applied to real data. Specifically, we estimate the model utilizing a comprehensive dataset that covers ESG scores, macroeconomic dynamics, and asset returns. The estimation process incorporates equilibrium restrictions and enables the extraction of the time-series of a crucial latent variable–ESG demand.

The model unfolds as follows. The agent's preferences are formulated through a modified version of Epstein and Zin (1989, 1991) to account for the ESG profile of the investment portfolio. In particular, beyond the conventional utility derived from physical consumption, the agent extracts nonfinancial benefits from holding sustainable assets. These ESG-related benefits constitute a second consumption good, and their proportion within the entire consumption bundle is contingent upon the demand for sustainable investments and its temporal dynamics.[1]

There are four sources of systematic risk in the economy. Two of these are short- and long-run consumption growth, similarly to conventional long-run risk based models. Complementing these are two sources related to ESG demand and supply, which interplay determines the cumulative nonpecuniary advantages for the agent. ESG demand and supply shocks then represent two sources of risk that are priced in the cross section of asset returns. Beyond the incremental contribution of the two ESG-related risk sources, there is also a convenience yield effect, which reflects the concept that an agent attuned to ESG considerations is willing to embrace a lower premium when holding green assets. The convenience yield terminology is adopted from Krishnamurthy and Vissing-Jorgensen (2012), who formulate consumption that contains convenience benefits from investing in liquid and safe U.S. Treasuries. In our setup, the convenience yield effect echoes the negative ESG-alpha relation in Pástor et al. (2021).

The dynamic framework introduces a series of implications. First, the convenience yield is not constant; rather, it dynamically adjusts in response to shifts in ESG demand and supply. Notably, a positive shock to ESG demand leads to an augmentation (diminution) of the convenience yield associated with green (brown) assets, thereby amplifying (reducing) their valuation and engendering a contemporaneous positive (negative) unexpected return. Second, as the agent's value function is concave in both ESG demand and supply, positive shocks to either quantity diminish the agent's marginal utility. Consequently, investors require (accept) a positive (negative) risk premium to hold assets whose returns exhibit positive (negative) covariance with such shocks. Specifically, since the returns of green (brown) assets positively (negatively) covary with ESG demand shocks, they are characterized by a positive (negative) ESG demand risk premium. The ESG demand risk premium adds to the convenience yield contribution, challenging the negative ESG-expected return relationship that characterizes the static setup. Indeed, in a dynamic setting, the ESG-expected return relation exhibits time variation and can eventually go either way.

We proceed to analyze the model empirically. The dataset encompasses the years spanning from 2007 to 2022. We categorize stocks based on their ESG scores, as provided by MSCI. This categorization results in the formation of green, brown, and green-neutral portfolios. The model is effectively represented through a linear state space, obtained by stacking the dynamics of consumption growth, aggregate ESG supply, aggregate ESG demand, portfolio ESG scores and excess returns, and the broader market excess return. The joint dynamics of the aforementioned variables is represented through a first-order structural vector autoregression. Given that expected consumption growth and ESG demand are unobservable, we employ the Kalman filter to estimate the model parameters. Interestingly, we initially observe that the market-implied estimate of ESG demand exhibits temporal patterns that align with trends in press attention

[1] The two-good economy extends the traditional consumption CAPM of Lucas (1978) and Breeden (1979). For instance, the second good is a luxury good in Ait-Sahalia et al. (2004), the service flow of durable goods in Yogo (2006), housing in Piazzesi et al. (2007), leisure in Van Binsbergen et al. (2012), and money in Lioui and Maio (2014). Nevertheless, in contrast to the aforementioned works, our model introduces a departure by intertwining consumption and portfolio selections in a nonseparable manner. This distinction arises due to the endogenous interplay between the portfolio's ESG signature, which determines the value of the second consumption commodity, and the underlying portfolio strategy.

towards ESG investing.

According to our estimation, the green-minus-brown portfolio exhibits a negative and statistically significant average expected return of -0.91% per annum. The negative expected return is mostly attributable to the higher exposure of the brown portfolio to short- and long-run consumption risks, leading to negative risk premia of -0.30% and -0.94%. The negative contribution of the convenience yield resulting from ESG nonpecuniary benefits (-0.37%) is partially offset by the positive risk premium associated with ESG demand (0.22%).

The analysis reveals the relationship between unexpected shocks in ESG demand and the contemporaneous realized asset returns. To be specific, the model-implied average expected excess return of the green portfolio is 7.90% per annum, while it is higher at 8.89% for the brown portfolio. However, throughout the sample, the unexpected ESG demand shocks induce a positive (negative) unexpected return of 1.52% (-2.01%) that adds to the conditional expected return of the green (brown) portfolio. Considering the combined effect of the conditional expected return and the unexpected return due to ESG demand shocks, the green-minus-brown portfolio average model-implied return is positive at 2.54%, close to the observed value.

Over recent years, the shift in ESG demand plays an even more pronounced role on the realized returns of the green-minus-brown portfolio. For instance, from 2016 to 2022, the effect of positive unanticipated ESG demand shocks on realized returns averages an impressive 8.11% per annum. This observation calls for caution when extrapolating future returns of ESG investments solely from historical returns. The proposed framework provides a structural decomposition of expected and unexpected green asset returns, quantifying the positive association between shifts in environmental concerns and unexpected returns of environmentally-friendly stocks advocated by Pástor et al. (2022) and Ardia et al. (2023).

While the common theme in the landscape of sustainable investing has centered around the combination of the three ESG dimensions, the growing concerns surrounding climate change suggest a shifting emphasis on the environmental dimension. For this reason, we also conduct an empirical analysis focusing on environmental-pillar scores, which confirms our core results. Indeed, the time series of aggregate demand for environmental sustainability exhibits an increase from the beginning of the sample until 2021, with a threefold increase over a decade. Focusing on the green-minus-brown portfolio, over the sample period, the environmental-sustainability demand risk premium is 0.41% per annum, partially offsetting the negative convenience yield premium equal to -0.66%. The positive return induced by shocks to environmental-sustainability demand equals 2.61% and largely offsets the negative average expected return of -1.02%.

We further illustrate the expected-realized return gap conducting impulse response experiments based on the estimated parameters. The cumulative return of the green-minus-brown portfolio reaches 5% following a positive one-standard deviation annual ESG demand shock. The positive effect of realized returns vanishes only about four years after the shock. Hence, with the positive contemporaneous effects of ESG demand shocks on realized returns, the green-minus-brown portfolio could deliver large positive average returns over extended horizons.

Finally, we show that an ESG-sensitive agent perceives conspicuous nonpecuniary benefits. Specifically, across the entire sample period, the estimated ESG benefits amount to 1.61% of total consumption. Narrowing our attention to the period after the Paris Agreement, from

2016 to 2022, the benefits amount to about 3.43% of the consumption bundle. This increase is attributable to the ascending trajectory of ESG demand during this period.

This paper contributes to several areas of the existing literature. First, we address the dynamic nature of ESG demand and supply in equilibrium asset pricing. Unlike previous studies that often focus on static ESG preferences or on transitions of ESG tastes across generations, our model captures the dynamics of ESG demand and supply. Our findings reveal that ESG demand shocks represent a prominent risk source characterized by diminishing marginal utility and a positive premium. Empirically, in contrast, ESG supply shocks have a secondary impact. Furthermore, our model sheds light on the conflicting forces that affect both the expected return on the green-minus-brown portfolio and the disparity between expected and realized returns associated with sustainable investing.

We also respond to the ongoing discussion on the predictability of returns based on ESG scores. Previous research has shown weak return predictability of the overall ESG rating and mixed results using different ESG proxies (e.g., Pedersen et al., 2021). Our analysis demonstrates that ESG demand shocks carry risk premia that could offset the negative ESG-expected return relation implied by the convenience yield of green assets. By combining these opposing influences with the positive contemporaneous effects of ESG demand shocks on realized returns, the green-minus-brown portfolio can yield large positive average returns over extended horizons.

This research also establishes a connection with studies exploring the uncertainty encompassing ESG concerns. Engle et al. (2020) employ a dynamic hedging approach to construct climate risk hedge portfolios, suggesting that innovations in climate news should be priced in the cross section. Their framework acknowledges the need for a green portfolio only when sustainability concerns vary over time. To compare, our equilibrium model based on nonpecuniary benefits implies a valuation impact of the ESG profile even when ESG preferences remain constant. Additionally, De Angelis et al. (2022) discuss firm adjustments to greenhouse emissions based on investors' sensitivity to climate externalities. They argue that uncertainty over future climate risks reduces the incentive to curb emissions and increases the cost of capital for sustainable firms, paralleling our finding of a positive ESG demand risk premium.

The remainder of this paper is structured as follows. Section 2 presents the economic setting. Section 3 describes the data. Section 4 introduces the estimation technique, describes the parameter estimates and model-implied asset returns, and displays the time-series implications of the model. Section 5 explores the quantitative implications of the estimated model, analyzing the impact of unexpected shocks to ESG demand and supply on asset prices and returns. The conclusion follows in Section 6.

2 Economic setting

This section develops an equilibrium model that considers the time-series dynamics of both ESG preferences and sustainability attributes. Our approach to preferences incorporates the notion that economic agents can harvest benefits from investing in sustainable assets beyond those obtained from the traditional physical consumption stream. Based on the proposed framework, we derive general expressions for the stochastic discount factor and the Euler equation, which jointly determine equilibrium expected returns. To enhance the model implications, we introduce additional structure concerning the dynamics of demand and supply for sustainable investing. This enables the development of interpretable expressions for the cross section of asset returns. A key focus lies in comprehending the expected and realized return differentials between *green* (sustainable) and *brown* (non-sustainable) assets.

2.1 Preferences

The economy is endowed with an infinitely-lived representative agent, who chooses a life-time consumption stream along with a trading strategy denoted by the vector of portfolio weights $\boldsymbol{\omega}_t = [\omega_{1,t}, \omega_{2,t}, \ldots, \omega_{N,t}]'$, where N is the number of risky assets and t is a time subscript. There is also a risk-free asset in zero net supply. The agent's preferences are formulated through a modified version of Epstein and Zin (1989, 1991) that accounts for the ESG profile of the investment universe.

In particular, the agent solves the optimization problem

$$U_t = \max_{C_t, \boldsymbol{\omega}_t} \left((1-\beta) A_t^{1-\frac{1}{\psi}} + \beta \mathrm{E}_t \left[U_{t+1}^{1-\gamma} \right]^{\frac{1}{\theta}} \right)^{\frac{1}{1-\frac{1}{\psi}}}, \tag{1}$$

$$A_t = C_t + \delta_t G_{W,t} \left(W_t - C_t \right), \tag{2}$$

$$W_{t+1} = \left(W_t - C_t \right) \left(R_{f,t+1} + \sum_{n=1}^{N} \omega_{n,t} \left(R_{n,t+1} - R_{f,t+1} \right) \right), \tag{3}$$

where U_t stands for the value function, A_t is a consumption bundle that we describe below, C_t denotes the physical consumption, W_t is the aggregate wealth prior to consumption, $W_t - C_t$ is the investable wealth, $R_{n,t+1}$ is the gross return on the n-th risky security, $R_{f,t+1}$ is the risk-free gross return, $\mathrm{E}_t[.]$ stands for the conditional expectation operator, $G_{W,t} = \sum_{n=1}^{N} \omega_{n,t} G_{n,t}$ is the ESG score of the wealth portfolio, $G_{n,t}$ is the ESG score of the n-th asset, with positive (negative) values representing green (brown) assets.[2] The zero case corresponds to ESG neutrality. The risk-free asset is assumed, without loss of generality, to be ESG neutral. When the risk-free asset departs from neutrality, the equilibrium results still hold, with $G_{n,t}$ standing for the asset ESG score in excess of the risk-free ESG score.

The preference parameters are defined as follows. β is the subjective discount factor, ψ is the intertemporal elasticity of substitution, γ is a measure of relative risk aversion, and $\theta = \frac{1-\gamma}{1-\frac{1}{\psi}}$. We introduce δ_t to capture ESG preference, with positive values indicating a preference for green assets and higher values representing stronger preference. Innovations in δ_t represent ESG demand shocks or, equivalently, unexpected changes in the preference for sustainable investing.

Our specification of preference shocks is novel, distinguishing it from previous work, such as Albuquerque et al. (2016), which considers shocks to the demand for physical consumption as the only consumption good. In contrast, in our model, ESG preference shocks drive the time variation of preference for sustainability relative to physical consumption, i.e., of the ESG share in the consumption bundle A_t. For a comprehensive analysis of the effects of multiple preference

[2] While the terms *green* and *brown* are often used to characterize environmental externalities, in this paper we refer to assets with high overall ESG profiles as green and those with low profiles as brown. In the empirical analysis, we examine the robustness of our results by restricting the focus on the environmental pillar scores.

shocks, Online Appendix A.1 presents the case accounting for both a preference shock loading on the entire bundle of consumption and an ESG preference shock.

Sustainability considerations encompass both demand and supply forces within the financial markets. The ESG preference parameter, denoted as δ_t, is indicative of the demand for sustainable investing and tends to rise in response to heightened concerns regarding environmental concerns, governance shortcomings, and social issues. On the supply side, the ESG score of aggregate wealth, $G_{W,t}$, represents the availability of more sustainable technologies, products, and services. Both demand and supply exhibit time variation, reflecting the evolutionary nature of ESG in our structural framework. It is worth noting that a zero ESG demand implies indifference towards ESG motives, while a zero ESG score indicates no positive or negative nonfinancial externalities. However, the scales of ESG demand δ_t and supply $G_{W,t}$ offer a degree of freedom in their choice, as these two quantities appear solely as a product in the agent's preferences in equation (2). Therefore, any combination of scales that yields the same product $\delta_t G_{W,t}$ is equivalent from a pricing perspective.

The consumption bundle A_t replaces the consumption good C_t in the original specification of Epstein and Zin (1989, 1991). The bundle consists of the physical good C_t and an additional component resulting from the nonpecuniary benefits associated with sustainable investing. The ESG-based component is equal to the product of ESG preferences δ_t, the greenness of aggregate wealth $G_{W,t}$, and the total amount of invested wealth $W_t - C_t$. From the perspective of an ESG-sensitive agent, a positive aggregate greenness $G_{W,t}$ makes the consumption bundle A_t more valuable than physical consumption C_t. The opposite holds for negative aggregate greenness.

The specification for the consumption bundle is a particular case of a common setup accounting for two goods with a constant elasticity of substitution, ϕ, and the share of the second good that is equal to δ_t: $A_t = (C_t^{1-\frac{1}{\phi}} + \delta_t \left(G_{W,t} \left(W_t - C_t\right)\right)^{1-\frac{1}{\phi}})^{\frac{1}{1-\frac{1}{\phi}}}$. While Online Appendix A.1 considers the general case of a finite ϕ and describes its implications, for ease of exposition the main text focuses on the limiting case of an infinite elasticity of substitution, which results in the additive expression in equation (2). This choice not only ensures tractability, but also aligns with the evolving literature on sustainable investing, where monetary and nonmonetary payoffs are additive (e.g., Pástor et al., 2021; Pedersen et al., 2021; Avramov et al., 2022). Furthermore, the nonlinearity in the consumption bundle would be eliminated through the log-linearization that we perform in the following to solve the model, leading to equivalent estimation outcomes. However, in contrast to the standard two-good economy, where the share of the two consumption goods remains constant, we introduce a novel level of flexibility allowing the share δ_t to vary over time, reflecting the dynamics of ESG demand.

Before concluding this subsection, we note that while Epstein-Zin preferences do not exhibit time separability, there is still a form of separability between consumption and portfolio choices (Epstein and Zin, 1989). In particular, the economic agent first chooses the optimal consumption plan subject to the budget constraint and subsequently determines the portfolio strategy that replicates the optimal consumption plan. A similar mechanism of separability also applies in a two-good economy with exogenous prices for the consumption goods (e.g., Yogo, 2006). However, in the setup developed here, consumption and portfolio choices exhibit nonseparability, as portfolio weights have an impact on the ESG profile of the aggregate wealth, $G_{W,t}$, which, in turn, affects the value of nonpecuniary benefits in the consumption bundle. In other words, the asset pricing effects of sustainable investing evolve endogenously because portfolio choice determines the value of the second consumption good, as well as the intertemporal evolution of wealth. This additional source of nonseparability due to sustainable investing would also apply when preferences are time-additive ($\theta = 1$).

2.2 Dynamic ESG equilibrium: A general outlook

We begin by deriving general asset pricing outcomes based on equations (1) through (3). The following proposition outlines the stochastic discount factor (SDF) and the Euler equation for the return of a generic asset, which can refer to the aggregate wealth portfolio, the market portfolio, or any individual asset. The derivation is in Online Appendix A.1.

Proposition 1. *In equilibrium, the Euler equation for the gross return on a generic asset n with an ESG score equal to G_n is given by*

$$\mathrm{E}_t \left[M_{t+1} R_{n,t+1} \right] = 1 - \delta_t G_{n,t}, \tag{4}$$

where M_{t+1}, the SDF, is formulated as

$$M_{t+1} = \beta^{\theta} \left(\frac{A_{t+1}}{A_t} \right)^{-\frac{\theta}{\psi}} \tilde{R}_{W,t+1}^{\theta-1}, \tag{5}$$

and $\tilde{R}_{W,t+1} = \frac{R_{W,t+1}}{1-\delta_t G_{W,t}}$ is the ESG-adjusted gross return on the consumption asset.[3]

The closed-form solution for the SDF maintains the Epstein-Zin tractability for asset pricing even in the presence of nonseparability between the value of the consumption bundle and the portfolio choice. According to the SDF in equation (5), there are two factors driving the risk premia in the economy.

The first factor represents the growth of the consumption bundle in (2), $\frac{A_{t+1}}{A_t}$, and is a generalization of the single-good consumption-CAPM. The factor can be further decomposed as the product of physical consumption growth, $\frac{C_{t+1}}{C_t}$, and the growth in the ratio of total consumption bundle to physical consumption, $\frac{A_{t+1}/C_{t+1}}{A_t/C_t} = \frac{1+\delta_{t+1} G_{W,t+1}(W_{t+1}-C_{t+1})/C_{t+1}}{1+\delta_t G_{W,t}(W_t - C_t)/C_t}$. This component represents the growth of the aggregate benefits from ESG investing relative to physical consumption, and depends on the variation in both demand for ESG through δ_t and aggregate supply through $G_{W,t}$.

The second factor accounts for the impact of ESG considerations on the return of aggregate wealth. It is expressed as: $\tilde{R}_{W,t+1} = \frac{R_{W,t+1}}{1-\delta_t G_{W,t}}$. From the perspective of an ESG-sensitive agent,

[3]The Euler equation (4) can be also written as

$$\mathrm{E}_t \left[\beta^{\theta} \left(\frac{A_{t+1}}{A_t} \right)^{-\frac{\theta}{\psi}} \tilde{R}_{W,t+1}^{\theta-1} \tilde{R}_{n,t+1} \right] = 1,$$

where $\tilde{R}_{n,t+1} = \frac{R_{n,t+1}}{1-\delta_t G_{n,t}}$ is the ESG-adjusted gross return on asset n. This expression bears similarity to the common solution for the Epstein-Zin framework, with the distinction that the growth rate of the consumption bundle $\frac{A_{t+1}}{A_t}$ replaces physical consumption growth $\frac{C_{t+1}}{C_t}$, and ESG-adjusted gross returns $\tilde{R}_{W,t+1}$ and $\tilde{R}_{n,t+1}$ replace unadjusted gross returns.

a positive aggregate greenness $G_{W,t}$ leads to a perceived return on aggregate wealth, $\tilde{R}_{W,t+1}$, that exceeds the actual return on wealth, $R_{W,t+1}$. Similarly, a higher preference for sustainable investing (higher δ_t) produces the same effect.

We now explore the implications of sustainable investing for expected asset returns. For a green-neutral asset, the right-hand side of (4) equals one, as in standard setups. However, for green (brown) assets the right-hand side is lower (greater) than one, due to positive (negative) convenience yield. The convenience yield, given by the product $\delta_t G_{n,t}$, reflects the notion that an ESG-preceptive agent is willing to compromise on a lower expected return for holding green assets due to the nonmonetary benefits they offer. The expected excess return implied by equation (4) is $\mathrm{E}_t\left[R_{n,t+1} - R_{f,t+1}\right] = -\frac{\mathrm{Cov}_t\left[R_{n,t+1}-R_{f,t+1}, M_{t+1}\right]}{\mathrm{E}_t[M_{t+1}]} - \frac{\delta_t G_{n,t}}{\mathrm{E}_t[M_{t+1}]}$, with the first and second terms representing the risk premium and the convenience yield premium, respectively.

The convenience yield effect echoes the negative ESG-alpha relation in Pástor et al. (2021). However, there are important differences in our dynamic setup. First, the convenience yield is not constant, but varies with ESG demand, δ_t, and the asset ESG score, $G_{n,t}$. Second, beyond the convenience yield, the expected return also depends on the covariances of returns with two ESG-related asset pricing factors. As a result, the risk premium channel can either reinforce or challenge the negative ESG-expected return relation that characterizes the static setting.

To analyze the implications for risk premia, it is useful to recognize that the value function (1) is concave in both ESG demand and supply (the proof is in Online Appendix A.1). Thus, positive shocks to δ_t or $G_{W,t}$ result in diminishing marginal utility, suggesting that the incremental benefits from holding green assets drop when preferences for sustainable investments grow larger and when the market gets greener. Then, ESG demand or supply shocks are negatively correlated with the SDF and are characterized by positive risk premia.[4] Consequently, assets with returns positively correlated with ESG demand or supply shocks yield a positive ESG-induced risk premium, while assets with negatively correlated returns exhibit the opposite effect.

At this general stage, in the absence of information about the exposures of green and brown assets to ESG shocks, the ESG-expected return relation is inconclusive. Nevertheless, by imposing reasonable structure on the economy in the subsection that follows, we are able to qualify the ESG-induced risk premium, shedding light on its direction and determinants. Specifically, as aggregate nonpecuniary benefits increase, an ESG-sensitive agent becomes more sensitive to ESG demand and supply shocks, demanding risk premia that rise with the volatility of these shocks. Moreover, green assets are associated with a positive risk premium due to ESG demand shocks, while a negative risk premium applies to brown assets. Consequently, the ESG demand risk premium is a force conflicting the negative ESG-expected return relation characterizing static setups. Essentially, the ESG-expected return relation could go either way.

Before concluding this subsection, we note that Online Appendix A.1 derives the Euler equation for more general cases. First, we consider a generic time-preference shock that applies

[4]The positive risk premium due to ESG demand and supply shocks follows from the concavity of preferences and is further elucidated when considering time additivity ($\theta = 1$). Then, the SDF in (5) simplifies to $M_{t+1} = \beta^{\theta}\left(\frac{C_{t+1}}{C_t}\right)^{-\gamma}\left(\frac{1+\delta_{t+1}G_{W,t+1}\left(W_{t+1}-C_{t+1}\right)/C_{t+1}}{1+\delta_t G_{W,t}(W_t-C_t)/C_t}\right)^{-\gamma}$. The last term indicates that ESG demand and supply shocks are negatively correlated with the SDF, resulting in a positive risk premium.

to the entire consumption bundle. The growth in time-preference for consumption appears in the SDF as an additional multiplicative factor that, as discussed in Albuquerque et al. (2016), would increase the market premium, by introducing a positive *valuation premium* due to time-varying demand for consumption, and would help obtaining an upward-sloping term structure of interest rates. Second, we also relax the assumption of an infinite elasticity of substitution between physical consumption and ESG externalities. Then, the convenience yield of any asset, green or brown, is attenuated when aggregate ESG supply grows larger. Indeed, a higher aggregate ESG supply reduces the marginal benefit of sustainability relative to physical consumption. Additionally, a new pricing factor, associated with the ratio of physical consumption relative to the value of the consumption bundle, appears in the SDF. As physical consumption and sustainability are not perfect substitutes, the agent favors assets delivering higher returns when physical consumption is low compared to the total value of the consumption bundle. These assets would then deliver lower expected returns in equilibrium.

In the following, we impose additional structure on the equilibrium to derive interpretable expressions for the cross-section of realized and expected returns.

2.3 Imposing structure on equilibrium

We formulate exogenous processes for consumption growth Δc_t, aggregate greenness $G_{W,t}$, and ESG preferences δ_t. For ease of interpretation, we assume that $\psi > 1$ ($\theta < 0$), which implies preference for early resolution of uncertainty and is consistent with a large body of work. We further assume that $\bar{\delta} > 0$ and $\bar{G}_W \geq 0$, suggesting that, in the long run, the representative agent prefers green to brown assets and the wealth portfolio is green (or green neutral).[5]

The exogenous processes are given by

$$\Delta c_{t+1} = \mu_c + x_t + \sigma_c \varepsilon_{c,t+1}, \tag{6}$$

$$x_{t+1} = \rho_x x_t + \sigma_x \varepsilon_{x,t+1}, \tag{7}$$

$$G_{W,t+1} = \mu_G + \rho_G G_{W,t} + \sigma_G \varepsilon_{G,t+1}, \tag{8}$$

$$\delta_{t+1} = \mu_\delta + \rho_\delta \delta_t + \sigma_\delta \varepsilon_{\delta,t+1}. \tag{9}$$

The consumption growth process (6) is homoskedastic. Consistent with the long-run risk framework, consumption growth has a predictable component driven by the mean-reverting long-run risk variable x_t (assuming $0 < \rho_x < 1$). Note that, while a persistent long-run risk variable x_t is useful to explain the constant component of the market premium, it does not interact with ESG demand or supply. Therefore, our findings regarding the incremental asset pricing implications of sustainable investing remain unaffected when the long-run risk component is muted, i.e., when $\sigma_x = \rho_x = 0$, resulting in identically and independently distributed (IID) consumption growth. The processes (8) and (9) also exhibit mean reversion (assuming $0 < \rho_G, \rho_\delta < 1$) with long-run means given by $\bar{G}_W = \frac{\mu_G}{1-\rho_G}$ and $\bar{\delta} = \frac{\mu_\delta}{1-\rho_\delta}$.[6] The innovations $\varepsilon_{c,t+1}$, $\varepsilon_{x,t+1}$, $\varepsilon_{G,t+1}$, and $\varepsilon_{\delta,t+1}$

[5] The analysis in Section 4 supports the hypothesis that the wealth portfolio is green in the long run.

[6] In the presence of mean-reverting state variables, there is a steady state equilibrium, which can be found through a fixed-point problem. Log-linearization is implemented around the steady state values. The specification also allows for quasi unit root processes (e.g., $\rho_G, \rho_\delta \approx 1$), accommodating for nearly random walk dynamics and still guaranteeing that the solution does not explode due to nonstationarity.

are assumed to be IID normal with zero mean and unit variance, as well as uncorrelated with each other contemporaneously and in all leads and lags. While the discussion that follows is based on the parsimonious specification above, in Online Appendix A.2, we consider a possible effect of the demand for sustainability on the supply side, allowing the drift of ESG supply in equation (8) to depend on the current level of ESG demand. The implications of this extension are discussed in Section 5.

To derive equilibrium outcomes, as detailed in Online Appendix A.2, we employ the log-linearization technique in Campbell and Shiller (1988), expressing the return on aggregate wealth as a function of the evolution of the price-to-consumption ratio, i.e., the logarithm of the ratio between investable wealth and consumption, $pc_t = \log \frac{W_t - C_t}{C_t}$. Likewise, we log-linearize the SDF in (5). The following proposition characterizes the price-to-consumption ratio, the dynamics of the SDF, and the risk-free rate.

Proposition 2. *The equilibrium price-to-consumption ratio, SDF dynamics, and risk-free rate (all in logs) are given by*

$$pc_t = A_{pc,0} + A_{pc,G} G_{W,t} + A_{pc,\delta}\delta_t + A_{pc,x} x_t, \tag{10}$$

$$m_{t+1} = m_0 + m_G G_{W,t} + m_\delta \delta_t + m_x x_t - \lambda_c \varepsilon_{c,t+1} - \lambda_G \varepsilon_{G,t+1} - \lambda_\delta \varepsilon_{\delta,t+1} - \lambda_x \varepsilon_{x,t+1}, \tag{11}$$

$$r_{f,t+1} = -m_0 - \frac{\lambda_c^2}{2} - \frac{\lambda_G^2}{2} - \frac{\lambda_\delta^2}{2} - \frac{\lambda_x^2}{2} - m_G G_{W,t} - m_\delta \delta_t - m_x x_t. \tag{12}$$

All the coefficients are derived and displayed in Online Appendix A.2, where we also show that $A_{pc,G}$, $A_{pc,\delta}$, $A_{pc,x}$, λ_c, λ_G, λ_δ, λ_x, m_G, m_δ *are all positive, while* $-1 < m_x < 0$.

The price-to-consumption ratio is an affine function of the state variables. The positive coefficients $A_{pc,G}$, $A_{pc,\delta}$, and $A_{pc,x}$ indicate that the price-to-consumption ratio is positively related with aggregate ESG supply $G_{W,t}$, ESG demand δ_t, and the long-run risk variable, x_t. Then, for a given level of physical consumption, an increase in aggregate ESG supply or demand leads to a higher value of the wealth portfolio. As shown in Online Appendix A.2, this mechanism also implies that the realized return on aggregate wealth is positively correlated with contemporaneous shocks to ESG supply and demand. Thus, an unanticipated rise in aggregate ESG benefits creates upward pressure on the value of the wealth portfolio and a higher contemporaneous realized return.

The log-linearized dynamics of the SDF in (11) are driven by four sources of risk, namely, shocks to (i) short-run consumption growth, $\varepsilon_{c,t+1}$, (ii) ESG supply, $\varepsilon_{G,t+1}$, (iii) ESG demand, $\varepsilon_{\delta,t+1}$, and (iv) long-run consumption growth, $\varepsilon_{x,t+1}$. The prices of the four risk sources, λ_c, λ_G, λ_δ, and λ_x, are constant and positive.[7] Thus, assets whose returns are positively (negatively) correlated with the systematic shocks yield a positive (negative) risk premium. Additionally, the prices of risk increase in the volatilities of the corresponding shocks, σ_c, σ_G, σ_δ, and σ_x.

The coefficients m_x, m_G, and m_δ drive the time variation of the drift of the SDF and, consequently, of the risk-free rate. As m_G and m_δ are positive, the risk-free rate is negatively

[7] The proof that λ_c and λ_x are positive is in the Online Appendix A.2. Considering the log-linearized model, it is more challenging to directly prove that λ_G and λ_δ are positive. However, as derived in Online Appendix A.1 and discussed in Section 2.2, these risk premia must be positive due to the concavity of the value function with respect to variations of $G_{W,t}$ and δ_t. In the context of the log-linearized model, we verify that λ_G and λ_δ are positive for a wide range of parameter values. The estimation in Section 4 also provides supporting evidence.

related to the aggregate greenness and ESG preference parameter. This is because an increase in ESG demand or supply leads to a higher ESG-adjusted return on the wealth portfolio. As a result, investors are motivated to increase their investments and reduce their consumption, leading to higher savings and a decrease in the risk-free rate. The constant terms $-\frac{\lambda_G^2}{2}$ and $-\frac{\lambda_\delta^2}{2}$ are present because ESG supply and demand shocks contribute to the risk perceived by the agent. These shocks lead to higher precautionary saving motives, resulting in a lower risk-free interest rate. Finally, consistent with the long-run risk literature, the risk-free rate exhibits an increasing relation with expected consumption growth, as $m_x < 0$. Indeed, an anticipated increase in future consumption levels encourages higher current consumption, which in turn leads to lower savings and a higher risk-free rate.

2.4 The cross section of asset returns

We proceed to examine the cross-section of asset returns, with a particular focus on the return differential between green and brown stocks. First, the dynamics of asset-n ESG score is formulated as

$$G_{n,t+1} = \mu_{Gn} + \rho_{Gn} G_{n,t} + \sigma_{Gn,G}\varepsilon_{G,t+1} + \sigma_{Gn}\varepsilon_{Gn,t+1}, \tag{13}$$

where $\varepsilon_{Gn,t+1}$ is IID normal and uncorrelated with all other innovations. When $0 < \rho_{Gn} < 1$, the process is mean-reverting with a long-run mean equal to $\bar{G}_n = \frac{\mu_{Gn}}{1-\rho_{Gn}}$. Unexpected innovations in the asset ESG score can covary with innovations in the aggregate greenness, $\varepsilon_{G,t+1}$. This reflects the idea that when green firms are incentivized to become even greener, both the aggregate market and a collection of green firms would exhibit an improved ESG profile. Conforming to intuition, estimation shows that the correlation between the market and stock-level ESG is, on average, positive for green, negative for brown, and zero for green-neutral firms. To characterize the market portfolio, we assume that the market ESG profile is identical to that of aggregate wealth, i.e., $G_{M,t} = G_{W,t}$, following the dynamics in Equation (8).[8]

We then define the dividend growth process as

$$\Delta d_{n,t+1} = \mu_{dn} + \rho_{dn,x} x_t + \sigma_{dn,c}\varepsilon_{c,t+1} + \sigma_{dn,dM}\varepsilon_{dM,t+1} + \sigma_{dn}\varepsilon_{dn,t+1}, \tag{14}$$

where the market and asset-specific innovations, $\varepsilon_{dM,t+1}$ and $\varepsilon_{dn,t+1}$, are IID normal and uncorrelated with all other innovations. Through the coefficient $\rho_{dn,x}$, the expected dividend growth is driven by a predictable component represented by the state variable x_t, which also drives consumption growth. We allow the unexpected component of dividend growth to vary with innovations in consumption growth, as well as with a common market dividend shock, $\varepsilon_{dM,t+1}$. For ease of interpretation, the dividend growth is parsimoniously formulated, while Online Appendix A describes a more general case where the dividend process in (14) has a drift influenced by δ_t and permits correlation with innovations in long-run risk, as well as in aggregate ESG demand and supply. The implications of the extended specification are discussed in Section 5.

To determine the equilibrium, we apply the Euler condition (4), log-linearizing the asset

[8]We make this assumption for empirical tractability, as we observe the ESG scores of traded firms to assess the market ESG profile, while the ESG profile of the wealth portfolio is unobservable. Otherwise, the market portfolio can be treated as any other risky asset.

return as in Campbell and Shiller (1988) and expressing it as a function of the price-to-dividend ratio, $pd_{n,t}$. The following proposition characterizes the price-to-dividend ratio, as well as the realized and expected return on any given risky asset, including the market portfolio. The proof is in Online Appendix A.3 for a generic asset and Online Appendix A.4 for the market portfolio.

Proposition 3. *The asset-n equilibrium price-to-dividend ratio, excess return dynamics, and expected excess return are formulated as*

$$pd_{n,t} = A_{n,0} + A_{n,G}G_{W,t} + A_{n,\delta}\delta_t + A_{n,x}x_t + A_{n,Gn}G_{n,t}, \tag{15}$$

$$\begin{aligned}\hat{r}_{n,t+1} = {} & \mathrm{E}_t\left[\hat{r}_{n,t+1}\right] + \sigma_{dn,c}\varepsilon_{c,t+1} + \kappa_{rn,pd}\left(A_{n,G}\sigma_G + A_{n,Gn}\sigma_{Gn,G}\right)\varepsilon_{G,t+1} \\ & + \kappa_{rn,pd}A_{n,\delta}\sigma_\delta\varepsilon_{\delta,t+1} + \kappa_{rn,pd}A_{n,x}\sigma_x\varepsilon_{x,t+1} \\ & + \kappa_{rn,pd}A_{n,Gn}\sigma_{Gn}\varepsilon_{Gn,t+1} + \sigma_{dn,dM}\varepsilon_{dM,t+1} + \sigma_{dn}\varepsilon_{dn,t+1},\end{aligned} \tag{16}$$

$$\begin{aligned}\mathrm{E}_t\left[\hat{r}_{n,t+1}\right] = {} & \underbrace{\sigma_{dn,c}}_{\mathrm{Cov}_t\left[\hat{r}_{n,t+1},\varepsilon_{c,t+1}\right]}\lambda_c + \underbrace{\kappa_{rn,pd}\left(A_{n,G}\sigma_G + A_{n,Gn}\sigma_{Gn,G}\right)}_{\mathrm{Cov}_t\left[\hat{r}_{n,t+1},\varepsilon_{G,t+1}\right]}\lambda_G \\ & + \underbrace{\kappa_{rn,pd}A_{n,\delta}\sigma_\delta}_{\mathrm{Cov}_t\left[\hat{r}_{n,t+1},\varepsilon_{\delta,t+1}\right]}\lambda_\delta + \underbrace{\kappa_{rn,pd}A_{n,x}\sigma_x}_{\mathrm{Cov}_t\left[\hat{r}_{n,t+1},\varepsilon_{x,t+1}\right]}\lambda_x - \frac{1}{2}\mathrm{Var}_t\left[\hat{r}_{n,t+1}\right] \\ & + \underbrace{\log\left(1-\bar{\delta}\bar{G}_n\right) - \frac{\bar{G}_n\left(\delta_t-\bar{\delta}\right)}{1-\bar{\delta}\bar{G}_n} - \frac{\bar{\delta}\left(G_{n,t}-\bar{G}_n\right)}{1-\bar{\delta}\bar{G}_n}}_{-y_{n,t}},\end{aligned} \tag{17}$$

where $\hat{r}_{n,t+1} = r_{n,t+1} - r_{f,t+1}$, $A_{n,G} = \frac{m_G}{1-\kappa_{rn,pd}\rho_G}$, $A_{n,\delta} = \frac{m_\delta+\bar{G}_n/(1-\bar{\delta}\bar{G}_n)}{1-\kappa_{rn,pd}\rho_\delta}$, $A_{n,x} = \frac{m_x+\rho_{dn,x}}{1-\kappa_{rn,pd}\rho_x}$, $A_{n,Gn} = \frac{\bar{\delta}/(1-\bar{\delta}\bar{G}_n)}{1-\kappa_{rn,pd}\rho_{Gn}}$, $\kappa_{rn,pd} = \frac{e^{\overline{pd}_n}}{1+e^{\overline{pd}_n}}$. $A_{n,0}$ *and* $\mathrm{Var}_t\left[\hat{r}_{n,t+1}\right]$ *are constant quantities described in Online Appendix A.3. The market portfolio* ($n = M$) *is characterized imposing* $G_{n,t} = G_{W,t}$, $\sigma_{dn,dM} = \sigma_{dM}$, $\sigma_{dn} = 0$, $\sigma_{Gn,G} = \sigma_G$, and $\sigma_{Gn} = 0$.

The price-to-dividend ratio in equation (15) is an affine function of the state variables $G_{W,t}$, δ_t, x_t, and $G_{n,t}$. The dependence on the aggregate ESG profile, $G_{W,t}$, evolves from the risk-free rate and is independent of the asset ESG score. As $A_{n,G} > 0$, an increase in aggregate greenness leads to a lower discount rate and results in a higher valuation of all risky assets.

The loadings on aggregate ESG demand, δ_t, play an essential role in explaining the cross section of stock returns. Specifically, $A_{n,\delta}$ is positive for green assets, while it becomes negative for assets with a sufficiently negative long-run ESG score, $\bar{G}_n$.[9] Therefore, when a positive ESG demand shock $\varepsilon_{\delta,t+1}$ occurs, the price of a green asset increases, leading to a positive unexpected return, as indicated by equation (16). This is because the asset provides greater nonpecuniary benefits upon a positive demand shock. Conversely, the price of brown assets decreases due to a stronger perception of their negative externalities. Hence, ESG demand shocks can generate positive differences in realized returns between green and brown assets.

The sensitivity to long-run risk shocks, represented by $A_{n,x}$, is subject to two conflicting

[9] The condition for $A_{n,\delta}$ to be positive is $\bar{G}_n > -\frac{m_\delta}{1-m_\delta\bar{\delta}}$. The threshold value is nonzero because ESG demand also negatively affects the risk-free rate, which impacts the discounting of future cashflows in the same direction for both green and brown assets. Based on the model estimates in Section 4, we empirically verify that the threshold value, $-\frac{m_\delta}{1-m_\delta\bar{\delta}}$, is close to zero, corresponding to an ESG-neutral asset. This is due to the negligible impact of ESG demand on the discount rate compared to its effect on the valuation of nonpecuniary benefits.

forces. First, higher expected consumption growth leads to a negative price effect, as future cashflows are discounted more heavily. Second, there is a positive price effect due to higher expected dividend growth. Prior research suggests that the latter effect is generally stronger, resulting in a positive value for $A_{n,x}$.

Finally, the firm's ESG profile, $G_{n,t}$, has an impact on stock valuation and realized returns. As $A_{n,Gn} > 0$, a positive innovation $\varepsilon_{Gn,t+1}$ leads to an increased stock valuation, driven by greater nonpecuniary benefits, and a contemporaneous positive unexpected return.

The expected excess return is determined by a combination of a time-varying convenience yield premium and four constant risk premia. The convenience yield premium, defined as the opposite of the convenience yield $y_{n,t}$, is driven by the processes δ_t and $G_{n,t}$. It is represented in the final line in equation (17), which represents the log-linearization of the term $1 - \delta_t G_{n,t}$ in the Euler equation (4). The convenience yield premium captures the time-varying nonpecuniary motives associated with the asset, resulting in a negative impact on expected returns for green stocks and a positive impact for brown stocks. The effect is more pronounced for higher levels of ESG demand. This component echoes the concept observed in single-period setups, where investors are willing to accept lower expected returns when holding green assets.

The remaining components of the expected excess return in (17) are constant through time. In particular, the risk premia are given by the covariances between asset returns and systematic sources of risk, scaled by the corresponding positive prices of risk. Among these, the exposure to ESG demand shocks $\varepsilon_{\delta,t+1}$ is particularly relevant. The covariance between realized returns and ESG demand shocks depends on the price sensitivity $A_{n,\delta}$, being thus positive for green and negative for sufficiently brown assets, with stronger dependence for assets deviating more from green neutrality.

An economic interpretation of the positive ESG demand risk premium for green assets is as follows. An ESG-perceptive investor holding a green asset is negatively affected by a decrease in ESG demand due to both lower aggregate nonpecuniary benefits and a lower financial valuation of the green asset. As the two effects reinforce each other rather than hedge, the risk premium for exposure to ESG demand shocks is positive for green assets. Conversely, a brown asset exhibits a valuation increase upon a negative ESG demand shock, thus representing a hedge against the decrease in the nonpecuniary benefits delivered by the wealth portfolio. Consequently, a negative ESG demand risk premium applies to brown assets. The ESG demand risk premium of a green-minus-brown portfolio is then positive. It becomes more pronounced as the volatility of ESG demand increases and can offset, at least partially, the negative ESG-expected return relation implied by the convenience yield.

The risk premium associated with ESG supply shocks is represented by the second term in equation (17). The sign of this component depends on the covariance between the asset and wealth portfolio ESG scores, $\sigma_{Gn,G}$. The empirical evidence discussed below shows that ESG supply is less volatile than the other sources of risk, implying that the corresponding risk premium is of second order. Finally, consistent with the existing literature, the exposures to short- and long-run consumption shocks positively contribute to the risk premium. It should be noted that the ESG demand and supply risk premia would exist even under additive preferences or a different specification of the consumption process. For instance, if consumption growth is

IID, the term involving λ_x vanishes, while all other considerations on risk premia remain intact.

The expected return on green assets consists of four positive risk premia contributions, while the convenience yield premium is negative. Brown assets exhibit a positive convenience yield premium, as well as positive short- and long-run consumption risk premia, but a negative risk premium for ESG demand shocks, as well as a risk premium for aggregate ESG supply shocks that can be either positive or negative. Consequently, the expected return on a portfolio that takes long positions in green and sells short brown assets exhibits a negative convenience yield premium, as observed in static setups, but a positive risk premium associate with the exposures to ESG demand shocks. Our setup does not impose specific restrictions related to the loadings on the other risk sources: (i) short-run consumption growth $\varepsilon_{c,t+1}$, (ii) long-run consumption growth $\varepsilon_{x,t+1}$, and (iii) aggregate ESG supply $\varepsilon_{G,t+1}$. In the empirical analysis that follows, we find that brown stocks have larger exposures to short- and long-run consumption shocks, while green stocks tend to have slightly larger exposure to aggregate ESG supply shocks.

In summary, the dynamic setup presents additional cross-sectional asset pricing implications compared to a static framework. Indeed, the ESG demand risk premium can offset the convenience yield premium associated with nonpecuniary benefits. Moreover, the important observation by Pástor et al. (2022) that green assets have realized higher average returns upon increasing sustainability concerns can be readily rationalized in a dynamic setup, as ESG demand shocks are associated with green assets realizing positive unexpected returns.

Having derived the asset pricing equilibrium, we can proceed to estimate the model based on consumption data, as well as observations on the market portfolio and individual stock returns, dividend-to-price ratios, and ESG scores.

3 Data

Our dataset relies on the ESG and environmental-pillar scores published by MSCI, widely recognized as a leading provider of ESG ratings among industry professionals and academic researchers. The data covers the period from January 2007 to December 2022 and consists of industry-adjusted scores based on the Intangible Value Assessment (IVA) methodology. The scores, ranging from 0 to 10, are regularly revised and published on a monthly basis. They do not represent an absolute measure of a firm's ESG profile, but provide an assessment relative to all other firms on a given date. For our analysis, we calculate percentile ranks of both ESG and environmental scores corresponding to each observation, normalizing them to the range between -0.5 and 0.5, following the approach by Engle et al. (2020).[10]

To construct ESG-sorted portfolios, we consider common stocks (share codes 10 and 11) traded on the NYSE/AMEX/Nasdaq exchanges, narrowing down the focus to firms with an available ESG rating. We obtain monthly total returns, dividends, and market capitalization from the Center for Research in Security Prices (CRSP). We exclude stocks that belong to the bottom percentile of market capitalization. We form three value-weighted monthly-rebalanced

[10]The scale is centered around zero, so that the median value represents an ESG-neutral asset, and the range is normalized to one for convenience. As noted in Section 2.1, there exists a degree of freedom in choosing the scales for ESG scores and ESG demand, which is unobservable in our analysis. By setting the scale of values for ESG scores, we ensure the econometric identifiability of ESG demand.

portfolios by sorting stocks on their prior ESG scores. The brown, neutral, and green portfolios consist of stocks with scores below the 30-th, between the 30-th and the 70-th, and above the 70-th percentiles, respectively. Portfolio-level ESG scores are computed by value-weighting the corresponding stock-level scores. The market portfolio is formed by value-weighting the contributions of all stocks in the available universe. Additionally, to conduct robustness checks, we form portfolios excluding stocks in the technology sector based on the Fama-French five-industry definitions. The risk-free return is the monthly return of the 1-month Treasury Bill.[11] Online Appendix B provides portfolio summary statistics and displays the time series of value-weighted scores by industry sector, as well as of the capitalization and composition of the portfolios by industry.

To calculate the aggregate nominal consumption, we follow the existing literature (e.g., Constantinides and Ghosh, 2011; David and Veronesi, 2013; Schorfheide et al., 2018) by considering the monthly time series of personal consumption expenditures for nondurable goods and services, provided by the Bureau of Economic Analysis and available on the Federal Reserve Economic Data website (series `PCEND` and `PCES`). We then use the Personal Consumption Expenditures Price Index (series `PCEPI`) and the U.S. population (series `POPTHM`) to calculate real per capita consumption.

4 Estimation

4.1 Estimation technique

To keep the focus on the incremental implications of ESG, we adopt several standard parameter values from the existing literature on consumption-based models. In particular, the subjective discount rate is $\beta = 0.998$, the intertemporal elasticity of substitution is $\psi = 1.5$, and the parameters describing the long-run risk dynamics are $\rho_x = 0.979$ and $\sigma_x = 0.00034$. Regarding ESG demand, we expect the effect of shocks to δ_t to be highly persistent. However, for the solution of the model, it is useful to assume that there exists an average value $\bar{\delta}$ around which the model can be log-linearized. For this reason, we follow Ireland (2015) by setting $\rho_\delta = 0.9999$, which formally preserves stationarity, while also constraining the dynamics of δ_t to be near unit root.

The remaining parameter space, denoted by Θ, is composed of economy-wide parameters, Θ_E, market parameters, Θ_M, and individual asset parameters, Θ_{br}, Θ_{neu}, and Θ_{gr}, for the brown, neutral, and green portfolios, respectively. More specifically, the economy-wide parameters, denoted by $\Theta_E = \{\gamma, \mu_c, \sigma_c, x_0, \bar{G}_W, \rho_G, \sigma_G, \delta_0, \bar{\delta}, \sigma_\delta\}$, include preference parameters, short- and long-run consumption growth, aggregate greenness, and ESG demand. Market parameters, $\Theta_M = \{\mu_{dM}, \rho_{dM,x}, \sigma_{dM,c}, \sigma_{dM}\}$, underlie the dynamics of the market dividend growth in (14). Asset-specific parameters are denoted by $\Theta_j = \{\mu_{dj}, \rho_{dj,x}, \sigma_{dj,c}, \sigma_{dj,dM}, \sigma_{dj}, \mu_{Gj}, \rho_{Gj}, \sigma_{Gj,G}, \sigma_{Gj}\}$, where $j = \{br, neu, gr\}$, and they underlie the dynamics of the dividend growth and the asset greenness.

The model can be represented through a linear state space obtained by stacking the dynamics

[11] We thank Kenneth French for providing industry definitions and risk-free returns through his website: `https://mba.tuck.dartmouth.edu/pages/faculty/ken.french/data_library.html`.

of consumption growth, aggregate ESG supply, ESG demand, long-run risk, portfolio ESG scores, the market excess return, as well as excess returns of the brown, green-neutral, and green portfolios. The joint dynamics is described through the vector autoregression

$$\boldsymbol{X}_{t+1} = \boldsymbol{A_X} + \boldsymbol{B_X}\boldsymbol{X}_t + \boldsymbol{\sigma_X}\varepsilon_{t+1}, \tag{18}$$

where

$$\boldsymbol{X}_t = \begin{bmatrix} \Delta c_t & G_{W,t} & \delta_t & x_t & G_{br,t} & G_{neu,t} & G_{gr,t} & \hat{r}_{M,t} & \hat{r}_{br,t} & \hat{r}_{neu,t} & \hat{r}_{gr,t} \end{bmatrix}', \tag{19}$$

$$\boldsymbol{A_X} = \begin{bmatrix} \mu_c & \mu_G & \mu_\delta & 0 & \mu_{Gbr} & \mu_{Gneu} & \mu_{Ggr} & \hat{r}_{M,0} & \hat{r}_{br,0} & \hat{r}_{neu,0} & \hat{r}_{gr,0} \end{bmatrix}', \tag{20}$$

$$\boldsymbol{\varepsilon}_t = \begin{bmatrix} \varepsilon_{c,t} & \varepsilon_{G,t} & \varepsilon_{\delta,t} & \varepsilon_{x,t} & \varepsilon_{Gbr,t} & \varepsilon_{Gneu,t} & \varepsilon_{Ggr,t} & \varepsilon_{dM,t} & \varepsilon_{dbr,t} & \varepsilon_{dneu,t} & \varepsilon_{dgr,t} \end{bmatrix}', \tag{21}$$

and the matrices $\boldsymbol{B_X}$ and $\boldsymbol{\sigma_X}$ are described in Online Appendix C. To account for the unobserved variables in the vector $\boldsymbol{X}_t$, namely ESG demand and long-run consumption growth, we employ the Kalman filter to estimate the system.

The transition equation in the state space is given by (18). The observable variables are the real monthly per capita consumption growth, the ESG scores and excess returns of the market, as well as of the three ESG-sorted portfolios. We stack these variables in the vector $\boldsymbol{Y}_t$:

$$\boldsymbol{Y}_t = \begin{bmatrix} \Delta c_t & G_{W,t} & G_{br,t} & G_{neu,t} & G_{gr,t} & \hat{r}_{M,t} & \hat{r}_{br,t} & \hat{r}_{neu,t} & \hat{r}_{gr,t} \end{bmatrix}'. \tag{22}$$

The observation equation of the system is then given by

$$\boldsymbol{Y}_t = \boldsymbol{H}\boldsymbol{X}_t. \tag{23}$$

Online Appendix C provides further details on the state-space representation, including the components of the $\boldsymbol{H}$ matrix, the Kalman filter implementation, and the restrictions on the parameter space. For instance, δ_t is constrained to be nonnegative and further $\bar{\delta}$ is set to be equal to the sample mean of δ_t. We also impose that the sample averages of observed price-to-dividend ratios are matched by the model-implied counterparts. This allows, together with the observation of asset returns, to pin down the parameters governing dividend growth.

In order to (i) address the finite-sample properties of the maximum likelihood estimates and (ii) impose constraints on the parameter space, which could render asymptotic inferences unreliable, we implement the methodology proposed by Efron and Tibshirani (1994, Ch. 6) and employed by Ireland (2015). In particular, we simulate 1000 joint trajectories of the variables in the model using the point estimates of the parameters. For each trajectory, we re-estimate the model based on the simulated data and, finally, we evaluate the standard errors per parameter as the standard deviations across all estimated values.

4.2 Estimating the model

We first present the time-series dynamics of aggregate ESG demand and supply, both displayed in Panel (a) of Figure 2. The ESG demand, δ_t, estimated through Kalman filter, exhibits similar patterns to those observed in the press attention given to sustainable investing (Figure 1). Specifically, δ_t shows a constant or slightly diminishing trend until 2014. Following the signing of the Paris Agreement on climate change at the end of 2015, it experiences a significant increase until 2021 and stabilizes in 2022. At the end of the sample, the value of δ_t is approximately six times larger than in 2016. Consequently, for an asset with a given ESG score, the ESG-based convenience yield at the end of the sample is also six times larger than in 2016.

The aggregate ESG supply, $G_{W,t}$, represents the value-weighted market ESG score. ESG supply is highly persistent and less volatile than ESG demand, as the latter is driven by market sentiment and can experience sudden shifts. Indeed, reallocation of capital across financial assets can be done quickly and with low costs, while adjusting ESG supply to meet sustainability criteria may involve high costs and longer time horizons due to its link to a firm's core business environment. The market portfolio only slightly deviates from green neutrality on average, but it becomes progressively greener in the second half of the sample. This shift is driven by profit-maximizing corporations responding to ESG trends for various reasons, including tax benefits, innovation stimulus, access to loans and grants, reduced cost of capital, and the attempt to cater to customers who prefer responsible corporations.[12]

The estimates for the model parameters are reported in Panel (a) of Table 1. The estimated risk aversion, γ, is 13.11, insignificantly different from 10, the value considered by Bansal and Yaron (2004) and in line with previous estimates (e.g., Constantinides and Ghosh, 2011; Schorfheide et al., 2018). The persistence of aggregate greenness, described in (8), is quite strong with ρ_G nearly equal to 0.99. The volatility σ_G is 0.01 and the sample mean $\bar{G}_W$ is 0.05. The ESG demand mean and volatility are $\bar{\delta} = 0.00046$ and $\sigma_\delta = 0.00004$.

The dynamics of $G_{W,t}$ and δ_t can be used to evaluate the ESG benefits formulated in (2) and their contribution to the total value of the consumption bundle. Indeed, the consumption bundle A_t equals the current value of consumption C_t times the expression $1+\delta_t G_{W,t} e^{pc_t}$, where pc_t is the logarithm of the ratio between investable wealth and consumption, given in equation (10). Over the entire sample period, the ESG nonmonetary benefits amount to 1.61% of the physical consumption on average, which is significant at conventional levels. ESG benefits rise to 3.43% of physical consumption between 2016 and 2022, due to increasing levels of ESG demand.

The prices of risk, namely λ_c, λ_G, λ_δ, and λ_x, as derived in Proposition 2, depend on the economy-wide parameters. Our empirical results are consistent with the inferences made in the theory section, confirming that all prices of risk are positive and statistically significant.

Consistent with the literature on long-run risk, the expected market dividend growth is leveraged relative to the expected consumption growth through the coefficient $\rho_{dM,x}$ in equation (14), estimated at 3.55 and highly significant. This implies that the market portfolio is strongly exposed to the long-run risk variable. Focusing on the dividend process of ESG-sorted portfolios, the expected dividend growth of the green portfolio is less exposed to long-run risk ($\rho_{dgr,x} = 3.38$) than the brown portfolio ($\rho_{dbr,x} = 3.64$), with a p-value for the difference lower than 0.05.

[12] Our assessment of the market greenness could be conservative. This is because, consistent with ESG raters who provide only a relative assessment of the sustainability profile of any rated firm, the median ESG score across stocks is zeroed out at any time period in the sample. Thus, possible shifts towards sustainability that could characterize the median corporation in the sample are not accounted for. The market ESG score still fluctuates, with a substantial upward trend after 2015, because larger market capitalization firms tend to be more sustainable than their smaller capitalization counterparts.

These findings are in line with the literature documenting that a better ESG profile reduces the risk exposure (e.g., Albuquerque et al., 2019; Ilhan et al., 2021). Intuitively, a higher standard of corporate ESG practice helps mitigate legal, regulatory, and operational risks.

The portfolio ESG scores are highly persistent, as the parameter ρ_{Gn} in equation (13) is 0.97 or above for all three portfolios. Thus, a shock to the ESG score of an asset is expected to have long-lasting price effects, as further analyzed in Section 5. The correlation between innovations in the ESG scores of the green portfolio and the market, measured through $\sigma_{Ggr,G}$, is positive and significant, while a negative and significant (although weaker) correlation applies to the brown portfolio. These findings suggest that greener assets have sustainability profiles that exhibit a stronger positive covariance with aggregate ESG supply shocks.

Next, we describe the conflicting forces underlying asset returns, analyzing the gap between expected and realized returns. As reported in annualized terms in Panel (a) of Table 2, the market portfolio exhibits an average annual excess return of 7.92% over the sample period, while the green and brown portfolios have average excess returns of 8.61% and 5.96%, respectively.

Focusing first on the market expected excess return, the model provides a clear decomposition mechanism through equation (17). Long-run risk shocks are associated with a risk premium equal to 9.63% per annum, accounting for a large part of the market premium. The ESG-based components of the market premium, namely the ESG supply risk premium, the ESG demand risk premium, and the average convenience yield, are all near zero, as the market portfolio only modestly departs from green neutrality. In recent years, the increasing ESG demand has implications for realized asset returns. Specifically, we calculate the average unexpected market return induced by ESG demand shocks, i.e., the annualized average of the expression $\kappa_{rM,pd}A_{M,\delta}\sigma_{\delta}\varepsilon_{\delta,t+1}$ in equation (16). As the market is near ESG neutral over the entire sample, the component of realized market returns induced by unexpected shocks to ESG demand is relatively mild, amounting to only 21 basis points per annum on average.

We proceed with the analysis of the expected excess return decomposition for ESG-sorted portfolios. Relative to the green portfolio, the brown portfolio has a higher risk premium associated with long-run consumption shocks (9.99% vs 9.05% per annum). According to equation (17), the ESG supply risk premium depends on the positive term $\kappa_{rn,pd}A_{n,G}\sigma_G$ and the term $\kappa_{rn,pd}A_{n,Gn}\sigma_{Gn,G}$, which is positive for the green and negative for the brown portfolios. While the first term dominates, the overall contribution of ESG supply risk premium to the expected return is negligible for all portfolios, as the volatility of aggregate and individual asset ESG scores is modest. In contrast, the ESG demand risk premium for the green portfolio is positive and economically significant at 0.10% per annum, consistent with a positive coefficient $A_{n,\delta}$ for green stocks. On the other hand, it is -0.12% for the brown portfolio, reflecting a negative $A_{n,\delta}$. This implies a positive and statistically significant 22-basis point ESG demand risk premium for the green-minus-brown portfolio.

The positive ESG demand risk premium partially offsets the convenience yield premium, which represents a negative contribution to the green-minus-brown expected return spread, averaging -0.37% over the full sample. Note that the convenience yield effect exhibits substantial fluctuations over the sample period. For example, during the period from 2016 to 2022, which follows the Paris Agreement, the average convenience yield premium of the green-minus-brown portfolio amounts to -0.68% per annum, almost twice the average value over the full sample.

Overall, the model-implied average expected excess return of the green portfolio is 7.90%, while it is higher at 8.89% for the brown portfolio. Consequently, the green-minus-brown portfolio has a negative average expected return of -1.00% per annum. However, throughout the sample, the unexpected shocks to ESG demand induce a positive and significant unexpected return, which amounts to 3.53%. This contribution, represented by the term $\kappa_{rn,pd} A_{n,\delta} \sigma_\delta \varepsilon_{\delta,t+1}$ in equation (16), adds to the conditional expected return. Considering the combined effect of the conditional expected return and the unexpected return due to ESG demand shocks, the green-minus-brown portfolio average return is positive and significant at 2.54%, consistent with the average return of 2.65% observed in the data.

Our model emphasizes that the conditional expected return and realized return of the green-minus-brown portfolio depend on several forces. It also provides a structural relation between unexpected shifts in ESG demand and realized returns. Notably, the effect of unanticipated ESG demand shocks on realized returns can be very sizable, implying that caution is necessary when using past realized returns to predict future returns of ESG investments. Looking ahead, the expected return on green stocks should diminish with the growing convenience yield. Consequently, if positive unexpected ESG demand shocks attenuate in the future, green assets may deliver lower performance.

The presence of time-varying ESG demand and the offsetting forces on expected and realized returns could explain the mixed evidence in the literature on return predictability of ESG ratings. To reinforce this observation, we analyze the time-series dynamics of the state variables and their implications for asset returns. The top-left panel in Figure 3 displays the expected consumption growth, represented by the conditionally deterministic component $\mu_c + x_t$ in equation (6), where x_t is obtained through the Kalman filter. The expected consumption growth is highly persistent and fluctuates between 0% and 4% per annum for most of the sample period, consistent with the existing literature (e.g., Schorfheide et al., 2018). However, following the 2008 financial crisis, an exception occurs as the expected consumption growth turns negative.

The ESG scores of the portfolios, displayed in the top-right graph, exhibit high persistence and do not show clear trends over time. According to our model, the expected excess return of a perfectly ESG-neutral asset is time invariant, as the convenience yield component in equation (17) is zero. This is evident in the second graph on the left of Figure 3, where the ESG-neutral portfolio exhibits an expected excess return that is nearly constant.

The expected excess returns of the green and brown portfolios display nearly symmetrical patterns, which can be attributed to the symmetry observed in the convenience yields. The convenience yields are indeed determined by the product of ESG demand, as shown in Figure 2a, which is the main driver of their time variation, and the portfolio ESG scores, which exhibit nearly opposite values throughout the sample. As a result, the convenience yield is positive for green and negative for brown stocks, with increasing absolute values towards the end of the sample, reflecting the growing ESG demand. For instance, the green portfolio exhibits an average convenience yield of 0.18% over the full sample, while the value is 0.68% in 2022.

The bottom-left graph of Figure 3 illustrates the total ESG premium, calculated as the net effect of convenience yield, ESG demand risk premium, and ESG supply risk premium. In periods of low ESG demand, the total ESG premium for green assets can slightly exceed that for ESG-neutral or brown assets. However, with the increase in ESG demand in the latter part of the sample, the convenience yield effect becomes dominant, leading to a largely negative total ESG premium for green assets and positive for brown assets.

The bottom-right graph displays the price-to-dividend ratios of both the market and ESG-sorted portfolios. These are highly correlated and primarily driven by the expected consumption growth variable, x_t. However, when focusing on the ESG portfolios, we observe that the model-implied price-to-dividend ratio of the green portfolio is lower than that of the other portfolios when ESG demand is low, while it grows higher as δ_t increases towards the end of the sample. This pattern emerges because the rise in ESG demand exerts a contemporaneous positive (negative) price pressure on green (brown) assets, as indicated by equation (15).

The contemporaneous price effect of ESG demand shocks has a sizable impact on realized returns, as displayed in equation (16). In particular, green assets realize returns that are positively correlated with ESG demand shocks, while brown asset returns are negatively correlated. Figure 4a highlights this effect, with the left graph showing the cumulative realized return of the green-minus-brown portfolio, the cumulative conditional expected return obtained by accumulating the expected return in equation (17), the cumulative unexpected return of ESG demand shocks, as expressed through the term $\kappa_{rn,pd} A_{n,\delta} \sigma_\delta \varepsilon_{\delta,t+1}$ in equation (16), as well as the sum of the expected and unexpected components.

Throughout the sample, the conditional expected return of the green-minus-brown portfolio is negative, resulting in a negative cumulative expected return that decreases over time. However, the cumulative realized return shows significant deviations from this expected pattern, particularly during periods of large shocks to ESG demand, as observed in Figure 3. This phenomenon becomes particularly evident in the most recent years of the sample, where positive shocks to ESG demand lead to substantial positive realized returns. As shown in the graph, the effect of shocks to δ_t, when added to the conditional expected return, is crucial in explaining the realized returns of the green-minus-brown portfolio. Over the entire 16-year long sample, the net increase in δ_t makes the realized return of the spread portfolio largely positive (about 41%), despite a negative cumulative conditional expected return of -16%.

The right graph in Figure 4a shows the conditional expected and realized returns accumulated over the prior 12 months. While the conditional expected return is slightly negative and shows little time variation, the 12-month realized return, as well as the expected return augmented by the effect of ESG demand shocks, are rather volatile and strongly correlated. Remarkably, between 2016 and 2022, the green-minus-brown portfolio achieves an average annualized return of 7.15%, despite an average expected return of -1.30%. This performance is attributed to the unexpected return induced by ESG demand shocks, amounting to 8.11%. The average expected return augmented by the effect of unexpected shocks to δ_t is then 6.81%, close to the realized value. The time-series evidence reinforces the notion that shifts in tastes for ESG play a crucial role in determining realized returns of assets with ESG profiles that depart from green neutrality. In the short run, the unexpected contribution to realized returns induced by ESG demand shocks can markedly dominate the expected return component.

While the results discussed above are based on composite ESG scores, we also estimate the model using environmental-pillar scores. Panel (b) of Figure 2 shows the time series of aggregate demand and supply for the environmental dimension of ESG. The value of δ_t exhibits a regular increase from the beginning of the sample until the end of 2021, with a threefold increase over ten years, followed by a decrease from 0.15% to 0.10% in 2022. Similar to the supply for composite ESG, the aggregate environmental-pillar score also displays a stable, slightly positive value. The parameter estimates in Panel (b) of Table 1 are consistent with those obtained using composite ESG scores, both at the aggregate and portfolio levels. Also in this case, the estimated risk aversion is insignificantly different from 10, and the four prices of risk are positive and statistically significant. The green-minus-brown portfolio return decomposition in Panel (b) of Table 2 also aligns with the findings obtained observing ESG scores, as the environmental-pillar demand risk premium is positive and significant at 0.41% per annum, partially offsetting the negative convenience yield premium of -0.66%. The positive return induced by shocks to δ_t equals 2.61% and adds to the negative average expected return of -1.02%, resulting in a total of 1.59% per annum, which closely aligns with the average observed return of 1.72%.

The time series evidence on portfolio-level conditional expected returns and price-to-dividend ratios in Online Appendix Figure A.3 confirms the results obtained for ESG scores. Similarly, Figure 4b, based on environmental-pillar scores, reinforces the findings on expected and realized returns of the green-minus-brown portfolio. For instance, over the period between 2016 and 2021, the average annualized return is 1.33%, despite an average expected return of -1.41%. This is because the unexpected return induced by shocks to δ_t amounts to 3.66% and its contribution largely offsets the negative average expected return. Interestingly, in 2022 the environmental-pillar green-minus-brown portfolio experienced a negative return, compared to the near-to-zero return of the equivalent portfolio based on composite ESG scores.

Finally, a potential concern is that the estimated growth in ESG demand could be driven largely by an increasing demand for stocks in the technology sector, which are often considered to have a high degree of sustainability. For this reason, we repeat the analysis excluding the stocks in the technology sector from the investable universe. The findings are described in Online Appendix D.2 and are consistent with those obtained when considering the entire universe. The outcome of this robustness check suggests that the dynamics of ESG demand are not primarily driven by stocks in the technology sector.

5 Implications of ESG demand and supply shocks

We next examine the asset pricing implications of ESG demand and supply shocks. The left graphs in Figure 5 focus on demand shocks. At time $t = 0$, the state variables are set equal to their sample averages. Then, a one-standard deviation positive annual shock is applied to ESG demand over 12 consecutive months.[13] In the first graph, it is evident that due to the persistence of ESG demand, δ_t rises and remains nearly fixed at the post-shock level. The second graph displays the conditional expected excess return of the green and brown portfolios. The brown portfolio has a higher expected return, and the gap even widens with positive ESG

[13] As the frequency used for the model estimation is monthly, the size of a one-standard deviation annual shock to δ_t is $\sigma_\delta\sqrt{12}$. Thus, we apply 12 positive consecutive monthly shocks of size $\frac{\sigma_\delta\sqrt{12}}{12}$ at months $t = 1, \ldots, 12$.

demand shocks due to the increasing convenience yield of green stocks, per equation (17).

The third graph shows the monthly realized portfolio excess returns. During the shock, the contemporaneous positive (negative) effect of an unexpected increase of ESG demand on realized returns of the green (brown) portfolio is sizable. This contribution is assessed based on the term $\kappa_{rn,pd} A_{n,\delta} \sigma_\delta \varepsilon_{\delta,t+1}$ in equation (16), where $A_{n,\delta}$ is positive for the green portfolio and negative otherwise. The green asset exhibits a realized monthly return that is 0.5% higher than the brown asset. After the end of the shock ($t = 12$ months), the realized return of the green-minus-brown portfolio is equal to the conditional expected return at -9 basis points.

The cumulative return of the spread portfolio (fourth graph) steeply increases during the shock, reaching about 5% at the end of the 1-year shock. Then, when the shock is shut down, it slowly diminishes due to the negative expected return. The positive effect of realized returns vanishes about 48 months following the end of the shock.

The experiment highlights that, while the expected green-minus-brown portfolio return is negative, unexpected positive ESG demand shocks have a substantial contemporaneous effect on realized returns. This effect is also evident from the valuation ratios, per equation (15). The green portfolio price-to-dividend ratio reflects a reduced expected cost of capital following the ESG demand shock, rising from 49.1 to 50.4. Conversely, the brown portfolio displays a negative price effect from 55.0 to 53.2.

The graphs on the right reflect the effects of a positive shock to aggregate ESG supply. The size of the annual unanticipated shock is +0.1, equally distributed throughout the 12 months, and reflects the ESG profile improvement of one decile on a scale ranging from the most brown asset to the most green. The aggregate ESG supply is less persistent ($\rho_G = 0.99$) than the aggregate demand, consequently, the effect of the shock vanishes, albeit rather slowly.

To understand the effect of an ESG supply shock on expected returns (second graph from top), it is important to recall that the ESG score of the green (brown) portfolio is positively (negatively) correlated with ESG supply, as $\sigma_{Ggr,G}$ ($\sigma_{Gbr,G}$) in equation (13) is positive (negative). Hence, with a positive aggregate shock, the convenience yield of the green asset increases and the expected excess return diminishes per equation (17). The opposite applies to the brown asset. The effect of ESG supply shocks is altogether milder relative to ESG demand shocks.

Consistent with equation (16), a positive shock to aggregate ESG implies a positive unexpected return, per the term $\kappa_{rn,pd} A_{n,G} \sigma_G \varepsilon_{G,t+1}$ with positive $A_{n,G}$, as well as an indirect effect due to the correlation of the shock with the asset ESG score, per the term $\kappa_{rn,pd} A_{n,Gn} \sigma_{Gn,G} \varepsilon_{G,t+1}$ with positive $A_{n,Gn}$. The first contribution depends on the negative effect on the risk-free rate, as displayed in equation (12), which implies a higher valuation of future cashflows. The second component reflects the change of the asset convenience yield in the presence of ESG preferences, which is positive for the green portfolio ($\sigma_{Gn,G} > 0$) and negative for the brown portfolio ($\sigma_{Gn,G} < 0$). The net effect is positive for both portfolios, as the risk-free rate effect dominates the convenience yield effect, and it is stronger for the green portfolio. However, the size of the unexpected return induced by an ESG supply shock is significantly smaller than that of an ESG demand shock. As the unexpected return resulting from the ESG supply shock is larger for the green portfolio, the negative expected return of the green-minus-brown portfolio is offset by its unexpected return contemporaneous to the shock. As a consequence, the realized return of the green-minus-brown portfolio is slightly positive during the shock, while it returns negative after the shock, reflecting the negative expected return.

Finally, following the ESG supply shock, the price-to-dividend ratio of both portfolios increases due to the lower discount rate, per the term $A_{n,G}G_{W,t}$ in (15). The green portfolio experiences a larger price increase than the brown portfolio, as the contemporaneous positive revision of the portfolio ESG score implies a positive price effect, per the term $A_{n,Gn}G_{n,t}$, which adds to the effect of a diminishing risk-free rate.

In the baseline analysis, we assume that the asset dividend growth in (14) is uncorrelated with innovations in both ESG demand and ESG scores. In Online Appendix A, we solve the model relaxing that assumption. An unexpected increase in ESG demand may, for instance, reinforce demand for green products, thus boosting the profits of green firms at the expense of brown firms. The graphs in Online Appendix Figure A.7 illustrate that, when the dividend growth of the green (brown) asset is positively (negatively) correlated with ESG demand, the expected return difference between the green and brown portfolios diminishes compared to the case with zero correlation. This is because the positive correlation implies a return contribution for the green-minus-brown portfolio that is also positively correlated with ESG demand, resulting in a higher ESG demand risk premium. Additionally, due to the positive impact on the dividend, the positive realized return gap in favor of the green asset contemporaneous to an ESG demand shock widens. Consequently, the positive effect of an ESG demand shock on the cumulative return of the green-minus-brown portfolio is more pronounced and takes a longer time to vanish compared to the scenario with zero correlation.

The graphs in Online Appendix Figure A.8 display the response to an annual shock to the ESG score of the green asset. When the correlation between dividend growth and the ESG score is zero, the effects on returns are qualitatively similar to those described for an aggregate ESG demand shock, while the impact on both expected and realized returns is slightly weaker. This is because a positive shock to the ESG score triggers an increase in the convenience yield, but does not lead to a reduction of the risk-free rate. A positive correlation between dividend growth and ESG score is plausible if an improvement in the firm's ESG profile triggers higher demand for goods and services, resulting in higher cashflows. Then, the realized return corresponding to the positive ESG score shock can be significantly higher than that in the baseline case. The correlation between dividend growth and ESG score could also be negative. For instance, this could result from increasing costs incurred for the improvement of the firm's sustainability profile. In this scenario, the negative cashflow effect could imply a lower, even negative, realized return contemporaneous to the unexpected ESG score improvement.

In Online Appendix E.2, we expand the specification of the processes in (8) and (13) to account for a dependence of the dynamics of ESG supply on ESG demand. Recognizing that the demand for sustainability drives the improvement in firms' ESG standards, we allow the drift of ESG scores to depend on the current level of ESG demand. The impulse response analysis in Online Appendix Figure A.9 demonstrates that, when the drift of ESG scores is positively related to ESG demand, the realized return contemporaneous to a positive ESG demand shock is higher than in the base case for both green and brown assets. This reflects the higher valuation of the assets due to their higher expected long-run nonpecuniary benefits induced by a positive

ESG preference shock. However, even when there is a strong dependence of ESG scores on ESG demand, the main model implications for expected and realized returns remain qualitatively unchanged compared to the baseline specification.

6 Conclusion

We study dynamic asset pricing in a general equilibrium framework, specifically examining the role of sustainable investing and its implications for expected and realized returns. Unlike previous studies that mostly concentrated on single-period setups, our approach offers insights into the return dynamics of ESG-sensitive assets.

In our model, the economic agent exhibits ESG perception and derives utility from both consuming goods and holding green assets. Notably, we account for the stochastic and persistent nature of the assets' ESG scores (supply) and the demand for sustainability. Within this equilibrium framework, we identify two incremental risk factors that arise from aggregate ESG demand and supply shocks.

Our analysis reveals that green assets demonstrate positive loadings on both ESG demand and supply shocks, resulting in a higher ESG-related risk premium compared to brown assets. This risk premium is offset by the association of green assets with time-varying positive convenience yield, which exerts downward pressure on expected returns. In addition to these two opposing forces, our findings suggest that positive ESG demand shocks can lead to green assets realizing large contemporaneous unexpected returns, resulting in a positive and substantial green-minus-brown realized return gap over extended investment horizons.

Furthermore, we use filtering techniques to reveal the time variation in the latent state of demand for sustainability. We document a substantial upward trend in ESG demand in recent years. Our research highlights ESG preference shocks as a novel risk source, characterized by a positive premium, while ESG supply shocks play a relatively minor role in comparison. Lastly, we emphasize the nonpecuniary benefits associated with sustainable investing, contributing a significant fraction of total consumption with an increasing trend.

In summary, by exploring dynamic asset pricing in a general equilibrium setting and considering the persistent and stochastic nature of ESG demand and supply shocks, we shed new light on the forces determining green and brown asset returns. The observed time-series trends in ESG demand and their influence on unexpected returns underscore the importance of incorporating ESG considerations when making long-horizon investment decisions. As sustainable investing continues to experience growth, our research supports the integration of multiple ESG risk factors into the financial landscape, thereby contributing to a better understanding of long-term investment opportunities.

We propose several avenues for future research. These include studying long-run asset allocation across characteristic-sorted portfolios with ESG preference shocks. Another area of exploration involves extending the model to account for heterogeneity in ESG preferences and uncertain beliefs about a firm's ESG profile. Future work could also focus on pricing debt instruments with ESG characteristics, such as green bonds (e.g., Flammer, 2021). Exploring the equilibrium in a production-based economy, considering financial costs and incentives of sustainability reforms, and analyzing the endogenous evolution of ESG supply in response to ESG demand is also a valuable research direction. Pursuing these areas of investigation will advance our understanding of sustainable investing and its long-run impact on financial markets.

References

Ait-Sahalia, Y., J. A. Parker, and M. Yogo (2004). Luxury goods and the equity premium. *The Journal of Finance 59*(6), 2959–3004.

Albuquerque, R., M. Eichenbaum, V. X. Luo, and S. Rebelo (2016). Valuation risk and asset pricing. *The Journal of Finance 71*(6), 2861–2904.

Albuquerque, R., Y. Koskinen, and C. Zhang (2019). Corporate social responsibility and firm risk: Theory and empirical evidence. *Management Science 65*(10), 4451–4469.

Ardia, D., K. Bluteau, K. Boudt, and K. Inghelbrecht (2023). Climate change concerns and the performance of green versus brown stocks. *Management Science*. Forthcoming.

Avramov, D., S. Cheng, A. Lioui, and A. Tarelli (2022). Sustainable investing with ESG rating uncertainty. *Journal of Financial Economics 145*(2), 642–664.

Bansal, R. and A. Yaron (2004). Risks for the long run: A potential resolution of asset pricing puzzles. *The Journal of Finance 59*(4), 1481–1509.

Berk, J. and J. H. van Binsbergen (2022). The impact of impact investing. *Available at SSRN 3909166*.

Breeden, D. T. (1979). An intertemporal asset pricing model with stochastic consumption and investment opportunities. *Journal of Financial Economics 7*(3), 265–296.

Campbell, J. Y. and J. H. Cochrane (1999). By force of habit: A consumption-based explanation of aggregate stock market behavior. *Journal of Political Economy 107*(2), 205–251.

Campbell, J. Y. and R. J. Shiller (1988). The dividend-price ratio and expectations of future dividends and discount factors. *The Review of Financial Studies 1*(3), 195–228.

Constantinides, G. M. and A. Ghosh (2011). Asset pricing tests with long-run risks in consumption growth. *The Review of Asset Pricing Studies 1*(1), 96–136.

David, A. and P. Veronesi (2013). What ties return volatilities to price valuations and fundamentals? *Journal of Political Economy 121*(4), 682–746.

De Angelis, T., P. Tankov, and O. D. Zerbib (2022). Climate impact investing. *Management Science*. Forthcoming.

Efron, B. and R. J. Tibshirani (1994). *An introduction to the bootstrap.* CRC Press.

Engle, R. F., S. Giglio, B. Kelly, H. Lee, and J. Stroebel (2020). Hedging climate change news. *The Review of Financial Studies 33*(3), 1184–1216.

Epstein, L. G. and S. E. Zin (1989). Substitution, Risk Aversion, and the Temporal Behavior of Consumption and Asset Returns: A Theoretical Framework. *Econometrica 57*(4), 937–969.

Epstein, L. G. and S. E. Zin (1991). Substitution, risk aversion, and the temporal behavior of consumption and asset returns: An empirical analysis. *Journal of Political Economy 99*(2), 263–286.

Flammer, C. (2021). Corporate green bonds. *Journal of Financial Economics 142*(2), 499–516.

Gomes, J., L. Kogan, and L. Zhang (2003). Equilibrium cross section of returns. *Journal of Political Economy 111*(4), 693–732.

Hamilton, J. D. (1994). *Time series analysis.* Princeton university press, Princeton.

Ilhan, E., Z. Sautner, and G. Vilkov (2021). Carbon tail risk. *The Review of Financial Studies 34*(3), 1540–1571.

Ireland, P. N. (2015). Monetary policy, bond risk premia, and the economy. *Journal of Monetary Economics 76*, 124–140.

Krishnamurthy, A. and A. Vissing-Jorgensen (2012). The aggregate demand for treasury debt. *Journal of Political Economy 120*(2), 233–267.

Lioui, A. and P. Maio (2014). Interest rate risk and the cross section of stock returns. *Journal of Financial and Quantitative Analysis 49*(2), 483–511.

Lucas, R. E. (1978). Asset prices in an exchange economy. *Econometrica*, 1429–1445.

Pástor, L., R. F. Stambaugh, and L. A. Taylor (2021). Sustainable investing in equilibrium. *Journal of Financial Economics 142*(2), 550–571.

Pástor, L., R. F. Stambaugh, and L. A. Taylor (2022). Dissecting green returns. *Journal of Financial Economics 146*(2), 403–424.

Pedersen, L. H., S. Fitzgibbons, and L. Pomorski (2021). Responsible investing: The ESG-efficient frontier. *Journal of Financial Economics 142*(2), 572–597.

Piazzesi, M., M. Schneider, and S. Tuzel (2007). Housing, consumption and asset pricing. *Journal of Financial Economics 83*(3), 531–569.

Schorfheide, F., D. Song, and A. Yaron (2018). Identifying long-run risks: A Bayesian mixed-frequency approach. *Econometrica 86*(2), 617–654.

Van Binsbergen, J. H., J. Fernández-Villaverde, R. S. Koijen, and J. Rubio-Ramírez (2012). The term structure of interest rates in a DSGE model with recursive preferences. *Journal of Monetary Economics 59*(7), 634–648.

Yogo, M. (2006). A consumption-based explanation of expected stock returns. *The Journal of Finance 61*(2), 539–580.

Figure 1: Trend in press attention to sustainable investing.

The figure shows the number of Factiva newspaper articles in English language on "sustainable/socially responsible/ethical/ESG" "investing/investment", relative to the total number of news on "investing/investment".

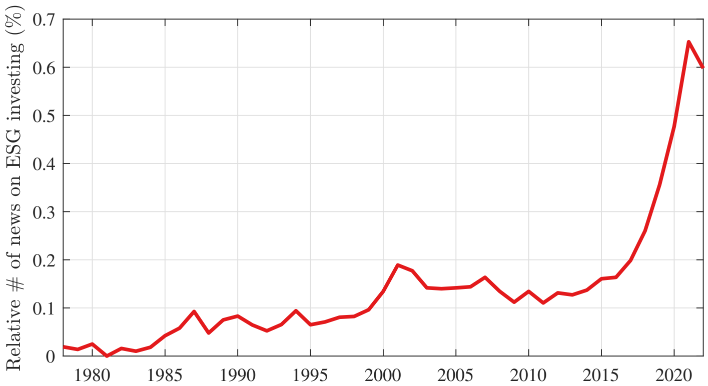

Figure 2: Time series of aggregate demand and supply for ESG and environmental attributes.

The figure shows the estimated time series of aggregate ESG demand, δ_t, and supply, $G_{W,t}$. The portfolios used for the estimation are obtained by value-weighting stocks sorted by their ESG scores in Panel (a) and environmental scores in Panel (b). The sample runs from January 2007 to December 2022.

(a) Estimation based on ESG scores

(b) Estimation based on environmental scores

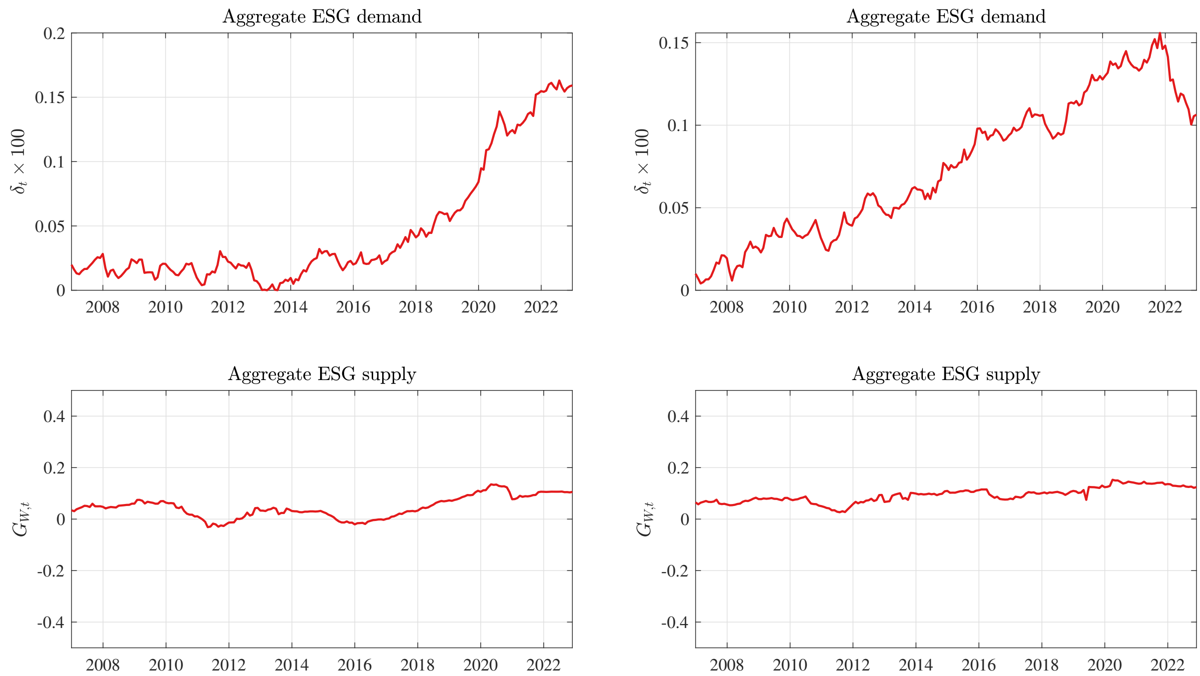

Figure 3: Time series of expected consumption growth, ESG scores, expected excess returns, and price-to-dividend ratios.

The figure shows the estimated time series of expected consumption growth, ESG scores, expected market and portfolio excess returns, convenience yields from ESG investing, total ESG premia, as well as price-to-annual dividend ratios. All quantities are annualized. The green, neutral, and brown portfolios are obtained sorting stocks by ESG score. The estimation is performed by maximum likelihood, observing the time series of market and portfolio returns, ESG scores, and consumption growth, as well as average price-to-dividend ratios. The sample runs from January 2007 to December 2022.

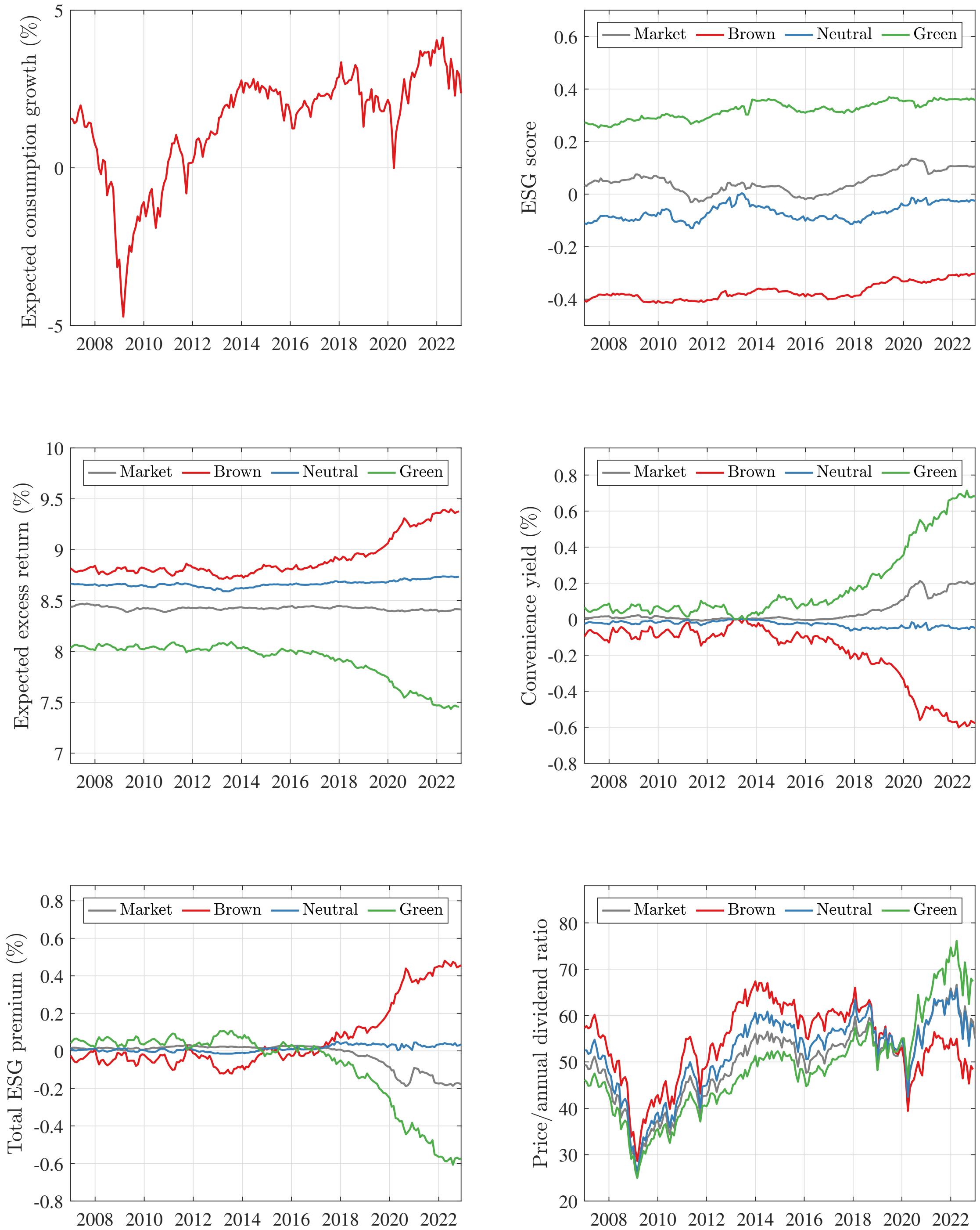

Figure 4: Returns of green-minus-brown portfolio.

The left graphs show the realized cumulative logarithmic return of the green-minus-brown portfolio, as well as the model-implied expected return, the unexpected return contribution attributable to ESG demand shocks, and the model-implied expected return augmented by the unexpected return contribution attributable to ESG demand shocks. The right graphs show the 12-month rolling logarithmic return of the same portfolio. The portfolios are obtained by value-weighting stocks sorted by their ESG scores in Panel (a) and environmental scores in Panel (b). The estimation is performed by maximum likelihood, observing the time series of market and portfolio returns, ESG or environmental ratings, and consumption growth, as well as average price-to-dividend ratios. The sample runs from January 2007 to December 2022.

(a) Green and brown portfolios based on ESG-scores

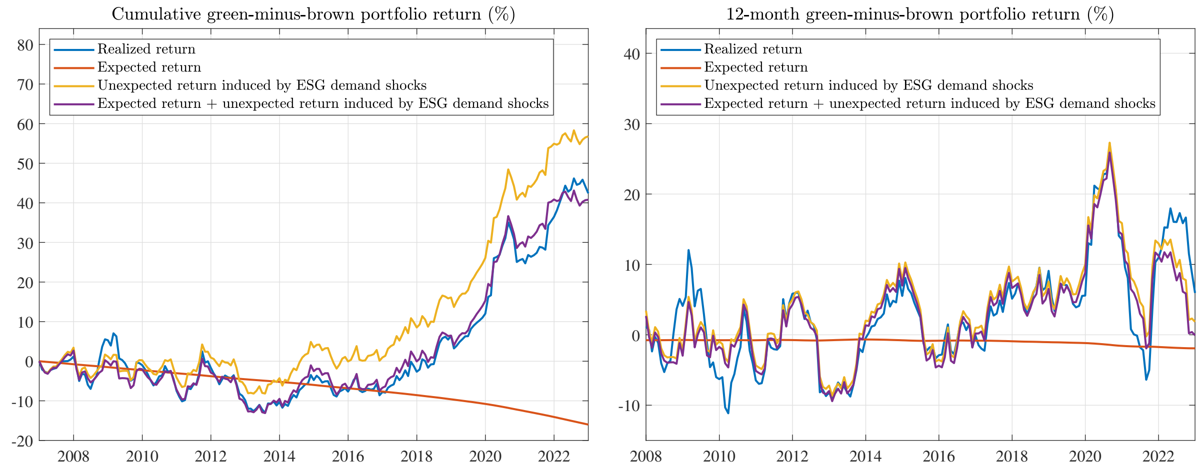

(b) Green and brown portfolios based on environmental scores

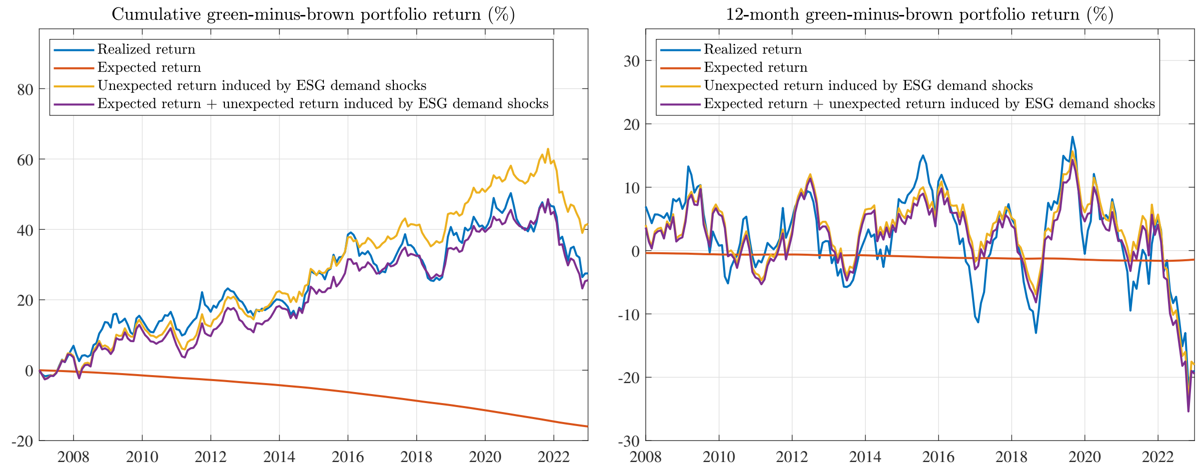

Figure 5: Response to annual one-standard deviation shock to aggregate ESG demand and supply.

The graphs on the left show responses to a one-standard deviation positive annual shock applied to δ_t. The graphs on the right show responses to a $+0.1$ annual shock to aggregate greenness. The expected and realized excess returns of the brown and green portfolios, the cumulative return of the green-minus-brown portfolio, and the price-to-annual dividend ratios of the brown and green portfolios are shown. The state variables are initially set at their average values and the shocks are equally distributed throughout 12 consecutive months.

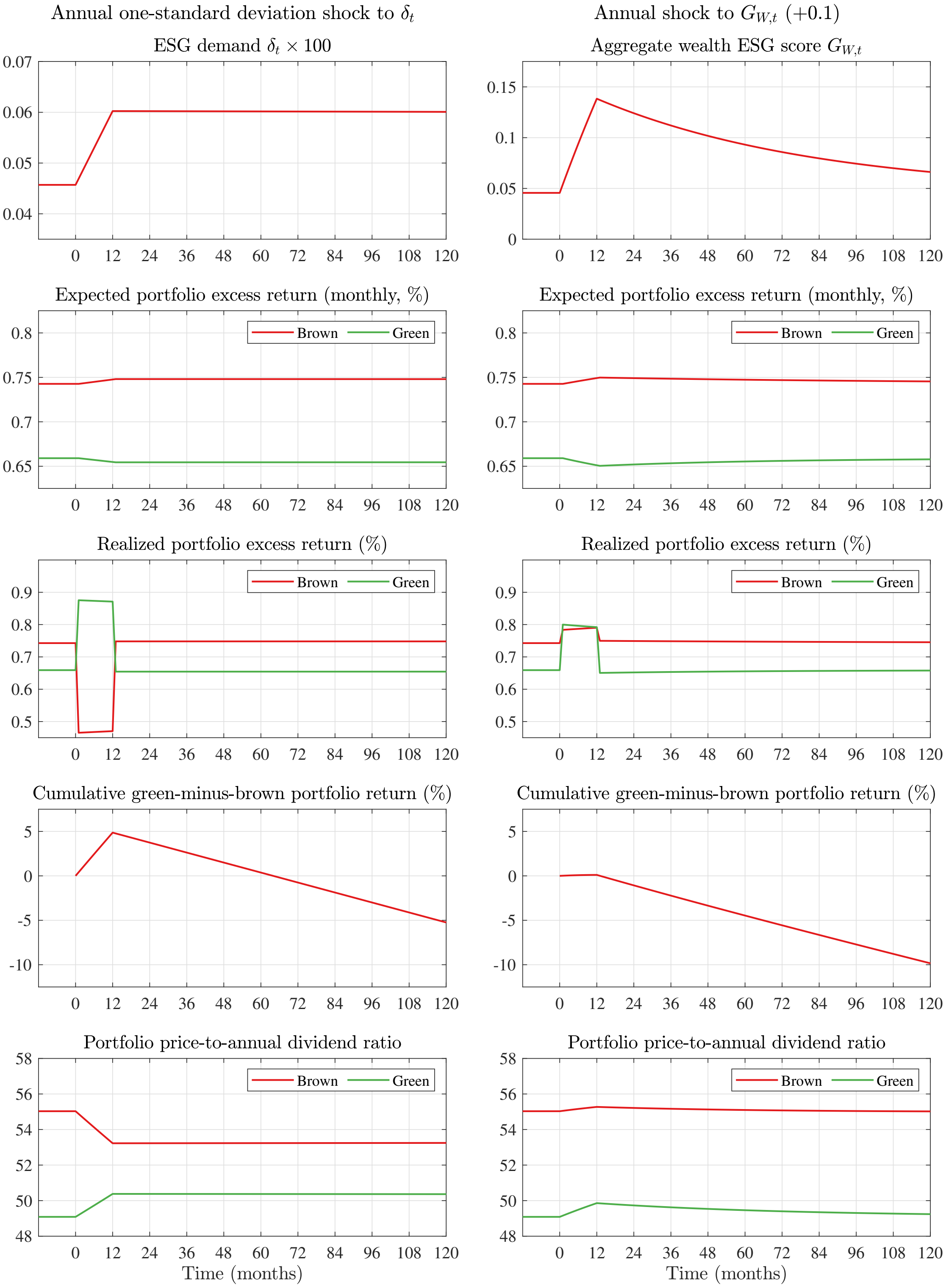

Table 1: Parameter estimates.

The table reports the estimated parameters for the baseline model specification. The subjective discount rate β is set at 0.998, the intertemporal elasticity of substitution ψ at 1.5, the long-run risk persistence ρ_x at 0.979, its volatility σ_x at 0.00034, and the persistence of ESG demand ρ_δ at 0.9999. The brown, neutral, and green portfolios are obtained by value-weighting stocks sorted by their ESG scores in Panel (a) and environmental scores in Panel (b). The estimation procedure is described in Section 4.1. The sample runs from January 2007 to December 2022.

(a) Estimation based on ESG scores

Economy-wide parameters (Θ_E) and market prices of risk

γ	μ_c	σ_c	x_0	μ_G	ρ_G	σ_G	δ_0	$\bar{\delta}$	σ_δ
13.11425	0.00142	0.01213	-0.00011	0.00063	0.98615	0.00993	0.00020	0.00046	0.00004
(3.21318)	(0.00133)	(0.00061)	(0.00372)	(0.00041)	(0.00898)	(0.00050)	(0.00014)	(0.00015)	(0.00000)
λ_c	λ_G	λ_δ	λ_x						
0.15902	0.00487	0.01072	0.18367						
(0.04053)	(0.00170)	(0.00277)	(0.04511)						

Market portfolio parameters (Θ_M)

μ_{dM}	$\rho_{dM,x}$	$\sigma_{dM,c}$	σ_{dM}
0.00629	3.54756	0.00032	0.01413
(0.00163)	(0.62219)	(0.00344)	(0.01143)

Brown portfolio parameters (Θ_{br})

μ_{dbr}	$\rho_{dbr,x}$	$\sigma_{dbr,c}$	$\sigma_{dbr,dM}$	σ_{dbr}	μ_{Gbr}	ρ_{Gbr}	σ_{GbrG}	σ_{Gbr}
0.00683	3.63920	0.00235	0.02306	0.00005	-0.00325	0.99124	-0.01618	0.01543
(0.00212)	(0.75289)	(0.00390)	(0.01618)	(0.00166)	(0.00373)	(0.01006)	(0.00139)	(0.00077)

Neutral portfolio parameters (Θ_{neu})

μ_{dneu}	$\rho_{dneu,x}$	$\sigma_{dneu,c}$	$\sigma_{dneu,dM}$	σ_{dneu}	μ_{Gneu}	ρ_{Gneu}	σ_{GneuG}	σ_{Gneu}
0.00656	3.71070	-0.00127	0.00658	0.00290	-0.00196	0.97152	0.00115	0.00863
(0.00139)	(0.60155)	(0.00354)	(0.01101)	(0.00116)	(0.00138)	(0.01999)	(0.00062)	(0.00044)

Green portfolio parameters (Θ_{gr})

μ_{dgr}	$\rho_{dgr,x}$	$\sigma_{dgr,c}$	$\sigma_{dgr,dM}$	σ_{dgr}	μ_{Ggr}	ρ_{Ggr}	σ_{GgrG}	σ_{Ggr}
0.00581	3.37996	0.00078	0.01692	0.00000	0.00566	0.98229	0.02059	0.01668
(0.00175)	(0.62662)	(0.00333)	(0.01239)	(0.00064)	(0.00348)	(0.01090)	(0.00161)	(0.00080)

(b) Estimation based on environmental scores

Economy-wide parameters (Θ_E) and market prices of risk

γ	μ_c	σ_c	x_0	μ_G	ρ_G	σ_G	δ_0	$\bar{\delta}$	σ_δ
11.90782	0.00126	0.01210	0.00060	0.00482	0.94828	0.01171	0.00010	0.00074	0.00004
(2.14109)	(0.00131)	(0.00061)	(0.00361)	(0.00143)	(0.01539)	(0.00059)	(0.00017)	(0.00020)	(0.00000)
λ_c	λ_G	λ_δ	λ_x						
0.14406	0.00447	0.01966	0.16618						
(0.02711)	(0.00150)	(0.00557)	(0.03100)						

Market portfolio parameters (Θ_M)

μ_{dM}	$\rho_{dM,x}$	$\sigma_{dM,c}$	σ_{dM}
0.00591	3.67321	0.00045	0.00360
(0.00130)	(0.44889)	(0.00351)	(0.01000)

Brown portfolio parameters (Θ_{br})

μ_{dbr}	$\rho_{dbr,x}$	$\sigma_{dbr,c}$	$\sigma_{dbr,dM}$	σ_{dbr}	μ_{Gbr}	ρ_{Gbr}	σ_{GbrG}	σ_{Gbr}
0.00635	3.83717	0.00021	0.01347	0.00243	-0.04111	0.88881	-0.01880	0.01983
(0.00159)	(0.54060)	(0.00390)	(0.01568)	(0.00140)	(0.01032)	(0.02790)	(0.00173)	(0.00098)

Neutral portfolio parameters (Θ_{neu})

μ_{dneu}	$\rho_{dneu,x}$	$\sigma_{dneu,c}$	$\sigma_{dneu,dM}$	σ_{dneu}	μ_{Gneu}	ρ_{Gneu}	σ_{GneuG}	σ_{Gneu}
0.00645	3.85533	0.00082	-0.00186	0.00002	-0.00747	0.88316	-0.00010	0.01124
(0.00131)	(0.48365)	(0.00373)	(0.01061)	(0.00061)	(0.00225)	(0.03513)	(0.00080)	(0.00057)

Green portfolio parameters (Θ_{gr})

μ_{dgr}	$\rho_{dgr,x}$	$\sigma_{dgr,c}$	$\sigma_{dgr,dM}$	σ_{dgr}	μ_{Ggr}	ρ_{Ggr}	σ_{GgrG}	σ_{Ggr}
0.00537	3.46500	0.00012	0.00488	0.00127	0.03025	0.91331	0.02521	0.01528
(0.00132)	(0.42140)	(0.00332)	(0.00975)	(0.00032)	(0.00772)	(0.02213)	(0.00170)	(0.00073)

Table 2: Decomposition of model-implied excess returns and average observed excess returns.

The table reports the observed and model-implied annualized excess returns, as well as the decomposition of model-implied excess returns. The brown, neutral, and green portfolios are obtained by value-weighting stocks sorted by their ESG scores in Panel (a) and environmental scores in Panel (b). The estimation procedure is described in Section 4.1. The sample runs from January 2007 to December 2022.

(a) Estimation based on ESG scores

Portfolio	Market	Brown	Neutral	Green	Green-brown
Model-implied short-run consumption risk premium	0.06%	0.45%	-0.24%	0.15%	-0.30%
	(0.71%)	(0.78%)	(0.77%)	(0.67%)	(0.27%)
Model-implied long-run consumption risk premium	9.63%	9.99%	10.21%	9.05%	-0.94%
	(2.03%)	(2.52%)	(2.00%)	(2.06%)	(0.58%)
Model-implied ESG supply risk premium	0.01%	0.00%	0.01%	0.01%	0.01%
	(0.01%)	(0.01%)	(0.01%)	(0.01%)	(0.00%)
Model-implied ESG demand risk premium	0.01%	-0.12%	-0.02%	0.10%	0.22%
	(0.00%)	(0.03%)	(0.01%)	(0.02%)	(0.06%)
Average model-implied convenience yield premium	-0.04%	0.19%	0.03%	-0.18%	-0.37%
	(0.01%)	(0.07%)	(0.01%)	(0.06%)	(0.13%)
Average model-implied expected excess return	8.40%	8.89%	8.65%	7.90%	-1.00%
	(1.93%)	(2.43%)	(1.79%)	(2.03%)	(0.62%)
Average ESG demand shock-induced return (δ-induced return)	0.21%	-2.01%	-0.38%	1.52%	3.53%
	(0.03%)	(0.19%)	(0.03%)	(0.15%)	(0.33%)
Average model-implied expected excess return + δ-induced return	8.61%	6.88%	8.27%	9.42%	2.54%
	(1.92%)	(2.45%)	(1.79%)	(1.98%)	(0.59%)
Average observed excess return	7.92%	5.96%	7.63%	8.61%	2.65%

(b) Estimation based on environmental scores

Portfolio	Market	Brown	Neutral	Green	Green-brown
Model-implied short-run consumption risk premium	0.08%	0.04%	0.14%	0.02%	-0.02%
	(0.69%)	(0.77%)	(0.73%)	(0.65%)	(0.30%)
Model-implied long-run consumption risk premium	9.10%	9.66%	9.69%	8.48%	-1.19%
	(1.41%)	(1.88%)	(1.46%)	(1.35%)	(0.78%)
Model-implied ESG supply risk premium	0.01%	0.01%	0.01%	0.01%	0.00%
	(0.01%)	(0.01%)	(0.01%)	(0.02%)	(0.00%)
Model-implied ESG demand risk premium	0.05%	-0.22%	-0.03%	0.19%	0.41%
	(0.02%)	(0.06%)	(0.01%)	(0.05%)	(0.12%)
Average model-implied convenience yield premium	-0.10%	0.33%	0.05%	-0.33%	-0.66%
	(0.02%)	(0.09%)	(0.01%)	(0.08%)	(0.17%)
Average model-implied expected excess return	7.89%	8.25%	8.44%	7.23%	-1.02%
	(1.27%)	(1.69%)	(1.30%)	(1.27%)	(0.83%)
Average ESG demand shock-induced return (δ-induced return)	0.30%	-1.42%	-0.26%	1.19%	2.61%
	(0.06%)	(0.21%)	(0.03%)	(0.19%)	(0.40%)
Average model-implied expected excess return + δ-induced return	8.19%	6.83%	8.18%	8.42%	1.59%
	(1.25%)	(1.72%)	(1.30%)	(1.20%)	(0.81%)
Average observed excess return	7.92%	6.72%	7.94%	8.44%	1.72%

Online Appendix to
“Dynamic ESG Equilibrium”

Doron Avramov   Abraham Lioui   Yang Liu   Andrea Tarelli

This Online Appendix presents the proofs and derivations, the summary statistics of the data, the estimation methodology, as well as the supplementary estimation and calibration material discussed in the paper.

Table of contents

A Derivations

A.1 Proof of Proposition 1 (Euler equation)

The optimization program is formulated as

$$U_t = \max_{C_t, \boldsymbol{\omega}_t} \left((1-\beta)\, \varphi_t A_t^{1-\frac{1}{\psi}} + \beta \mathrm{E}_t \left[U_{t+1}^{1-\gamma} \right]^{\frac{1}{\theta}} \right)^{\frac{1}{1-\frac{1}{\psi}}}, \tag{A.1}$$

$$A_t = \left(C_t^{1-\frac{1}{\phi}} + \delta_t S_t^{1-\frac{1}{\phi}} \right)^{\frac{1}{1-\frac{1}{\phi}}} = C_t \left(1 + \delta_t \left(\frac{S_t}{C_t} \right)^{1-\frac{1}{\phi}} \right)^{\frac{1}{1-\frac{1}{\phi}}}, \tag{A.2}$$

$$S_t = G_{W,t} \left(W_t - C_t \right), \tag{A.3}$$

where $G_{W,t}=\sum_{n=1}^{N}\omega_{n,t}G_{n,t}$ is the aggregate greenness (ESG supply), φ_t is a variable reflecting shocks to the time rate of preference (Albuquerque et al., 2016, Schorfheide et al., 2018), and δ_t represents time-varying preferences for ESG (demand). Note that, in the most general case where ϕ can be finite, the aggregate ESG supply must be nonnegative. In the main text, we develop the analysis considering additive preferences, i.e., $\phi \to +\infty$, in which case $G_{W,t}$ can take any value. The budget constraint states that $W_{t+1}=(W_t-C_t)\,R_{W,t+1}$, where $R_{W,t+1}=R_{f,t+1}+\sum_{n=1}^{N}\omega_{n,t}\,(R_{n,t+1}-R_{f,t+1})$. At the optimum, the value function depends on wealth only, that is $U_t=J\,(W_t)$. The agent then optimizes

$$J\,(W_t)=\max_{C_t,\boldsymbol{\omega}_t}\left((1-\beta)\,\varphi_t A_t^{1-\frac{1}{\psi}}+\beta \mathrm{E}_t\left[J\,(W_{t+1})^{1-\gamma}\right]^{\frac{1}{\theta}}\right)^{\frac{1}{1-\frac{1}{\psi}}}. \tag{A.4}$$

The first order condition with respect to consumption is given by

$$0=(1-\beta)\,\varphi_t A_t^{-\frac{1}{\psi}}\frac{\partial A_t}{\partial C_t}-\beta \mathrm{E}_t\left[J\,(W_{t+1})^{1-\gamma}\right]^{\frac{1}{\theta}-1}\mathrm{E}_t\left[J\,(W_{t+1})^{-\gamma}\frac{\partial J\,(W_{t+1})}{\partial W_{t+1}}R_{W,t+1}\right], \tag{A.5}$$

where $\frac{\partial A_t}{\partial C_t}=\left(\frac{A_t}{C_t}\right)^{\frac{1}{\phi}}-\left(\frac{A_t}{S_t}\right)^{\frac{1}{\phi}}\delta_t G_{W,t}$ and $\lim\limits_{\phi\to+\infty}\frac{\partial A_t}{\partial C_t}=1-\delta_t G_{W,t}$. Next, the first order condition with respect to $\omega_{n,t}$ is given by

$$\begin{aligned}0=&\beta \mathrm{E}_t\left[J\,(W_{t+1})^{1-\gamma}\right]^{\frac{1}{\theta}-1}\mathrm{E}_t\left[J\,(W_{t+1})^{-\gamma}\frac{\partial J\,(W_{t+1})}{\partial W_{t+1}}\,(R_{n,t+1}-R_{f,t+1})\right]\\&+(1-\beta)\,\varphi_t A_t^{-\frac{1}{\psi}}\frac{\partial A_t}{\partial S_t}G_{n,t}.\end{aligned} \tag{A.6}$$

As $\frac{\partial A_t}{\partial S_t}=\left(\frac{A_t}{S_t}\right)^{\frac{1}{\phi}}\delta_t$ and $\lim\limits_{\phi\to+\infty}\frac{\partial A_t}{\partial S_t}=\delta_t$, multiplying (A.6) by $\omega_{n,t}$ and summing across assets yields

$$\begin{aligned}0=&\beta \mathrm{E}_t\left[J\,(W_{t+1})^{1-\gamma}\right]^{\frac{1}{\theta}-1}\mathrm{E}_t\left[J\,(W_{t+1})^{-\gamma}\frac{\partial J\,(W_{t+1})}{\partial W_{t+1}}R_{W,t+1}\right]\\&-\beta \mathrm{E}_t\left[J\,(W_{t+1})^{1-\gamma}\right]^{\frac{1}{\theta}-1}\mathrm{E}_t\left[J\,(W_{t+1})^{-\gamma}\frac{\partial J\,(W_{t+1})}{\partial W_{t+1}}R_{f,t+1}\right]\\&+(1-\beta)\,\varphi_t A_t^{-\frac{1}{\psi}}\frac{\partial A_t}{\partial S_t}G_{W,t}.\end{aligned} \tag{A.7}$$

Noting that

$$\frac{\partial A_t}{\partial C_t}+\frac{\partial A_t}{\partial S_t}G_{W,t}=\left(1+\delta_t\left(\frac{S_t}{C_t}\right)^{1-\frac{1}{\phi}}\right)^{\frac{1}{\phi-1}}=\left(\frac{A_t}{C_t}\right)^{\frac{1}{\phi}}, \tag{A.8}$$

which tends to one for $\phi\to+\infty$, and combining (A.5) and (A.7), we obtain

$$\mathrm{E}_t\left[M_{t+1}R_{f,t+1}\right]=1. \tag{A.9}$$

This is the Euler equation for the risk-free gross return, where the stochastic discount factor

(SDF) is formulated as

$$M_{t+1}=\beta\frac{\mathrm{E}_t\left[J\left(W_{t+1}\right)^{1-\gamma}\right]^{\frac{1}{\theta}-1}J\left(W_{t+1}\right)^{-\gamma}\frac{\partial J(W_{t+1})}{\partial W_{t+1}}}{\left(1-\beta\right)\varphi_t A_t^{-\frac{1}{\psi}}\left(\frac{A_t}{C_t}\right)^{\frac{1}{\phi}}}. \tag{A.10}$$

From (A.6), we can express the Euler equation for excess return on a generic asset as

$$\mathrm{E}_t\left[M_{t+1}\left(R_{n,t+1}-R_{f,t+1}\right)\right]=-\left(\frac{S_t}{C_t}\right)^{-\frac{1}{\phi}}\delta_t G_{n,t}. \tag{A.11}$$

Note that, for $\phi\to+\infty$, the Euler equation becomes $\mathrm{E}_t\left[M_{t+1}\left(R_{n,t+1}-R_{f,t+1}\right)\right]=-\delta_t G_{n,t}$, hence, $\mathrm{E}_t\left[R_{n,t+1}-R_{f,t+1}\right]=-\frac{\mathrm{Cov}_t\left[R_{n,t+1}-R_{f,t+1},M_{t+1}\right]}{\mathrm{E}_t[M_{t+1}]}-\frac{\delta_t G_{n,t}}{\mathrm{E}_t[M_{t+1}]}$. Summing (A.9) and (A.11), we obtain the Euler equation for the gross return on a generic asset:

$$\mathrm{E}_t\left[M_{t+1}R_{n,t+1}\right]=1-\left(\frac{S_t}{C_t}\right)^{-\frac{1}{\phi}}\delta_t G_{n,t}. \tag{A.12}$$

We next derive an explicit solution for the value function. To start, we guess $J\left(W_t\right)=\Phi_t W_t$. Then, equations (A.4) and (A.5) can be expressed as

$$\beta\mathrm{E}_t\left[\Phi_{t+1}^{1-\gamma}W_{t+1}^{1-\gamma}\right]^{\frac{1}{\theta}}=\Phi_t^{1-\frac{1}{\psi}}W_t^{1-\frac{1}{\psi}}-\left(1-\beta\right)\varphi_t A_t^{1-\frac{1}{\psi}} \tag{A.13}$$

and

$$0=\left(1-\beta\right)\varphi_t A_t^{-\frac{1}{\psi}}\frac{\partial A_t}{\partial C_t}\left(W_t-C_t\right)-\beta\mathrm{E}_t\left[\Phi_{t+1}^{1-\gamma}W_{t+1}^{1-\gamma}\right]^{\frac{1}{\theta}}, \tag{A.14}$$

respectively. Combining both equations yields

$$\Phi_t=\left(1-\beta\right)^{\frac{1}{1-\frac{1}{\psi}}}\varphi_t^{\frac{1}{1-\frac{1}{\psi}}}\left(\frac{A_t}{C_t}\right)^{\frac{1}{\phi}\frac{1}{1-\frac{1}{\psi}}}\left(\frac{W_t}{A_t}\right)^{\frac{\frac{1}{\psi}}{1-\frac{1}{\psi}}}. \tag{A.15}$$

Then, M_{t+1} in (A.10) can be developed as

$$M_{t+1}=\beta^{\theta}\left(\frac{\varphi_{t+1}}{\varphi_t}\right)^{\theta}\left(\frac{A_{t+1}}{A_t}\right)^{-\frac{\theta}{\psi}}\left(\frac{\frac{C_{t+1}}{A_{t+1}}}{\frac{C_t}{A_t}}\right)^{-\frac{\theta}{\phi}}\left(\frac{R_{W,t+1}}{1-\left(\frac{S_t}{C_t}\right)^{-\frac{1}{\phi}}\delta_t G_{W,t}}\right)^{\theta-1}, \tag{A.16}$$

where $R_{W,t+1}=\frac{W_{t+1}}{W_t-C_t}$. Defining $\tilde{R}_{W,t+1}=\frac{R_{W,t+1}}{1-\left(\frac{S_t}{C_t}\right)^{-\frac{1}{\phi}}\delta_t G_{W,t}}$ and $\tilde{R}_{n,t+1}=\frac{R_{n,t+1}}{1-\left(\frac{S_t}{C_t}\right)^{-\frac{1}{\phi}}\delta_t G_{n,t}}$, the Euler equation in (A.12) can be equivalently expressed as

$$\mathrm{E}_t\left[M_{t+1}\tilde{R}_{n,t+1}\right]=1, \tag{A.17}$$

where

$$M_{t+1}=\beta^{\theta}\left(\frac{\varphi_{t+1}}{\varphi_t}\right)^{\theta}\left(\frac{A_{t+1}}{A_t}\right)^{-\frac{\theta}{\psi}}\left(\frac{\frac{C_{t+1}}{A_{t+1}}}{\frac{C_t}{A_t}}\right)^{-\frac{\theta}{\phi}}\tilde{R}_{W,t+1}^{\theta-1}. \tag{A.18}$$

Before considering the simplified case discussed in the text, where the time-preference shock φ_t is muted and ϕ approaches infinity, we briefly comment on the incremental contribution of the extended version.

Similar to Albuquerque et al. (2016), the growth in time preference $\frac{\varphi_{t+1}}{\varphi_t}$ establishes an additional multiplicative factor to the SDF in equation (5). That is, allowing time-preference shocks helps matching the market premium by considering a positive *valuation premium* of the market portfolio due to time-varying demand for consumption. It also improves the model ability to generate an upward-sloping term structure of interest rates.

The implications of a finite elasticity of substitution ϕ are twofold. First, as implied by the term $(S_t/C_t)^{-\frac{1}{\phi}}$ in equation (A.12), which diminishes in S_t, the convenience yield of any asset, green or brown, is attenuated when aggregate ESG supply grows larger relative to physical consumption. Second, the factor $\left(\frac{C_{t+1}/A_{t+1}}{C_t/A_t}\right)^{-\frac{\theta}{\phi}}$ appears in the SDF (A.16). To analyze its contribution, consider the case where preferences are time additive ($\theta = 1$), so that the factor depending on the return on wealth can be excluded. The SDF then increases when the share of physical consumption C_t relative to the consumption bundle A_t diminishes. As physical consumption and sustainability are not perfect substitutes, the agent favors assets that deliver higher returns in times when physical consumption is low relative to the value of the consumption bundle. Such assets would deliver lower expected returns in equilibrium. Both the effects described above become more prominent when the elasticity of substitution diminishes.

In what follows, we assume $\varphi_t = 1$ and $\phi \to +\infty$. The Euler equation (A.12) and the corresponding SDF in (A.16) can be expressed as

$$\mathrm{E}_t\left[M_{t+1}\tilde{R}_{n,t+1}\right] = 1, \tag{A.19}$$

$$M_{t+1} = \beta^{\theta}\left(\frac{A_{t+1}}{A_t}\right)^{-\frac{\theta}{\psi}}\tilde{R}_{W,t+1}^{\theta-1}, \tag{A.20}$$

where $\tilde{R}_{W,t+1} = \frac{R_{W,t+1}}{1-\delta_t G_{W,t}}$ and $\tilde{R}_{n,t+1} = \frac{R_{n,t+1}}{1-\delta_t G_{n,t}}$ are the ESG-adjusted gross returns on the consumption asset and on a generic asset, respectively. The Euler equation undertakes the standard form only when the financial return is replaced by the ESG-adjusted return.

We then calculate the logarithm of the SDF, $m_{t+1} = \log M_{t+1}$:

$$\begin{aligned} m_{t+1} = {} & \theta\log\beta - \frac{\theta}{\psi}\Delta c_{t+1} + (\theta-1)\left(r_{W,t+1} - \log\left(1-\delta_t G_{W,t}\right)\right) \\ & - \frac{\theta}{\psi}\log\left(\frac{1+\delta_{t+1}\frac{W_{t+1}-C_{t+1}}{C_{t+1}}G_{W,t+1}}{1+\delta_t\frac{W_t-C_t}{C_t}G_{W,t}}\right), \end{aligned} \tag{A.21}$$

where $\Delta c_{t+1} = \log\frac{C_{t+1}}{C_t}$ and $r_{W,t+1} = \log\frac{W_{t+1}}{W_t-C_t}$ is the logarithmic return on financial wealth. The expected excess return of a generic asset then satisfies the following relation

$$\mathrm{E}_t\left[r_{n,t+1} - r_{f,t+1}\right] + \frac{1}{2}\mathrm{Var}_t\left[r_{n,t+1}\right] = -\mathrm{Cov}_t\left[m_{t+1}, r_{n,t+1}\right] - y_{n,t}, \tag{A.22}$$

where $r_{n,t+1} = \log R_{n,t+1}$, $r_{f,t+1} = \log R_{f,t+1}$, and $y_{n,t} = -\log\left(1-\delta_t G_{n,t}\right)$.

Finally, we aim to determine the concavity of the value function with respect to $G_{W,t}$ and

δ_t. We start evaluating the first derivatives:

$$\begin{aligned}
\frac{\partial J(W_t)}{\partial G_{W,t}} &= (1-\beta)\left((1-\beta)A_t^{1-\frac{1}{\psi}} + \beta \mathrm{E}_t\left[U_{t+1}^{1-\gamma}\right]^{\frac{1}{\theta}}\right)^{\frac{1}{1-\frac{1}{\psi}}-1} A_t^{-\frac{1}{\psi}}\delta_t(W_t - C_t) \\
&= (1-\beta)J(W_t)^{\frac{1}{\psi}} A_t^{-\frac{1}{\psi}}\delta_t(W_t - C_t), \qquad \text{(A.23)} \\
\frac{\partial J(W_t)}{\partial \delta_t} &= (1-\beta)\left((1-\beta)A_t^{1-\frac{1}{\psi}} + \beta \mathrm{E}_t\left[U_{t+1}^{1-\gamma}\right]^{\frac{1}{\theta}}\right)^{\frac{1}{1-\frac{1}{\psi}}-1} A_t^{-\frac{1}{\psi}} G_{W,t}(W_t - C_t) \\
&= (1-\beta)J(W_t)^{\frac{1}{\psi}} A_t^{-\frac{1}{\psi}} G_{W,t}(W_t - C_t), \qquad \text{(A.24)}
\end{aligned}$$

which, respectively, are positive for $\delta_t > 0$ and $G_{W,t} > 0$.

The second derivatives are

$$\begin{aligned}
\frac{\partial^2 J(W_t)}{\partial G_{W,t}^2} &= -\frac{1}{\psi}(1-\beta)J(W_t)^{\frac{1}{\psi}} A_t^{-\frac{1}{\psi}-1}\delta_t^2(W_t - C_t)^2 \\
&\quad \cdot \frac{\beta \mathrm{E}_t\left[J(W_{t+1})^{1-\gamma}\right]^{\frac{1}{\theta}}}{(1-\beta)A_t^{1-\frac{1}{\psi}} + \beta \mathrm{E}_t\left[J(W_{t+1})^{1-\gamma}\right]^{\frac{1}{\theta}}} < 0, \qquad \text{(A.25)} \\
\frac{\partial^2 J(W_t)}{\partial \delta_t^2} &= -\frac{1}{\psi}(1-\beta)J(W_t)^{\frac{1}{\psi}} A_t^{-\frac{1}{\psi}-1} G_{W,t}^2(W_t - C_t)^2 \\
&\quad \cdot \frac{\beta \mathrm{E}_t\left[J(W_{t+1})^{1-\gamma}\right]^{\frac{1}{\theta}}}{(1-\beta)A_t^{1-\frac{1}{\psi}} + \beta \mathrm{E}_t\left[J(W_{t+1})^{1-\gamma}\right]^{\frac{1}{\theta}}} < 0, \qquad \text{(A.26)}
\end{aligned}$$

which are both negative. The value function is thus concave in both $G_{W,t}$ and δ_t.

A.2 Proof of Proposition 2 (stochastic discount factor)

The time-t investable wealth is $P_t = W_t - C_t$, i.e., wealth after consumption, and is conventionally called *price* of the consumption asset (wealth portfolio). The return on wealth between time t and time $t+1$ is:

$$\begin{aligned}
r_{W,t+1} &= \log\left(\frac{W_{t+1}}{W_t - C_t}\right) = \log\left(\frac{P_{t+1} + C_{t+1}}{P_t}\right) = \log\left(\frac{\frac{P_{t+1}}{C_{t+1}} + 1}{\frac{P_t}{C_t}}\frac{C_{t+1}}{C_t}\right) \\
&= \log\left(1 + e^{pc_{t+1}}\right) - pc_t + \Delta c_{t+1}, \qquad \text{(A.27)}
\end{aligned}$$

where $pc_t = \log \frac{P_t}{C_t}$ is the log price/consumption ratio. We perform the Campbell and Shiller (1988) log-linearization by developing the first-order Taylor expansion of the first term around the average model-implied log price-to-consumption ratio $\overline{pc}$:

$$\begin{aligned}
\log\left(1 + e^{pc_{t+1}}\right) &\simeq \log\left(1 + e^{pc_{t+1}}\right)\Big|_{\overline{pc}} + \frac{\mathrm{d}}{\mathrm{d}pc_{t+1}}\log\left(1 + e^{pc_{t+1}}\right)\Big|_{\overline{pc}}\left(pc_{t+1} - \overline{pc}\right) \\
&= \log\left(1 + e^{\overline{pc}}\right) + \frac{e^{\overline{pc}}}{1 + e^{\overline{pc}}}\left(pc_{t+1} - \overline{pc}\right). \qquad \text{(A.28)}
\end{aligned}$$

Then,

$$r_{W,t+1} \simeq \kappa_{rW,0} + \kappa_{rW,pc} pc_{t+1} - pc_t + \Delta c_{t+1}, \tag{A.29}$$

where $\kappa_{rW,pc} = \frac{e^{\overline{pc}}}{1+e^{\overline{pc}}}$, $\kappa_{rW,0} = \log\left(1 + e^{\overline{pc}}\right) - \kappa_{rW,pc}\overline{pc}$, with $\overline{pc}$ being determined as the solution of a fixed-point problem. Following the same logic, we perform two additional approximations. The first is given by

$$\begin{aligned}\log\left(1 + e^{pc_t}\delta_t G_{W,t}\right) &\simeq \log\left(1 + e^{\overline{pc}}\bar{\delta}\bar{G}_W\right) + \frac{e^{\overline{pc}}\bar{G}_W}{1 + e^{\overline{pc}}\bar{\delta}\bar{G}_W}\left(\delta_t - \bar{\delta}\right) \\ &\quad + \frac{e^{\overline{pc}}\bar{\delta}}{1 + e^{\overline{pc}}\bar{\delta}\bar{G}_W}\left(G_{W,t} - \bar{G}_W\right) + \frac{e^{\overline{pc}}\bar{\delta}\bar{G}_W}{1 + e^{\overline{pc}}\bar{\delta}\bar{G}_W}\left(pc_t - \overline{pc}\right) \\ &= \kappa_{m,0} + \kappa_{m,\delta}\delta_t + \kappa_{m,G}G_{W,t} + \kappa_{m,pc}pc_t,\end{aligned} \tag{A.30}$$

where $\kappa_{m,\delta} = \frac{e^{\overline{pc}}\bar{G}_W}{1+e^{\overline{pc}}\bar{\delta}\bar{G}_W}$, $\kappa_{m,G} = \frac{e^{\overline{pc}}\bar{\delta}}{1+e^{\overline{pc}}\bar{\delta}\bar{G}_W}$, $\kappa_{m,pc} = \frac{e^{\overline{pc}}\bar{\delta}\bar{G}_W}{1+e^{\overline{pc}}\bar{\delta}\bar{G}_W}$, and $\kappa_{m,0} = \log\left(1 + e^{\overline{pc}}\bar{\delta}\bar{G}_W\right) - \kappa_{m,\delta}\bar{\delta} - \kappa_{m,G}\bar{G}_W - \kappa_{m,pc}\overline{pc}$. The second approximation is

$$\begin{aligned}\log\left(1 - \delta_t G_{W,t}\right) &\simeq \log\left(1 - \bar{\delta}\bar{G}_W\right) - \frac{\bar{G}_W}{1 - \bar{\delta}\bar{G}_W}\left(\delta_t - \bar{\delta}\right) - \frac{\bar{\delta}}{1 - \bar{\delta}\bar{G}_W}\left(G_{W,t} - \bar{G}_W\right) \\ &= \kappa_{W,0} + \kappa_{W,\delta}\delta_t + \kappa_{W,G}G_{W,t},\end{aligned} \tag{A.31}$$

where $\kappa_{W,\delta} = -\frac{\bar{G}_W}{1-\bar{\delta}\bar{G}_W}$, $\kappa_{W,G} = -\frac{\bar{\delta}}{1-\bar{\delta}\bar{G}_W}$, and $\kappa_{W,0} = \log\left(1 - \bar{\delta}\bar{G}_W\right) - \kappa_{W,\delta}\bar{\delta} - \kappa_{W,G}\bar{G}_W$. Then, we can rewrite the SDF in (A.21) as

$$\begin{aligned}m_{t+1} &\simeq \theta\log\beta - \frac{\theta}{\psi}\Delta c_{t+1} + (\theta - 1)\, r_{W,t+1} - (\theta - 1)\left(\kappa_{W,0} + \kappa_{W,\delta}\delta_t + \kappa_{W,G}G_{W,t}\right) \\ &\quad - \frac{\theta}{\psi}\kappa_{m,\delta}\Delta\delta_{t+1} - \frac{\theta}{\psi}\kappa_{m,G}\Delta G_{W,t+1} - \frac{\theta}{\psi}\kappa_{m,pc}\Delta pc_{t+1}.\end{aligned} \tag{A.32}$$

As introduced in Section 2.3, we specify four dynamic processes:

$$\Delta c_{t+1} = \mu_c + x_t + \sigma_c\varepsilon_{c,t+1}, \tag{A.33}$$

$$G_{W,t+1} = \mu_G + \rho_G G_{W,t} + \rho_{G,\delta}\delta_t + \sigma_G\varepsilon_{G,t+1}, \tag{A.34}$$

$$\delta_{t+1} = \mu_\delta + \rho_\delta\delta_t + \sigma_\delta\varepsilon_{\delta,t+1}, \tag{A.35}$$

$$x_{t+1} = \rho_x x_t + \sigma_x\varepsilon_{x,t+1}, \tag{A.36}$$

where $G_{W,t+1}$ and δ_{t+1} are mean reverting, $\mu_G = (1 - \rho_G)\,\bar{G}_W - \rho_{G,\delta}\bar{\delta}$, and $\mu_\delta = (1 - \rho_\delta)\,\bar{\delta}$. Based on (A.31), we rewrite the Euler equation as:

$$\mathrm{E}_t\left[e^{m_{t+1} + r_{W,t+1}}\right] = e^{\kappa_{W,0} + \kappa_{W,\delta}\delta_t + \kappa_{W,G}G_{W,t}}. \tag{A.37}$$

To characterize the SDF, we make the following guess on the functional form of the price-to-consumption ratio:

$$pc_t = A_{pc,0} + A_{pc,G}G_{W,t} + A_{pc,\delta}\delta_t + A_{pc,x}x_t. \tag{A.38}$$

Then, substituting in equation (A.29), it follows that

$$\begin{aligned}
r_{W,t+1} &\simeq \kappa_{rW,0} + \kappa_{rW,pc} pc_{t+1} - pc_t + \Delta c_{t+1} \\
&= \kappa_{rW,0} + A_{pc,0}\left(\kappa_{rW,pc} - 1\right) + A_{pc,G}\left(\kappa_{rW,pc} G_{W,t+1} - G_{W,t}\right) \\
&\quad + A_{pc,\delta}\left(\kappa_{rW,pc}\delta_{t+1} - \delta_t\right) + A_{pc,x}\left(\kappa_{rW,pc} x_{t+1} - x_t\right) + \Delta c_{t+1}.
\end{aligned} \tag{A.39}$$

Summing equations (A.32) and (A.39), we further obtain

$$\begin{aligned}
& m_{t+1} + r_{W,t+1} = \\
& \theta \log \beta - (\theta - 1)\kappa_{W,0} + (1-\gamma)\mu_c + \theta\kappa_{rW,0} + \theta A_{pc,0}\left(\kappa_{rW,pc} - 1\right) \\
& + \theta\kappa_{rW,pc}\left(A_{pc,\delta}\mu_\delta + A_{pc,G}\mu_G\right) \\
& - \frac{\theta}{\psi}\left(\left(\kappa_{m,G} + \kappa_{m,pc}A_{pc,G}\right)\mu_G + \left(\kappa_{m,\delta} + \kappa_{m,pc}A_{pc,\delta}\right)\mu_\delta\right) \\
& + \left(\theta A_{pc,G}\left(\kappa_{rW,pc}\rho_G - 1 - \frac{\kappa_{m,pc}}{\psi}\left(\rho_G - 1\right)\right) - (\theta - 1)\kappa_{W,G} - \frac{\theta}{\psi}\kappa_{m,G}\left(\rho_G - 1\right)\right) G_{W,t} \\
& + \begin{pmatrix} \theta A_{pc,\delta}\left(\kappa_{rW,pc}\rho_\delta - 1 - \frac{\kappa_{m,pc}}{\psi}\left(\rho_\delta - 1\right)\right) - (\theta-1)\kappa_{W,\delta} - \frac{\theta}{\psi}\kappa_{m,\delta}\left(\rho_\delta - 1\right) \\ + \left(\theta A_{pc,G}\left(\kappa_{rW,pc} - \frac{\kappa_{m,pc}}{\psi}\right) - \frac{\theta}{\psi}\kappa_{m,G}\right)\rho_{G,\delta} \end{pmatrix} \delta_t \\
& + \left((1-\gamma) + \theta A_{pc,x}\left(\kappa_{rW,pc}\rho_x - 1 - \frac{\kappa_{m,pc}}{\psi}\left(\rho_x - 1\right)\right)\right) x_t \\
& + (1-\gamma)\sigma_c \varepsilon_{c,t+1} \\
& + \left(\theta A_{pc,G}\left(\kappa_{rW,pc} - \frac{\kappa_{m,pc}}{\psi}\right) - \frac{\theta}{\psi}\kappa_{m,G}\right)\sigma_G \varepsilon_{G,t+1} \\
& + \left(\left(\theta A_{pc,\delta}\left(\kappa_{rW,pc} - \frac{\kappa_{m,pc}}{\psi}\right) - \frac{\theta}{\psi}\kappa_{m,\delta}\right)\sigma_\delta\right)\varepsilon_{\delta,t+1} \\
& + \theta A_{pc,x}\left(\kappa_{rW,pc} - \frac{\kappa_{m,pc}}{\psi}\right)\sigma_x \varepsilon_{x,t+1}.
\end{aligned} \tag{A.40}$$

As $\mathrm{E}_t\left[e^{m_{t+1}+r_{W,t+1}}\right] = e^{\kappa_{W,0}+\kappa_{W,\delta}\delta_t+\kappa_{W,G}G_{W,t}}$, we can solve for the coefficients:

$$A_{pc,0} = \frac{1}{\theta\left(1 - \kappa_{rW,pc}\right)} \begin{pmatrix} \theta\log\beta - \theta\kappa_{W,0} + (1-\gamma)\mu_c \\ +\theta\kappa_{rW,0} + \theta\kappa_{rW,pc}\left(A_{pc,G}\mu_G + A_{pc,\delta}\mu_\delta\right) \\ -\frac{\theta}{\psi}\left(\kappa_{m,G} + \kappa_{m,pc}A_{pc,G}\right)\mu_G \\ -\frac{\theta}{\psi}\left(\kappa_{m,\delta} + \kappa_{m,pc}A_{pc,\delta}\right)\mu_\delta \\ +\frac{(1-\gamma)^2\sigma_c^2}{2} + \frac{\left(\theta A_{pc,G}\left(\kappa_{rW,pc} - \frac{\kappa_{m,pc}}{\psi}\right) - \frac{\theta}{\psi}\kappa_{m,G}\right)^2\sigma_G^2}{2} \\ +\frac{\left(\theta A_{pc,\delta}\left(\kappa_{rW,pc} - \frac{\kappa_{m,pc}}{\psi}\right) - \frac{\theta}{\psi}\kappa_{m,\delta}\right)^2\sigma_\delta^2}{2} \\ +\frac{\left(\theta\kappa_{rW,pc} - \frac{\theta}{\psi}\kappa_{m,pc}\right)^2 A_{pc,x}^2\sigma_x^2}{2} \end{pmatrix}, \tag{A.41}$$

$$A_{pc,G} = \frac{\kappa_{m,G}\left(1 - \rho_G\right) - \psi\kappa_{W,G}}{\psi - \kappa_{m,pc} - \left(\psi\kappa_{rW,pc} - \kappa_{m,pc}\right)\rho_G} = \frac{\kappa_{m,G} - \frac{\psi}{1-\rho_G}\kappa_{W,G}}{\psi\frac{1-\kappa_{rW,pc}\rho_G}{1-\rho_G} - \kappa_{m,pc}}, \tag{A.42}$$

$$A_{pc,\delta} = \frac{\kappa_{m,\delta}\left(1 - \rho_\delta\right) - \psi\kappa_{W,\delta} + \left(\left(\psi\kappa_{rW,pc} - \kappa_{m,pc}\right)A_{pc,G} - \kappa_{m,G}\right)\rho_{G,\delta}}{\psi - \kappa_{m,pc} - \left(\psi\kappa_{rW,pc} - \kappa_{m,pc}\right)\rho_\delta}$$

$$= \frac{\kappa_{m,\delta} - \frac{\psi}{1-\rho_\delta}\kappa_{W,\delta}}{\psi\frac{1-\kappa_{rW,pc}\rho_\delta}{1-\rho_\delta} - \kappa_{m,pc}} + \frac{\frac{\psi\kappa_{rW,pc}-\kappa_{m,pc}}{1-\rho_\delta}A_{pc,G} - \frac{\kappa_{m,G}}{1-\rho_\delta}}{\psi\frac{1-\kappa_{rW,pc}\rho_\delta}{1-\rho_\delta} - \kappa_{m,pc}}\rho_{G,\delta}, \tag{A.43}$$

$$A_{pc,x} = \frac{\psi - 1}{\psi - \kappa_{m,pc} - \left(\psi\kappa_{rW,pc} - \kappa_{m,pc}\right)\rho_x} = \frac{\frac{\psi-1}{1-\rho_x}}{\psi\frac{1-\kappa_{rW,pc}\rho_x}{1-\rho_x} - \kappa_{m,pc}}. \tag{A.44}$$

A sufficient condition for the coefficients $A_{pc,G}$, $A_{pc,\delta}$, and $A_{pc,x}$ to be positive is that $\rho_{G,\delta} = 0$, $\psi > 1$, $\bar{\delta} \geq 0$, and $\bar{G}_W \geq 0$. m_{t+1} in (A.32) can be then written as

$$\begin{aligned}
m_{t+1} \simeq{}& \theta\log\beta - \gamma\mu_c + (\theta-1)\left(\kappa_{rW,0} - \kappa_{W,0} + A_{pc,0}\left(\kappa_{rW,pc} - 1\right)\right) \\
&+ (\theta-1)\,\kappa_{rW,pc}\left(A_{pc,G}\mu_G + A_{pc,\delta}\mu_\delta\right) \\
&- \frac{\theta}{\psi}\left(\left(\kappa_{m,\delta} + \kappa_{m,pc}A_{pc,\delta}\right)\mu_\delta + \left(\kappa_{m,G} + \kappa_{m,pc}A_{pc,G}\right)\mu_G\right) \\
&+ \left((\theta-1)\left(A_{pc,G}\left(\kappa_{rW,pc}\rho_G - 1\right) - \kappa_{W,G}\right) - \frac{\theta}{\psi}\left(\kappa_{m,G} + \kappa_{m,pc}A_{pc,G}\right)\left(\rho_G - 1\right)\right)G_{W,t} \\
&+ \left(\begin{array}{l} (\theta-1)\left(A_{pc,\delta}\left(\kappa_{rW,pc}\rho_\delta - 1\right) - \kappa_{W,\delta}\right) - \frac{\theta}{\psi}\left(\kappa_{m,\delta} + \kappa_{m,pc}A_{pc,\delta}\right)\left(\rho_\delta - 1\right) \\ + \left((\theta-1)\,A_{pc,G}\kappa_{rW,pc} - \frac{\theta}{\psi}\left(\kappa_{m,G} + \kappa_{m,pc}A_{pc,G}\right)\right)\rho_{G,\delta} \end{array}\right)\delta_t \\
&+ \left(-\gamma + \left((\theta-1)\left(\kappa_{rW,pc}\rho_x - 1\right) - \frac{\theta}{\psi}\kappa_{m,pc}\left(\rho_x - 1\right)\right)A_{pc,x}\right)x_t \\
&- \gamma\sigma_c\varepsilon_{c,t+1} \\
&+ \left((\theta-1)\,A_{pc,G}\kappa_{rW,pc} - \frac{\theta}{\psi}\left(\kappa_{m,pc}A_{pc,G} + \kappa_{m,G}\right)\right)\sigma_G\varepsilon_{G,t+1} \\
&+ \left((\theta-1)\,A_{pc,\delta}\kappa_{rW,pc} - \frac{\theta}{\psi}\left(\kappa_{m,pc}A_{pc,\delta} + \kappa_{m,\delta}\right)\right)\sigma_\delta\varepsilon_{\delta,t+1} \\
&+ \left((\theta-1)\,\kappa_{rW,pc} - \frac{\theta}{\psi}\kappa_{m,pc}\right)A_{pc,x}\sigma_x\varepsilon_{x,t+1}.
\end{aligned} \tag{A.45}$$

We can identify the market prices of risk by rewriting m_{t+1} as:

$$m_{t+1} = m_0 + m_G G_{W,t} + m_\delta\delta_t + m_x x_t - \lambda_c\varepsilon_{c,t+1} - \lambda_G\varepsilon_{G,t+1} - \lambda_\delta\varepsilon_{\delta,t+1} - \lambda_x\varepsilon_{x,t+1}, \tag{A.46}$$

where

$$\begin{aligned}
m_0 ={}& \theta\log\beta - \gamma\mu_c + (\theta-1)\left(\kappa_{rW,0} - \kappa_{W,0} + A_{pc,0}\left(\kappa_{rW,pc} - 1\right)\right) \\
&+ (\theta-1)\,\kappa_{rW,pc}\left(A_{pc,G}\mu_G + A_{pc,\delta}\mu_\delta\right) \\
&- \frac{\theta}{\psi}\left(\left(\kappa_{m,\delta} + \kappa_{m,pc}A_{pc,\delta}\right)\mu_\delta + \left(\kappa_{m,G} + \kappa_{m,pc}A_{pc,G}\right)\mu_G\right),
\end{aligned} \tag{A.47}$$

$$\begin{aligned}
m_G &= (\theta-1)\left(A_{pc,G}\left(\kappa_{rW,pc}\rho_G - 1\right) - \kappa_{W,G}\right) - \frac{\theta}{\psi}\left(\kappa_{m,G} + \kappa_{m,pc}A_{pc,G}\right)\left(\rho_G - 1\right) \\
&= \frac{\frac{\kappa_{m,G}}{\psi}\left(1-\rho_G\right) - \kappa_{W,G}\frac{\kappa_{m,pc}}{\psi}\frac{1-\rho_G}{1-\kappa_{rW,pc}\rho_G}}{1 - \frac{\kappa_{m,pc}}{\psi}\frac{1-\rho_G}{1-\kappa_{rW,pc}\rho_G}},
\end{aligned} \tag{A.48}$$

$$\begin{aligned}
m_\delta ={}& (\theta-1)\left(A_{pc,\delta}\left(\kappa_{rW,pc}\rho_\delta - 1\right) - \kappa_{W,\delta}\right) - \frac{\theta}{\psi}\left(\kappa_{m,\delta} + \kappa_{m,pc}A_{pc,\delta}\right)\left(\rho_\delta - 1\right) \\
&+ \left((\theta-1)\,A_{pc,G}\kappa_{rW,pc} - \frac{\theta}{\psi}\left(\kappa_{m,G} + \kappa_{m,pc}A_{pc,G}\right)\right)\rho_{G,\delta}
\end{aligned}$$

$$
\begin{aligned}
&= \frac{\frac{\kappa_{m,\delta}}{\psi}\left(1-\rho_\delta\right)-\kappa_{W,\delta}\frac{\kappa_{m,pc}}{\psi}\frac{1-\rho_\delta}{1-\kappa_{rW,pc}\rho_\delta}}{1-\frac{\kappa_{m,pc}}{\psi}\frac{1-\rho_\delta}{1-\kappa_{rW,pc}\rho_\delta}} \\
&\quad + \left(\left(\theta-1\right)A_{pc,G}\kappa_{rW,pc}-\frac{\theta}{\psi}\left(\kappa_{m,G}+\kappa_{m,pc}A_{pc,G}\right)\right)\rho_{G,\delta}, \qquad \text{(A.49)} \\
m_x &= -\gamma+\left(\left(\theta-1\right)\left(\kappa_{rW,pc}\rho_x-1\right)-\frac{\theta}{\psi}\kappa_{m,pc}\left(\rho_x-1\right)\right)A_{pc,x} \\
&= -\frac{1}{\psi}\frac{1-\kappa_{m,pc}\frac{1-\rho_x}{1-\kappa_{rW,pc}\rho_x}}{1-\frac{\kappa_{m,pc}}{\psi}\frac{1-\rho_x}{1-\kappa_{rW,pc}\rho_x}}, \qquad \text{(A.50)} \\
\lambda_c &= \gamma\sigma_c, \qquad \text{(A.51)} \\
\lambda_G &= \left(\left(1-\theta\right)\kappa_{rW,pc}A_{pc,G}+\frac{\theta}{\psi}\left(\kappa_{m,G}+\kappa_{m,pc}A_{pc,G}\right)\right)\sigma_G, \qquad \text{(A.52)} \\
\lambda_\delta &= \left(\left(1-\theta\right)\kappa_{rW,pc}A_{pc,\delta}+\frac{\theta}{\psi}\left(\kappa_{m,\delta}+\kappa_{m,pc}A_{pc,\delta}\right)\right)\sigma_\delta \qquad \text{(A.53)} \\
\lambda_x &= \left(\left(1-\theta\right)\kappa_{rW,pc}+\frac{\theta}{\psi}\kappa_{m,pc}\right)A_{pc,x}\sigma_x \\
&= \left(\frac{\gamma\psi-1}{\psi-1}\kappa_{rW,pc}-\frac{\gamma-1}{\psi-1}\kappa_{m,pc}\right)A_{pc,x}\sigma_x. \qquad \text{(A.54)}
\end{aligned}
$$

Assuming that $\left|\bar{\delta}\bar{G}_W\right|<1$, it follows that $m_x<0$. Assuming that $\psi>1$, $\bar{\delta}\geq 0$, and $\bar{G}_W\geq 0$ is a sufficient condition for $m_G, m_\delta>0$, as well as $-1<m_x<0$. As for the market prices of risk, it is useful to notice that $\kappa_{rW,pc}>\kappa_{m,pc}$. It turns out that $\lambda_c,\lambda_x>0$ at all times. The signs of λ_G and λ_δ depend on both positive and negative contributions. For instance, for $\theta<0$, they are characterized by positive contributions stemming from the impact of shocks to $G_{W,t}$ and δ_t on the return on aggregate wealth, while negative contributions arise from the effect on the ESG factor. However, the concavity of expected utility with respect to $G_{W,t}$ and δ_t implies a diminishing marginal utility of such variables, and thus positive risk premia.

The return on wealth can be formulated as

$$
\begin{aligned}
r_{W,t+1} = &\underbrace{\kappa_{rW,0}+A_{pc,0}\left(\kappa_{rW,pc}-1\right)+A_{pc,G}\kappa_{rW,pc}\mu_G+A_{pc,\delta}\kappa_{rW,pc}\mu_\delta+\mu_c}_{r_{W,0}} \\
&+A_{pc,G}\left(\kappa_{rW,pc}\rho_G-1\right)G_{W,t}+A_{pc,\delta}\left(\kappa_{rW,pc}\rho_\delta-1\right)\delta_t \\
&+\left(A_{pc,x}\left(\kappa_{rW,pc}\rho_x-1\right)+1\right)x_t \\
&+A_{pc,G}\kappa_{rW,pc}\sigma_G\varepsilon_{G,t+1}+A_{pc,\delta}\kappa_{rW,pc}\sigma_\delta\varepsilon_{\delta,t+1} \\
&+A_{pc,x}\kappa_{rW,pc}\sigma_x\varepsilon_{x,t+1}+\sigma_c\varepsilon_{c,t+1}. \qquad \text{(A.55)}
\end{aligned}
$$

As $A_{pc,G}$, $A_{pc,\delta}$, and $A_{pc,x}$ are positive, the return on wealth is positively correlated with the shocks $\varepsilon_{G,t+1}$, $\varepsilon_{\delta,t+1}$, $\varepsilon_{x,t+1}$, and $\varepsilon_{c,t+1}$. The expected excess return of the consumption asset can be expressed as

$$
\mathrm{E}_t\left[r_{W,t+1}-r_{f,t+1}\right] = \underbrace{\sigma_c}_{\mathrm{Cov}_t\left[r_{W,t+1},\varepsilon_{c,t+1}\right]}\lambda_c+\underbrace{\kappa_{rW,pc}A_{pc,G}\sigma_G}_{\mathrm{Cov}_t\left[r_{W,t+1},\varepsilon_{G,t+1}\right]}\lambda_G
$$

$$
\begin{aligned}
&+ \underbrace{\kappa_{rW,pc} A_{pc,\delta} \sigma_\delta}_{\mathrm{Cov}_t\left[r_{W,t+1},\varepsilon_{\delta,t+1}\right]} \lambda_\delta + \underbrace{\kappa_{rW,pc} A_{pc,x} \sigma_x}_{\mathrm{Cov}_t\left[r_{W,t+1},\varepsilon_{x,t+1}\right]} \lambda_x - \frac{1}{2}\mathrm{Var}_t\left[r_{W,t+1}\right] \\
&\underbrace{+ \kappa_{W,0} - \frac{\bar{\delta}}{1-\bar{\delta}\bar{G}_W} G_{W,t} - \frac{\bar{G}_W}{1-\bar{\delta}\bar{G}_W} \delta_t}_{-y_{W,t}} .
\end{aligned} \tag{A.56}
$$

To determine the risk-free rate of return, we express the Euler equation as

$$
\mathrm{E}_t\left[e^{m_{t+1}+r_{f,t+1}}\right] = 1. \tag{A.57}
$$

As $r_{f,t+1}$ is known at time t, it follows that $\mathrm{E}_t\left[e^{r_{f,t+1}}\right] = e^{\mathrm{E}_t\left[r_{f,t+1}\right]}$. Thus, the risk-free rate of return is given by

$$
r_{f,t+1} = -\log \mathrm{E}_t\left[e^{m_{t+1}}\right]. \tag{A.58}
$$

Using (A.46):

$$
\begin{aligned}
\mathrm{E}_t\left[e^{m_{t+1}}\right] &= \mathrm{E}_t\left[e^{m_0 + m_G G_{W,t} + m_\delta \delta_t + m_x x_t - \lambda_c \varepsilon_{c,t+1} - \lambda_G \varepsilon_{G,t+1} - \lambda_\delta \varepsilon_{\delta,t+1} - \lambda_x \varepsilon_{x,t+1}}\right] \\
&= e^{m_0 + m_G G_{W,t} + m_\delta \delta_t + m_x x_t + \frac{\lambda_c^2}{2} + \frac{\lambda_G^2}{2} + \frac{\lambda_\delta^2}{2} + \frac{\lambda_x^2}{2}} .
\end{aligned} \tag{A.59}
$$

Then, using (A.38) yields

$$
r_{f,t+1} = \underbrace{-m_0 - \frac{\lambda_c^2}{2} - \frac{\lambda_G^2}{2} - \frac{\lambda_\delta^2}{2} - \frac{\lambda_x^2}{2}}_{r_{f,0}} \underbrace{-m_G}_{r_{f,G}} G_{W,t} \underbrace{-m_\delta}_{r_{f,\delta}} \delta_t \underbrace{-m_x}_{r_{f,x}} x_t. \tag{A.60}
$$

A.3 Proof of Proposition 3 (risky asset return)

For an arbitrary risky asset, the Euler equation reads:

$$
\mathrm{E}_t\left[M_{t+1} R_{n,t+1}\right] = 1 - \delta_t G_{n,t}. \tag{A.61}
$$

Similarly to (A.31), we can write

$$
\log\left(1 - \delta_t G_{n,t}\right) \simeq \kappa_{n,0} + \kappa_{n,Gn} G_{n,t} + \kappa_{n,\delta} \delta_t, \tag{A.62}
$$

where $\kappa_{n,Gn} = -\frac{\bar{\delta}}{1-\bar{\delta}\bar{G}_n}$, $\kappa_{n,\delta} = -\frac{\bar{G}_n}{1-\bar{\delta}\bar{G}_n}$, and $\kappa_{n,0} = \log\left(1 - \bar{\delta}\bar{G}_n\right) - \kappa_{n,Gn}\bar{G}_n - \kappa_{n,\delta}\bar{\delta}$.

Similar to the approach followed in Online Appendix A.2 for the return on aggregate wealth, we adopt the log-linearization technique introduced by Campbell and Shiller (1988) to express the logarithmic return on the risky asset as follows:

$$
r_{n,t+1} \simeq \kappa_{rn,0} + \kappa_{rn,pd} pd_{n,t+1} - pd_{n,t} + \Delta d_{n,t+1}, \tag{A.63}
$$

where $\kappa_{rn,pd} = \frac{e^{\overline{pd}_n}}{1+e^{\overline{pd}_n}}$ and $\kappa_{rn,0} = \log\left(1 + e^{\overline{pd}_n}\right) - \kappa_{rn,pd}\overline{pd}_n$. Consider the following dynamics:

$$
G_{n,t+1} = \mu_{Gn} + \rho_{Gn} G_{n,t} + \rho_{Gn,\delta} \delta_t + \sigma_{Gn,G} \varepsilon_{G,t+1} + \sigma_{Gn} \varepsilon_{Gn,t+1}, \tag{A.64}
$$

$$
\begin{aligned}
\Delta d_{n,t+1} = & \mu_{dn} + \rho_{dn,x} x_t + \rho_{dn,\delta}\delta_t + \sigma_{dn,c}\varepsilon_{c,t+1} + \sigma_{dn,G}\varepsilon_{G,t+1} + \sigma_{dn,\delta}\varepsilon_{\delta,t+1} + \sigma_{dn,x}\varepsilon_{x,t+1} \\
& + \sigma_{dn,Gn}\varepsilon_{Gn,t+1} + \sigma_{dn,dM}\varepsilon_{dM,t+1} + \sigma_{dn}\varepsilon_{dn,t+1},
\end{aligned} \tag{A.65}
$$

where $\mu_{Gn} = (1-\rho_{Gn})\,\bar{G}_n - \rho_{Gn,\delta}\bar{\bar{\delta}}$. We make the guess:

$$
pd_{n,t} = A_{n,0} + A_{n,G} G_{W,t} + A_{n,\delta}\delta_t + A_{n,x} x_t + A_{n,Gn} G_{n,t}. \tag{A.66}
$$

We then write the log asset return as:

$$
\begin{aligned}
r_{n,t+1} \simeq & \underbrace{\kappa_{rn,0} + \kappa_{rn,pd}\left(A_{n,0} + A_{n,G}\mu_G + A_{n,\delta}\mu_\delta + A_{n,Gn}\mu_{Gn}\right) - A_{n,0} + \mu_{dn}}_{r_{n,0}} \\
& + \underbrace{\left(\kappa_{rn,pd}\rho_G - 1\right) A_{n,G}}_{r_{n,G}} G_{W,t} \\
& + \underbrace{\left(\left(\kappa_{rn,pd}\rho_\delta - 1\right) A_{n,\delta} + \kappa_{rn,pd}\left(A_{n,G}\rho_{G,\delta} + A_{n,Gn}\rho_{Gn,\delta}\right) + \rho_{dn,\delta}\right)}_{r_{n,\delta}} \delta_t \\
& + \underbrace{\left(\left(\kappa_{rn,pd}\rho_x - 1\right) A_{n,x} + \rho_{dn,x}\right)}_{r_{n,x}} x_t + \underbrace{\left(\kappa_{rn,pd}\rho_{Gn} - 1\right) A_{n,Gn}}_{r_{n,Gn}} G_{n,t} \\
& + \underbrace{\sigma_{dn,c}}_{\sigma_{rn,c}} \varepsilon_{c,t+1} + \underbrace{\left(\kappa_{rn,pd}\left(A_{n,G}\sigma_G + A_{n,Gn}\sigma_{Gn,G}\right) + \sigma_{dn,G}\right)}_{\sigma_{rn,G}} \varepsilon_{G,t+1} \\
& + \underbrace{\left(\kappa_{rn,pd} A_{n,\delta}\sigma_\delta + \sigma_{dn,\delta}\right)}_{\sigma_{rn,\delta}} \varepsilon_{\delta,t+1} \\
& + \underbrace{\left(\kappa_{rn,pd} A_{n,x}\sigma_x + \sigma_{dn,x}\right)}_{\sigma_{rn,x}} \varepsilon_{x,t+1} + \underbrace{\left(\kappa_{rn,pd} A_{n,Gn}\sigma_{Gn} + \sigma_{dn,Gn}\right)}_{\sigma_{rn,Gn}} \varepsilon_{Gn,t+1} \\
& + \underbrace{\sigma_{dn,dM}}_{\sigma_{rn,dM}} \varepsilon_{dM,t+1} + \underbrace{\sigma_{dn}}_{\sigma_{rn,dn}} \varepsilon_{dn,t+1}.
\end{aligned} \tag{A.67}
$$

We apply the Euler condition

$$
\mathrm{E}_t\left[e^{m_{t+1}+r_{n,t+1}}\right] = e^{\kappa_{n,0}+\kappa_{n,Gn}G_{n,t}+\kappa_{n,\delta}\delta_t}, \tag{A.68}
$$

where

$$
\begin{aligned}
m_{t+1} + r_{n,t+1} \simeq & m_0 + \kappa_{rn,0} + \left(\kappa_{rn,pd} - 1\right) A_{n,0} + \kappa_{rn,pd}\left(A_{n,G}\mu_G + A_{n,\delta}\mu_\delta + A_{n,Gn}\mu_{Gn}\right) + \mu_{dn} \\
& + \left(m_G + \left(\kappa_{rn,pd}\rho_G - 1\right) A_{n,G}\right) G_{W,t} \\
& + \left(m_\delta + \left(\kappa_{rn,pd}\rho_\delta - 1\right) A_{n,\delta} + \kappa_{rn,pd}\left(A_{n,G}\rho_{G,\delta} + A_{n,Gn}\rho_{Gn,\delta}\right) + \rho_{dn,\delta}\right) \delta_t \\
& + \left(m_x + \left(\kappa_{rn,pd}\rho_x - 1\right) A_{n,x} + \rho_{dn,x}\right) x_t \\
& + \left(\kappa_{rn,pd}\rho_{Gn} - 1\right) A_{n,Gn} G_{n,t} \\
& + \left(-\lambda_c + \sigma_{dn,c}\right) \varepsilon_{c,t+1} \\
& + \left(-\lambda_G + \kappa_{rn,pd}\left(A_{n,G}\sigma_G + A_{n,Gn}\sigma_{Gn,G}\right) + \sigma_{dn,G}\right) \varepsilon_{G,t+1} \\
& + \left(-\lambda_\delta + \kappa_{rn,pd} A_{n,\delta}\sigma_\delta + \sigma_{dn,\delta}\right) \varepsilon_{\delta,t+1} \\
& + \left(-\lambda_x + \kappa_{rn,pd} A_{n,x}\sigma_x + \sigma_{dn,x}\right) \varepsilon_{x,t+1}
\end{aligned}
$$

$$+ \left(\kappa_{rn,pd} A_{n,Gn} \sigma_{Gn} + \sigma_{dn,Gn}\right) \varepsilon_{Gn,t+1}$$
$$+ \sigma_{dn,dM} \varepsilon_{dM,t+1} + \sigma_{dn} \varepsilon_{dn,t+1}. \tag{A.69}$$

Therefore

$$\begin{aligned}
0 = {} & m_0 + \kappa_{rn,0} + \left(\kappa_{rn,pd} - 1\right) A_{n,0} + \kappa_{rn,pd} \left(A_{n,G} \mu_G + A_{n,\delta} \mu_\delta + A_{n,Gn} \mu_{Gn}\right) + \mu_{dn} \\
& - \kappa_{n,0} + \frac{\left(-\lambda_c + \sigma_{dn,c}\right)^2}{2} + \frac{\left(-\lambda_G + \kappa_{rn,pd} \left(A_{n,G} \sigma_G + A_{n,Gn} \sigma_{Gn,G}\right) + \sigma_{dn,G}\right)^2}{2} \\
& + \frac{\left(-\lambda_\delta + \kappa_{rn,pd} A_{n,\delta} \sigma_\delta + \sigma_{dn,\delta}\right)^2}{2} + \frac{\left(-\lambda_x + \kappa_{rn,pd} A_{n,x} \sigma_x + \sigma_{dn,x}\right)^2}{2} \\
& + \frac{\left(\kappa_{rn,pd} A_{n,Gn} \sigma_{Gn} + \sigma_{dn,Gn}\right)^2}{2} + \frac{\sigma_{dn,dM}^2}{2} + \frac{\sigma_{dn}^2}{2} \\
& + \left(m_G + \left(\kappa_{rn,pd} \rho_G - 1\right) A_{n,G}\right) G_{W,t} \\
& + \left(m_\delta + \left(\kappa_{rn,pd} \rho_\delta - 1\right) A_{n,\delta} + \kappa_{rn,pd} \left(A_{n,G} \rho_{G,\delta} + A_{n,Gn} \rho_{Gn,\delta}\right) + \rho_{dn,\delta} - \kappa_{n,\delta}\right) \delta_t \\
& + \left(m_x + \left(\kappa_{rn,pd} \rho_x - 1\right) A_{n,x} + \rho_{dn,x}\right) x_t \\
& + \left(\left(\kappa_{rn,pd} \rho_{Gn} - 1\right) A_{n,Gn} - \kappa_{n,Gn}\right) G_{n,t}.
\end{aligned} \tag{A.70}$$

Finally, the coefficients in (A.66) are

$$A_{n,0} = \frac{1}{1 - \kappa_{rn,pd}} \left(\begin{array}{l} m_0 + \kappa_{rn,0} + \kappa_{rn,pd} \left(A_{n,G} \mu_G + A_{n,\delta} \mu_\delta + A_{n,Gn} \mu_{Gn}\right) \\ + \mu_{dn} - \kappa_{n,0} \\ + \frac{\left(-\lambda_c + \sigma_{dn,c}\right)^2}{2} + \frac{\left(-\lambda_G + \kappa_{rn,pd}\left(A_{n,G} \sigma_G + A_{n,Gn} \sigma_{Gn,G}\right) + \sigma_{dn,G}\right)^2}{2} \\ + \frac{\left(-\lambda_\delta + \kappa_{rn,pd} A_{n,\delta} \sigma_\delta + \sigma_{dn,\delta}\right)^2}{2} + \frac{\left(-\lambda_x + \kappa_{rn,pd} A_{n,x} \sigma_x + \sigma_{dn,x}\right)^2}{2} \\ + \frac{\left(\kappa_{rn,pd} A_{n,Gn} \sigma_{Gn} + \sigma_{dn,Gn}\right)^2}{2} + \frac{\sigma_{dn,dM}^2}{2} + \frac{\sigma_{dn}^2}{2} \end{array} \right), \tag{A.71}$$

$$A_{n,G} = \frac{m_G}{1 - \kappa_{rn,pd} \rho_G}, \tag{A.72}$$

$$A_{n,\delta} = \frac{m_\delta + \kappa_{rn,pd} \left(A_{n,G} \rho_{G,\delta} + A_{n,Gn} \rho_{Gn,\delta}\right) + \rho_{dn,\delta} - \kappa_{n,\delta}}{1 - \kappa_{rn,pd} \rho_\delta}, \tag{A.73}$$

$$A_{n,x} = \frac{m_x + \rho_{dn,x}}{1 - \kappa_{rn,pd} \rho_x}, \tag{A.74}$$

$$A_{n,Gn} = \frac{-\kappa_{n,Gn}}{1 - \kappa_{rn,pd} \rho_{Gn}}. \tag{A.75}$$

Note that $A_{n,Gn} > 0$ and that the return coefficient on $G_{n,t}$ is $r_{n,Gn} = \kappa_{n,Gn} < 0$. Furthermore, $A_{n,G} > 0$, and thus $r_{n,G} < 0$, when $\psi > 1$. Finally, $A_{n,\delta}$ is positive when $\bar{G}_n > -\frac{m_\delta + \kappa_{rn,pd}\left(A_{n,G} \rho_{G,\delta} + A_{n,Gn} \rho_{Gn,\delta}\right) + \rho_{dn,\delta}}{1 - \left(m_\delta + \kappa_{rn,pd}\left(A_{n,G} \rho_{G,\delta} + A_{n,Gn} \rho_{Gn,\delta}\right) + \rho_{dn,\delta}\right) \bar{\delta}}$. We can also rewrite the return on an asset as follows

$$r_{n,t+1} \simeq \underbrace{\begin{pmatrix} -m_0 + \kappa_{n,0} \\ -\frac{\left(-\lambda_c+\sigma_{dn,c}\right)^2}{2} - \frac{\left(-\lambda_G+\kappa_{rn,pd}\left(A_{n,G}\sigma_G+A_{n,Gn}\sigma_{Gn,G}\right)+\sigma_{dn,G}\right)^2}{2} \\ -\frac{\left(-\lambda_\delta+\kappa_{rn,pd}A_{n,\delta}\sigma_\delta+\sigma_{dn,\delta}\right)^2}{2} - \frac{\left(-\lambda_x+\kappa_{rn,pd}A_{n,x}\sigma_x+\sigma_{dn,x}\right)^2}{2} \\ -\frac{\left(\kappa_{rn,pd}A_{n,Gn}\sigma_{Gn}+\sigma_{dn,Gn}\right)^2}{2} - \frac{\sigma^2_{dn,dM}}{2} - \frac{\sigma^2_{dn}}{2} \end{pmatrix}}_{r_{n,0}}$$

$$\begin{aligned} &\underbrace{-m_G}_{r_{n,G}} G_{W,t} + \underbrace{\left(\kappa_{n,\delta} - m_\delta\right)}_{r_{n,\delta}} \delta_t \underbrace{-m_x}_{r_{n,x}} x_t + \underbrace{\kappa_{n,Gn}}_{r_{n,Gn}} G_{n,t} \\ &+ \underbrace{\sigma_{dn,c}}_{\sigma_{rn,c}} \varepsilon_{c,t+1} + \underbrace{\left(\kappa_{rn,pd}A_{n,G}\sigma_G + \kappa_{rn,pd}A_{n,Gn}\sigma_{Gn,G} + \sigma_{dn,G}\right)}_{\sigma_{rn,G}} \varepsilon_{G,t+1} \\ &+ \underbrace{\left(\kappa_{rn,pd}A_{n,\delta}\sigma_\delta + \sigma_{dn,\delta}\right)}_{\sigma_{rn,\delta}} \varepsilon_{\delta,t+1} + \underbrace{\left(\kappa_{rn,pd}A_{n,x}\sigma_x + \sigma_{dn,x}\right)}_{\sigma_{rn,x}} \varepsilon_{x,t+1} \\ &+ \underbrace{\left(\kappa_{rn,pd}A_{n,Gn}\sigma_{Gn} + \sigma_{dn,Gn}\right)}_{\sigma_{rn,Gn}} \varepsilon_{Gn,t+1} + \underbrace{\sigma_{dn,dM}}_{\sigma_{rn,dM}} \varepsilon_{dM,t+1} + \underbrace{\sigma_{dn}}_{\sigma_{rn,dn}} \varepsilon_{dn,t+1}. \end{aligned} \tag{A.76}$$

Recalling (12), the excess return $\hat{r}_{n,t+1} = r_{n,t+1} - r_{f,t+1}$ can be expressed as

$$\hat{r}_{n,t+1} \simeq \underbrace{\begin{pmatrix} \kappa_{n,0} - \frac{\left(-\lambda_c+\sigma_{dn,c}\right)^2}{2} - \frac{\left(-\lambda_G+\kappa_{rn,pd}\left(A_{n,G}\sigma_G+A_{n,Gn}\sigma_{Gn,G}\right)+\sigma_{dn,G}\right)^2}{2} \\ -\frac{\left(-\lambda_\delta+\kappa_{rn,pd}A_{n,\delta}\sigma_\delta+\sigma_{dn,\delta}\right)^2}{2} - \frac{\left(-\lambda_x+\kappa_{rn,pd}A_{n,x}\sigma_x+\sigma_{dn,x}\right)^2}{2} \\ -\frac{\left(\kappa_{rn,pd}A_{n,Gn}\sigma_{Gn}+\sigma_{dn,Gn}\right)^2}{2} - \frac{\sigma^2_{dn,dM}}{2} - \frac{\sigma^2_{dn}}{2} + \frac{\lambda_c^2}{2} + \frac{\lambda_G^2}{2} + \frac{\lambda_\delta^2}{2} + \frac{\lambda_x^2}{2} \end{pmatrix}}_{\hat{r}_{n,0}}$$

$$\begin{aligned} &+ \underbrace{\kappa_{n,\delta}}_{\hat{r}_{n,\delta}} \delta_t + \underbrace{\kappa_{n,Gn}}_{\hat{r}_{n,Gn}} G_{n,t} \\ &+ \underbrace{\sigma_{dn,c}}_{\sigma_{rn,c}} \varepsilon_{c,t+1} + \underbrace{\left(\kappa_{rn,pd}A_{n,G}\sigma_G + \kappa_{rn,pd}A_{n,Gn}\sigma_{Gn,G} + \sigma_{dn,G}\right)}_{\sigma_{rn,G}} \varepsilon_{G,t+1} \\ &+ \underbrace{\left(\kappa_{rn,pd}A_{n,\delta}\sigma_\delta + \sigma_{dn,\delta}\right)}_{\sigma_{rn,\delta}} \varepsilon_{\delta,t+1} + \underbrace{\left(\kappa_{rn,pd}A_{n,x}\sigma_x + \sigma_{dn,x}\right)}_{\sigma_{rn,x}} \varepsilon_{x,t+1} \\ &+ \underbrace{\left(\kappa_{rn,pd}A_{n,Gn}\sigma_{Gn} + \sigma_{dn,Gn}\right)}_{\sigma_{rn,Gn}} \varepsilon_{Gn,t+1} + \underbrace{\sigma_{dn,dM}}_{\sigma_{rn,dM}} \varepsilon_{dM,t+1} + \underbrace{\sigma_{dn}}_{\sigma_{rn,dn}} \varepsilon_{dn,t+1}. \end{aligned} \tag{A.77}$$

The first two lines represent the conditional expected excess return, $\mathrm{E}_t\left[\hat{r}_{n,t+1}\right]$, which can be further developed as

$$\begin{aligned} \mathrm{E}_t\left[\hat{r}_{n,t+1}\right] = {} & \sigma_{dn,c}\lambda_c + \kappa_{rn,pd}\left(A_{n,G}\sigma_G + A_{n,Gn}\sigma_{Gn,G}\right)\lambda_G \\ & + \kappa_{rn,pd}A_{n,\delta}\sigma_\delta\lambda_\delta + \kappa_{rn,pd}A_{n,x}\sigma_x\lambda_x - \frac{1}{2}\mathrm{Var}_t\left[\hat{r}_{n,t+1}\right] \\ & + \underbrace{\log\left(1 - \bar{\delta}\bar{G}_n\right) - \frac{\bar{G}_n\left(\delta_t - \bar{\delta}\right)}{1 - \bar{\delta}\bar{G}_n} - \frac{\bar{\delta}\left(G_{n,t} - \bar{G}_n\right)}{1 - \bar{\delta}\bar{G}_n}}_{-y_{n,t}}, \end{aligned} \tag{A.78}$$

where

$$\begin{aligned}\mathrm{Var}_t\left[\hat{r}_{n,t+1}\right] = \sigma_{dn,c}^2 &+ \left(\kappa_{rn,pd}\left(A_{n,G}\sigma_G + A_{n,Gn}\sigma_{Gn,G}\right) + \sigma_{dn,G}\right)^2 \\ &+ \left(\kappa_{rn,pd}A_{n,\delta}\sigma_\delta + \sigma_{dn,\delta}\right)^2 + \left(\kappa_{rn,pd}A_{n,x}\sigma_x + \sigma_{dn,x}\right)^2 \\ &+ \left(\kappa_{rn,pd}A_{n,Gn}\sigma_{Gn} + \sigma_{dn,Gn}\right)^2 + \sigma_{dn,dM}^2 + \sigma_{dn}^2. \end{aligned} \tag{A.79}$$

Proposition 3 is obtained imposing $\rho_{dn,\delta} = \sigma_{dn,G} = \sigma_{dn,\delta} = \sigma_{dn,x} = \sigma_{dn,Gn} = 0$.

A.4 Proof of Proposition 3 (market return)

For the market portfolio, we assume $G_{M,t} = G_{W,t}$. Then, we can express the Euler condition (A.12) as

$$\mathrm{E}_t\left[M_{t+1}R_{M,t+1}\right] = 1 - \delta_t G_{W,t}. \tag{A.80}$$

Recalling (A.31), we can write $\log\left(1 - \delta_t G_{W,t}\right) \simeq \kappa_{W,0} + \kappa_{W,G}G_{W,t} + \kappa_{W,\delta}\delta_t$.

We use the following log-linearization for the return of the market portfolio:

$$r_{M,t+1} \simeq \kappa_{rM,0} + \kappa_{rM,pd}pd_{M,t+1} - pd_{M,t} + \Delta d_{M,t+1}, \tag{A.81}$$

where $\kappa_{rM,pd} = \frac{e^{\overline{pd}_M}}{1+e^{\overline{pd}_M}}$ and $\kappa_{rM,0} = \log\left(1 + e^{\overline{pd}_M}\right) - \kappa_{rM,pd}\overline{pd}_M$. Consider the following dynamics:

$$\begin{aligned}\Delta d_{M,t+1} = &\mu_{dM} + \rho_{dM,x}x_t + \rho_{dM,\delta}\delta_t \\ &+ \sigma_{dM,c}\varepsilon_{c,t+1} + \sigma_{dM,G}\varepsilon_{G,t+1} + \sigma_{dM,\delta}\varepsilon_{\delta,t+1} + \sigma_{dM,x}\varepsilon_{x,t+1} + \sigma_{dM}\varepsilon_{dM,t+1}. \end{aligned} \tag{A.82}$$

We make the guess:

$$pd_{M,t} = A_{M,0} + A_{M,G}G_{W,t} + A_{M,\delta}\delta_t + A_{M,x}x_t. \tag{A.83}$$

We then write the log market return as:

$$\begin{aligned} r_{M,t+1} \simeq &\underbrace{\kappa_{rM,0} + \kappa_{rM,pd}\left(A_{M,0} + A_{M,G}\mu_G + A_{M,\delta}\mu_\delta\right) - A_{M,0} + \mu_{dM}}_{r_{M,0}} \\ &+ \underbrace{\left(\kappa_{rM,pd}\rho_G - 1\right)A_{M,G}}_{r_{M,G}} G_{W,t} + \underbrace{\left(\left(\kappa_{rM,pd}\rho_\delta - 1\right)A_{M,\delta} + \rho_{dM,\delta} + \kappa_{rM,pd}A_{M,G}\rho_{G,\delta}\right)}_{r_{M,\delta}}\delta_t \\ &+ \underbrace{\left(\left(\kappa_{rM,pd}\rho_x - 1\right)A_{M,x} + \rho_{dM,x}\right)}_{r_{M,x}} x_t \\ &+ \underbrace{\sigma_{dM,c}}_{\sigma_{rM,c}}\varepsilon_{c,t+1} + \underbrace{\left(\kappa_{rM,pd}A_{M,G}\sigma_G + \sigma_{dM,G}\right)}_{\sigma_{rM,G}}\varepsilon_{G,t+1} \\ &+ \underbrace{\left(\kappa_{rM,pd}A_{M,\delta}\sigma_\delta + \sigma_{dM,\delta}\right)}_{\sigma_{rM,\delta}}\varepsilon_{\delta,t+1} \\ &+ \underbrace{\left(\kappa_{rM,pd}A_{M,x}\sigma_x + \sigma_{dM,x}\right)}_{\sigma_{rM,x}}\varepsilon_{x,t+1} + \underbrace{\sigma_{dM}}_{\sigma_{rM,dM}}\varepsilon_{dM,t+1}. \end{aligned} \tag{A.84}$$

We apply the Euler condition

$$\mathrm{E}_t\left[e^{m_{t+1}+r_{M,t+1}}\right] \simeq e^{\kappa_{W,0}+\kappa_{W,G}G_{W,t}+\kappa_{W,\delta}\delta_t}, \tag{A.85}$$

where

$$\begin{aligned} m_{t+1}+r_{M,t+1} \simeq\, & \kappa_{rM,0}+\kappa_{rM,pd}\left(A_{M,0}+A_{M,G}\mu_G+A_{M,\delta}\mu_\delta\right)-A_{M,0}+\mu_{dM}+m_0 \\ & +\left(\left(\kappa_{rM,pd}\rho_G-1\right)A_{M,G}+m_G\right)G_{W,t} \\ & +\left(\left(\kappa_{rM,pd}\rho_\delta-1\right)A_{M,\delta}+\rho_{dM,\delta}+\kappa_{rM,pd}A_{M,G}\rho_{G,\delta}+m_\delta\right)\delta_t \\ & +\left(\left(\kappa_{rM,pd}\rho_x-1\right)A_{M,x}+\rho_{dM,x}+m_x\right)x_t \\ & +\left(\sigma_{dM,c}-\lambda_c\right)\varepsilon_{c,t+1}+\left(\kappa_{rM,pd}A_{M,G}\sigma_G+\sigma_{dM,G}-\lambda_G\right)\varepsilon_{G,t+1} \\ & +\left(\kappa_{rM,pd}A_{M,\delta}\sigma_\delta+\sigma_{dM,\delta}-\lambda_\delta\right)\varepsilon_{\delta,t+1} \\ & +\left(\kappa_{rM,pd}A_{M,x}\sigma_x+\sigma_{dM,x}-\lambda_x\right)\varepsilon_{x,t+1}+\sigma_{dM}\varepsilon_{dM,t+1}. \end{aligned} \tag{A.86}$$

Therefore,

$$\begin{aligned} 0 \simeq\, & \kappa_{rM,0}+\kappa_{rM,pd}\left(A_{M,G}\mu_G+A_{M,\delta}\mu_\delta\right)+\left(\kappa_{rM,pd}-1\right)A_{M,0}+\mu_{dM}+m_0 \\ & -\kappa_{W,0}+\frac{\left(\sigma_{dM,c}-\lambda_c\right)^2}{2}+\frac{\left(\kappa_{rM,pd}A_{M,G}\sigma_G+\sigma_{dM,G}-\lambda_G\right)^2}{2} \\ & +\frac{\left(\kappa_{rM,pd}A_{M,\delta}\sigma_\delta+\sigma_{dM,\delta}-\lambda_\delta\right)^2}{2} \\ & +\frac{\left(\kappa_{rM,pd}A_{M,x}\sigma_x+\sigma_{dM,x}-\lambda_x\right)^2}{2}+\frac{\sigma_{dM}^2}{2} \\ & +\left(\left(\kappa_{rM,pd}\rho_G-1\right)A_{M,G}+m_G-\kappa_{W,G}\right)G_{W,t} \\ & +\left(\left(\kappa_{rM,pd}\rho_\delta-1\right)A_{M,\delta}+\rho_{dM,\delta}+\kappa_{rM,pd}A_{M,G}\rho_{G,\delta}+m_\delta-\kappa_{W,\delta}\right)\delta_t \\ & +\left(\left(\kappa_{rM,pd}\rho_x-1\right)A_{M,x}+\rho_{dM,x}+m_x\right)x_t. \end{aligned} \tag{A.87}$$

Finally, the coefficients in (A.83) are

$$A_{M,0}=\frac{1}{1-\kappa_{rM,pd}}\left(\begin{array}{l} \kappa_{rM,0}+\kappa_{rM,pd}\left(A_{M,G}\mu_G+A_{M,\delta}\mu_\delta\right)+\mu_{dM}+m_0 \\ -\kappa_{W,0}+\frac{\sigma_{dM}^2}{2}+\frac{\left(\sigma_{dM,c}-\lambda_c\right)^2}{2}+\frac{\left(\kappa_{rM,pd}A_{M,G}\sigma_G+\sigma_{dM,G}-\lambda_G\right)^2}{2} \\ +\frac{\left(\kappa_{rM,pd}A_{M,\delta}\sigma_\delta+\sigma_{dM,\delta}-\lambda_\delta\right)^2}{2}+\frac{\left(\kappa_{rM,pd}A_{M,x}\sigma_x+\sigma_{dM,x}-\lambda_x\right)^2}{2} \end{array}\right), \tag{A.88}$$

$$A_{M,G}=\frac{m_G-\kappa_{W,G}}{1-\kappa_{rM,pd}\rho_G}, \tag{A.89}$$

$$A_{M,\delta}=\frac{m_\delta+\rho_{dM,\delta}-\kappa_{W,\delta}+\kappa_{rM,pd}A_{M,G}\rho_{G,\delta}}{1-\kappa_{rM,pd}\rho_\delta}, \tag{A.90}$$

$$A_{M,x}=\frac{m_x+\rho_{dM,x}}{1-\kappa_{rM,pd}\rho_x}. \tag{A.91}$$

The return can be then rewritten as

$$
\begin{aligned}
r_{M,t+1} \simeq & \underbrace{\begin{pmatrix} -m_0 + \kappa_{W,0} - \frac{\left(\sigma_{dM,c}-\lambda_c\right)^2}{2} - \frac{\left(\kappa_{rM,pd}A_{M,G}\sigma_G+\sigma_{dM,G}-\lambda_G\right)^2}{2} \\ -\frac{\left(\kappa_{rM,pd}A_{M,\delta}\sigma_\delta+\sigma_{dM,\delta}-\lambda_\delta\right)^2}{2} - \frac{\left(\kappa_{rM,pd}A_{M,x}\sigma_x+\sigma_{dM,x}-\lambda_x\right)^2}{2} - \frac{\sigma_{dM}^2}{2} \end{pmatrix}}_{r_{M,0}} \\
& + \underbrace{\left(\kappa_{W,G} - m_G\right)}_{r_{M,G}} G_{W,t} + \underbrace{\left(\kappa_{W,\delta} - m_\delta\right)}_{r_{M,\delta}} \delta_t \underbrace{-m_x}_{r_{M,x}} x_t \\
& + \underbrace{\sigma_{dM,c}}_{\sigma_{rM,c}} \varepsilon_{c,t+1} + \underbrace{\left(\kappa_{rM,pd}A_{M,G}\sigma_G + \sigma_{dM,G}\right)}_{\sigma_{rM,G}} \varepsilon_{G,t+1} \\
& + \underbrace{\left(\kappa_{rM,pd}A_{M,\delta}\sigma_\delta + \sigma_{dM,\delta}\right)}_{\sigma_{rM,\delta}} \varepsilon_{\delta,t+1} \\
& + \underbrace{\left(\kappa_{rM,pd}A_{M,x}\sigma_x + \sigma_{dM,x}\right)}_{\sigma_{rM,x}} \varepsilon_{x,t+1} + \underbrace{\sigma_{dM}}_{\sigma_{rM,dM}} \varepsilon_{dM,t+1}.
\end{aligned} \tag{A.92}
$$

Recalling (12), the excess return $\hat{r}_{M,t+1} = r_{M,t+1} - r_{f,t+1}$ is thus

$$
\begin{aligned}
\hat{r}_{M,t+1} \simeq & \underbrace{\begin{pmatrix} \kappa_{W,0} - \frac{\left(\sigma_{dM,c}-\lambda_c\right)^2}{2} - \frac{\left(\kappa_{rM,pd}A_{M,G}\sigma_G+\sigma_{dM,G}-\lambda_G\right)^2}{2} \\ -\frac{\left(\kappa_{rM,pd}A_{M,\delta}\sigma_\delta+\sigma_{dM,\delta}-\lambda_\delta\right)^2}{2} - \frac{\left(\kappa_{rM,pd}A_{M,x}\sigma_x+\sigma_{dM,x}-\lambda_x\right)^2}{2} \\ -\frac{\sigma_{dM}^2}{2} + \frac{\lambda_c^2}{2} + \frac{\lambda_G^2}{2} + \frac{\lambda_\delta^2}{2} + \frac{\lambda_x^2}{2} \end{pmatrix}}_{\hat{r}_{M,0}} \\
& + \underbrace{\kappa_{W,G}}_{\hat{r}_{M,G}} G_{W,t} + \underbrace{\kappa_{W,\delta}}_{\hat{r}_{M,\delta}} \delta_t \\
& + \underbrace{\sigma_{dM,c}}_{\sigma_{rM,c}} \varepsilon_{c,t+1} + \underbrace{\left(\kappa_{rM,pd}A_{M,G}\sigma_G + \sigma_{dM,G}\right)}_{\sigma_{rM,G}} \varepsilon_{G,t+1} \\
& + \underbrace{\left(\kappa_{rM,pd}A_{M,\delta}\sigma_\delta + \sigma_{dM,\delta}\right)}_{\sigma_{rM,\delta}} \varepsilon_{\delta,t+1} \\
& + \underbrace{\left(\kappa_{rM,pd}A_{M,x}\sigma_x + \sigma_{dM,x}\right)}_{\sigma_{rM,x}} \varepsilon_{x,t+1} + \underbrace{\sigma_{dM}}_{\sigma_{rM,dM}} \varepsilon_{dM,t+1}.
\end{aligned} \tag{A.93}
$$

$\psi > 1$ is a sufficient condition for $A_{M,G} > 0$. When $\rho_{G,\delta} = 0$, if in addition $\bar{G}_W > -\frac{m_\delta+\rho_{dM,\delta}}{1-\bar{\delta}\left(m_\delta+\rho_{dM,\delta}\right)}$, then $A_{M,\delta} > 0$ ($\bar{G}_W > 0$ is a sufficient condition for the positivity of $A_{M,\delta}$). In this case, expected returns are negatively correlated with G_t and δ_t, as $r_{M,G}, r_{M,\delta} < 0$. The market portfolio in Proposition 3 is characterized imposing $\rho_{G,\delta} = \rho_{dM,\delta} = \sigma_{dM,G} = \sigma_{dM,\delta} = \sigma_{dM,x} = 0$.

B Summary statistics

Table A.1 tabulates the summary statistics of the value-weighted portfolios sorted by prior ESG and environmental scores, constructed following the methodology outlined in Section 3. Panel (a) refers to portfolios constructed using the entire universe, while Panel (b) is based on the universe excluding stocks in the technology sector.

Next, we analyze the weighted-average ESG profile by industry of the stocks in our sample. To do so, we adopt the Fama-French five-industry definitions and identify stocks in our sample based on their SIC codes. The time series of capitalization-weighted ESG and environmental-pillar scores for each of the industry sectors are shown in Figure A.1. As displayed in Panel (a), no specific industry sector exhibits an ESG score that is consistently above or below the others. Furthermore, the industry-level ESG scores are always comprised between -0.1 and 0.2. These observations imply that, according to the ESG scores used for the analysis, no industry sector is specifically green or brown.

We also assess the prominence of each industry sector in the market portfolio, as well as in the ESG and environmental-pillar sorted portfolios. The left graphs in Figure A.2 illustrate, for each portfolio, the time series of the ratios between the total capitalization of each industry sector and the overall market capitalization. Similarly, the right graphs display the time series of the ratios between the number of stocks within a specific sector and the total number of stocks in the universe.

C Estimation methodology

To perform the estimation, we use the Kalman filter (Hamilton, 1994) to write a likelihood function that is then numerically maximized relative to the parameter space. We first develop the state space representation, jointly considering the equations representing the dynamics of consumption growth in (6), aggregate ESG supply and demand in (8) and (9), long-run risk in (7), the grenness of portfolio j ($j = \{br, neu, gr\}$) in (13), market excess return in (A.93), and individual portfolio excess returns in (A.77):

$$\Delta c_{t+1} = \mu_c + x_t + \sigma_c \varepsilon_{c,t+1}, \tag{C.1}$$

$$G_{W,t+1} = \mu_G + \rho_G G_{W,t} + \rho_{G,\delta}\delta_t + \sigma_G \varepsilon_{G,t+1}, \tag{C.2}$$

$$\delta_{t+1} = \mu_\delta + \rho_\delta \delta_t + \sigma_\delta \varepsilon_{\delta,t+1}, \tag{C.3}$$

$$x_{t+1} = \rho_x x_t + \sigma_x \varepsilon_{x,t+1}, \tag{C.4}$$

$$G_{j,t+1} = \mu_{Gj} + \rho_{Gj,\delta}\delta_t + \rho_{Gj} G_{j,t} + \sigma_{Gj,G}\varepsilon_{G,t+1} + \sigma_{Gj}\varepsilon_{Gj,t+1}, \tag{C.5}$$

$$\begin{aligned} \hat{r}_{M,t+1} \simeq\ & \hat{r}_{M,0} + \hat{r}_{M,G} G_{W,t} + \hat{r}_{M,\delta}\delta_t + \hat{r}_{M,x} x_t \\ & + \sigma_{rM,c}\varepsilon_{c,t+1} + \sigma_{rM,G}\varepsilon_{G,t+1} + \sigma_{rM,\delta}\varepsilon_{\delta,t+1} \\ & + \sigma_{rM,x}\varepsilon_{x,t+1} + \sigma_{rM,dM}\varepsilon_{dM,t+1}, \end{aligned} \tag{C.6}$$

$$\begin{aligned} \hat{r}_{j,t+1} \simeq\ & \hat{r}_{j,0} + \hat{r}_{j,G} G_{W,t} + \hat{r}_{j,\delta}\delta_t + \hat{r}_{j,x} x_t + \hat{r}_{j,Gj} G_{j,t} \\ & + \sigma_{rj,c}\varepsilon_{c,t+1} + \sigma_{rj,G}\varepsilon_{G,t+1} + \sigma_{rj,\delta}\varepsilon_{\delta,t+1} + \sigma_{rj,x}\varepsilon_{x,t+1} \\ & + \sigma_{rj,Gj}\varepsilon_{Gj,t+1} + \sigma_{rj,dM}\varepsilon_{dM,t+1} + \sigma_{rj,dj}\varepsilon_{dj,t+1}. \end{aligned} \tag{C.7}$$

Note that the right-hand side depends on the current value of the state variables $G_{W,t}$, δ_t, x_t, and $G_{j,t}$, as well as on the innovations $\varepsilon_{c,t+1}$, $\varepsilon_{G,t+1}$, $\varepsilon_{\delta,t+1}$, $\varepsilon_{x,t+1}$, $\varepsilon_{Gj,t+1}$, $\varepsilon_{dM,t+1}$, and $\varepsilon_{dj,t+1}$. The equations can be stacked through a VAR representation:

$$\boldsymbol{X}_{t+1} = \boldsymbol{A_X} + \boldsymbol{B_X}\boldsymbol{X}_t + \boldsymbol{\sigma_X}\boldsymbol{\varepsilon}_{t+1}, \tag{C.8}$$

where:

$$\boldsymbol{X}_t = \begin{bmatrix} \Delta c_t \\ G_{W,t} \\ \delta_t \\ x_t \\ \vdots \\ G_{j,t} \\ \vdots \\ \hat{r}_{M,t+1} \\ \vdots \\ \hat{r}_{j,t+1} \\ \vdots \end{bmatrix}, \quad \boldsymbol{A}_{\boldsymbol{X}} = \begin{bmatrix} \mu_c \\ \mu_G \\ \mu_\delta \\ 0 \\ \vdots \\ \mu_{Gj} \\ \vdots \\ \hat{r}_{M,0} \\ \vdots \\ \hat{r}_{j,0} \\ \vdots \end{bmatrix}, \quad \boldsymbol{\varepsilon}_{t+1} = \begin{bmatrix} \varepsilon_{c,t+1} \\ \varepsilon_{G,t+1} \\ \varepsilon_{\delta,t+1} \\ \varepsilon_{x,t+1} \\ \vdots \\ \varepsilon_{Gj,t+1} \\ \vdots \\ \varepsilon_{dM,t+1} \\ \vdots \\ \varepsilon_{dj,t+1} \\ \vdots \end{bmatrix}, \tag{C.9}$$

$$\boldsymbol{B}_{\boldsymbol{X}} = \begin{bmatrix} 0 & 0 & 0 & 1 & \cdots & 0 & \cdots & 0 & 0 & \cdots & 0 & \cdots \\ 0 & \rho_G & \rho_{G,\delta} & 0 & \cdots & 0 & \cdots & 0 & 0 & \cdots & 0 & \cdots \\ 0 & 0 & \rho_\delta & 0 & \cdots & 0 & \cdots & 0 & 0 & \cdots & 0 & \cdots \\ 0 & 0 & 0 & \rho_x & \cdots & 0 & \cdots & 0 & 0 & \cdots & 0 & \cdots \\ \vdots & \vdots & \vdots & \vdots & \ddots & 0 & 0 & 0 & 0 & \cdots & 0 & \cdots \\ 0 & 0 & \rho_{Gj,\delta} & 0 & 0 & \rho_{Gj} & 0 & 0 & 0 & \cdots & 0 & \cdots \\ \vdots & \vdots & \vdots & \vdots & 0 & 0 & \ddots & 0 & 0 & \cdots & 0 & \cdots \\ 0 & \hat{r}_{M,G} & \hat{r}_{M,\delta} & \hat{r}_{M,x} & \cdots & 0 & \cdots & 0 & 0 & \cdots & 0 & \cdots \\ \vdots & \vdots & \vdots & \vdots & \ddots & 0 & 0 & 0 & 0 & \cdots & 0 & \cdots \\ 0 & \hat{r}_{j,G} & \hat{r}_{j,\delta} & \hat{r}_{j,x} & 0 & \hat{r}_{j,Gj} & 0 & 0 & 0 & \cdots & 0 & \cdots \\ \vdots & \vdots & \vdots & \vdots & 0 & 0 & \ddots & 0 & 0 & \cdots & 0 & \cdots \end{bmatrix}, \tag{C.10}$$

$$\boldsymbol{\sigma}_{\boldsymbol{X}} = \begin{bmatrix} \sigma_c & 0 & 0 & 0 & 0 & 0 & 0 & 0 & \cdots & 0 & \cdots \\ 0 & \sigma_G & 0 & 0 & 0 & 0 & 0 & 0 & \cdots & 0 & \cdots \\ 0 & 0 & \sigma_\delta & 0 & 0 & 0 & 0 & 0 & \cdots & 0 & \cdots \\ 0 & 0 & 0 & \sigma_x & 0 & 0 & 0 & 0 & \cdots & 0 & \cdots \\ \vdots & \vdots & \vdots & \vdots & \ddots & 0 & 0 & \vdots & \cdots & 0 & \cdots \\ 0 & \sigma_{Gj,G} & 0 & 0 & 0 & \sigma_{Gj} & 0 & 0 & \cdots & 0 & \cdots \\ \vdots & \vdots & \vdots & \vdots & 0 & 0 & \ddots & \vdots & \cdots & 0 & \cdots \\ \sigma_{rM,c} & \sigma_{rM,G} & \sigma_{rM,\delta} & \sigma_{rM,x} & \cdots & 0 & \cdots & \sigma_{rM,dM} & \cdots & 0 & \cdots \\ \vdots & \vdots & \vdots & \vdots & \ddots & 0 & 0 & \vdots & \ddots & 0 & 0 \\ \sigma_{rj,c} & \sigma_{rj,G} & \sigma_{rj,\delta} & \sigma_{rj,x} & 0 & \sigma_{rj,Gj} & 0 & \sigma_{rj,dM} & 0 & \sigma_{rj,dj} & 0 \\ \vdots & \vdots & \vdots & \vdots & 0 & 0 & \ddots & \vdots & 0 & 0 & \ddots \end{bmatrix}. \tag{C.11}$$

We consider as observables the real monthly consumption growth, the ESG scores of the market (proxying for the greenness of the aggregate wealth portfolio) and its excess return, as well as the ESG scores of the portfolios and their monthly returns. We stack these variables in the vector $\boldsymbol{Y}_t$:

$$\boldsymbol{Y}_t = \begin{bmatrix} \Delta c_t & G_{W,t} & \cdots & G_{j,t} & \cdots & \hat{r}_{M,t} & \cdots & \hat{r}_{j,t} & \cdots \end{bmatrix}'. \tag{C.12}$$

The observation equation of the Kalman filter (with zero observation errors) is given by

$$\boldsymbol{Y}_t = \boldsymbol{H}\boldsymbol{X}_t, \tag{C.13}$$

and $\boldsymbol{H}$ is a sparse matrix loading with unit weights the elements of $\boldsymbol{X}_t$ that belong to $\boldsymbol{Y}_t$:

$$\boldsymbol{H} = \begin{bmatrix} 1 & 0 & 0 & 0 & 0 & 0 & \cdots & 0 \\ 0 & 1 & 0 & 0 & 0 & 0 & \cdots & 0 \\ 0 & 0 & 0 & 0 & 1 & 0 & \cdots & 0 \\ 0 & 0 & 0 & 0 & 0 & 1 & \cdots & 0 \\ \vdots & \vdots & \vdots & \vdots & \vdots & \vdots & \ddots & \vdots \\ 0 & 0 & 0 & 0 & 0 & 0 & 0 & 1 \end{bmatrix}. \tag{C.14}$$

The prediction stage is described by the following transition equations, which provide the time-t conditional expectation and covariances of the state variables in $t+1$:

$$\boldsymbol{X}_{t+1|t} = \boldsymbol{A}_{\boldsymbol{X}} + \boldsymbol{B}_{\boldsymbol{X}}\boldsymbol{X}_{t|t}, \tag{C.15}$$

$$\boldsymbol{\Sigma}^X_{t+1|t} = \boldsymbol{B}_{\boldsymbol{X}}\boldsymbol{\Sigma}^X_{t|t}\boldsymbol{B}'_{\boldsymbol{X}} + \boldsymbol{\sigma}_{\boldsymbol{X}}\boldsymbol{\sigma}'_{\boldsymbol{X}}, \tag{C.16}$$

$\boldsymbol{X}_{1|0}$ is initialized considering the initial values of the observable variables, complemented by δ_0 and x_0, which belong to the parameter space and represent the unobservable initial values of the processes δ_t and x_t. $\boldsymbol{\Sigma}^X_{1|0}$ is initialized at $\boldsymbol{\sigma}_{\boldsymbol{X}}\boldsymbol{\sigma}'_{\boldsymbol{X}}$. The predicted vector of observables is thus $\boldsymbol{Y}_{t+1|t} = \boldsymbol{H}\boldsymbol{X}_{t+1|t}$. The updating equations, which consider the $t+1$ observed values $\boldsymbol{Y}_{t+1}$, are then

$$\boldsymbol{X}_{t+1|t+1} = \boldsymbol{X}_{t+1|t} + \boldsymbol{K}_{t+1}\left(\boldsymbol{Y}_{t+1} - \boldsymbol{H}\boldsymbol{X}_{t+1|t}\right), \tag{C.17}$$

$$\boldsymbol{\Sigma}^X_{t+1|t+1} = \boldsymbol{\Sigma}^X_{t+1|t} - \boldsymbol{K}_{t+1}\left(\boldsymbol{H}\boldsymbol{\Sigma}^X_{t+1|t}\boldsymbol{H}'\right)\boldsymbol{K}'_{t+1}, \tag{C.18}$$

where $\boldsymbol{K}_{t+1} = \boldsymbol{\Sigma}^X_{t+1|t}\boldsymbol{H}'\left(\boldsymbol{H}\boldsymbol{\Sigma}^X_{t+1|t}\boldsymbol{H}'\right)^{-1}$ is the Kalman gain. Given a candidate set of model parameters Θ, equations (C.15) through (C.18) are evaluated recursively. Then, for each time step, the following log-likelihood function is evaluated

$$\begin{aligned} \ell_{t+1}(\Theta) = & -\frac{n}{2}\log(2\pi) - \frac{1}{2}\log\left|\boldsymbol{H}\boldsymbol{\Sigma}^X_{t+1|t}\boldsymbol{H}'\right| \\ & -\frac{1}{2}\left(\boldsymbol{Y}_t - \boldsymbol{H}\boldsymbol{X}_{t+1|t}\right)'\left(\boldsymbol{H}\boldsymbol{\Sigma}^X_{t+1|t}\boldsymbol{H}'\right)^{-1}\left(\boldsymbol{Y}_t - \boldsymbol{H}\boldsymbol{X}_{t+1|t}\right). \end{aligned} \tag{C.19}$$

The total log-likelihood, $\ell(\Theta) = \sum_{t=1}^{T} \ell_t(\Theta)$, is numerically maximized with respect to the parameter space Θ to obtain the model estimates. In the optimization, we impose the long-run means of the aggregate ESG score, $\bar{G}_W$, and the individual asset scores, $\bar{G}_n$, to be equal to their sample means. Similarly, $\bar{\delta}$ is equal the sample mean of the filtered state variable δ_t. We further set the long-run means of the model-implied price-to-dividend ratios of the market portfolios and individual assets to match the sample average of the observed price-to-dividend ratios. Finally, δ_t is restricted to be nonnegative.

D Supplementary empirical findings

D.1 Supplementary empirical findings based on environmental-pillar scores

Figure A.3 displays time-series findings obtained by estimating the model using environmental-pillar scores. In particular, the figure shows the expected consumption growth, as well as environmental scores, expected excess returns, convenience yields, total ESG premium, and price-to-dividend ratios of the market portfolio and of the portfolios constructed by sorting stocks based on their environmental-pillar scores.

D.2 Supplementary empirical findings excluding stocks in the technology sector

We report the empirical results obtained by estimating the model when stocks in the technology sector are excluded from the investable universe. In each of the tables and figures mentioned below, the findings are obtained observing ESG scores in Panel (a) and environmental-pillar scores in Panel (b).

Figure A.4 displays the time series of aggregate demand and supply for ESG and environmental attributes. ESG demand exhibits a very similar pattern to that obtained using the entire universe (Figure 2a), while demand for environmental attributes reaches even higher values than for the baseline findings in Figure 2b.

Table A.2 reports the parameter estimates, with findings overall in line with those obtained considering the entire universe (Table 1). For instance, risk aversion is insignificantly different from 10, the prices of risk are all positive and significant, and the brown portfolio is more exposed to long-run risk shocks than the green portfolio ($\rho_{dbr} > \rho_{dgr}$).

Table A.3 reports the model-implied decomposition of excess returns. Similar to the baseline findings in Table 2, the green-minus-brown displays a positive and significant ESG demand risk premium, which partially offsets the negative average convenience yield premium. The positive and significant average unexpected return induced by shocks to ESG demand adds to the negative conditional expected return and is essential to match the positive return observed in the data.

Finally, Figures A.5 and A.6 display time-series evidence that is consistent with that obtained considering the entire universe, shown in Figures 3, A.3, and 4.

E Supplementary calibration exercises

E.1 Shocks to ESG demand and ESG score in the presence of correlated cashflows

In this section, we perform a set of supplementary analyses studying the impact of dividend growth rates that are correlated with shocks to ESG demand or ESG scores.

In the first analysis, dividend growth is allowed to be correlated with innovations of ESG demand and of the asset's ESG score. This implies relaxing the hypothesis that the coefficients $\sigma_{dn,\delta}$ and $\sigma_{dn,Gn}$, appearing in equation (A.65), are equal to zero.

To allow for a conditional correlation between dividend growth and ESG demand, we consider the baseline parameter values reported in Section 4.2 and replace $\sigma_{dn,\delta}$ (which baseline value is zero) and σ_{dn} with $\tilde{\sigma}_{dn,\delta}$ and $\tilde{\sigma}_{dn}$, respectively, such that i) the conditional correlation between dividend growth and ESG demand equals the value we aim to impose, $\text{Corr}_t\left[\Delta d_{n,t+1}, \delta_{t+1}\right]$, and ii) the total dividend growth volatility, $\sigma_{dn,tot}$, is the same as the estimated one:

$$\sigma_{dn,tot} = \sqrt{\sigma_{dn,c}^2 + \sigma_{dn,G}^2 + \sigma_{dn,\delta}^2 + \sigma_{dn,x}^2 + \sigma_{dn,Gn}^2 + \sigma_{dn,dM}^2 + \sigma_{dn}^2}, \tag{E.1}$$

$$\tilde{\sigma}_{dn,\delta} = \sigma_{dn,tot} \cdot \text{Corr}_t\left[\Delta d_{n,t+1}, \delta_{t+1}\right], \tag{E.2}$$

$$\tilde{\sigma}_{dn} = \sqrt{\sigma_{dn,tot}^2 - \left(\sigma_{dn,c}^2 + \sigma_{dn,G}^2 + \tilde{\sigma}_{dn,\delta}^2 + \sigma_{dn,x}^2 + \sigma_{dn,Gn}^2 + \sigma_{dn,dM}^2\right)}. \tag{E.3}$$

The graphs in Figure A.7 show that, when dividend growth is positively correlated with ESG demand, the expected return of the green-minus-brown spread portfolio increases relative to the zero correlation case, while a negative correlation implies a lower expected return. This is because the positive correlation implies a return contribution that is also positively correlated with ESG demand, and thus a higher loading on the positive price of risk of ESG demand. If the green (brown) asset's dividend growth is positively (negatively) correlated with ESG demand, during a positive ESG demand shock the positive realized return gap in favor of the green asset widens, while the equilibrium expected return gap in favor of the brown asset shrinks. In this case, the positive effect on the cumulative return of the green-minus-brown portfolio is stronger and vanishes over a longer period relative to the zero correlation case.

Similarly, to allow for a conditional correlation between dividend growth and the asset's ESG score, $\text{Corr}_t\left[\Delta d_{n,t+1}, G_{n,t+1}\right]$, we determine $\tilde{\sigma}_{dn,Gn}$ and $\tilde{\sigma}_{dn}$ such that:

$$\sigma_{dn,tot} = \sqrt{\sigma_{dn,c}^2 + \sigma_{dn,G}^2 + \sigma_{dn,\delta}^2 + \sigma_{dn,x}^2 + \sigma_{dn,Gn}^2 + \sigma_{dn,dM}^2 + \sigma_{dn}^2}, \tag{E.4}$$

$$\tilde{\sigma}_{dn,Gn} = \sigma_{dn,tot} \cdot \text{Corr}_t\left[\Delta d_{n,t+1}, G_{n,t+1}\right], \tag{E.5}$$

$$\tilde{\sigma}_{dn} = \sqrt{\sigma_{dn,tot}^2 - \left(\sigma_{dn,c}^2 + \sigma_{dn,G}^2 + \sigma_{dn,\delta}^2 + \sigma_{dn,x}^2 + \tilde{\sigma}_{dn,Gn}^2 + \sigma_{dn,dM}^2\right)}. \tag{E.6}$$

The graphs in Figure A.8 show the response to an annual shock to the ESG score of the green asset. When the correlation between the dividend growth and the ESG score is zero, the effects on returns are qualitatively similar to those described for an aggregate ESG demand shock, while the impact on both expected and realized returns is slightly weaker. This is because a positive shock to the ESG score triggers only an increase in the convenience yield, but does not imply a reducing risk-free rate.

A positive correlation between dividend growth and ESG score is plausible if an improvement of the firm's ESG profile triggers a higher demand for goods and services and thus higher cashflows. Then, the realized return corresponding to the positive ESG score shock can be significantly higher than that in the baseline case. The correlation between dividend growth and ESG score could yet be negative. For instance, this could result from increasing costs incurred for the improvement of the firm's sustainability profile. Then, the negative cashflow effect could imply a lower, even negative, realized return due to the unexpected ESG score improvement.

E.2 Effect of ESG demand on ESG supply

The graphs in Figure A.9 show the responses to a one-standard deviation positive annual shock applied to ESG demand when the parameters $\rho_{G,\delta}$ and $\rho_{Gn,\delta}$ in equations (A.34) and (A.64) are allowed to be nonzero. Positive values would capture the endogenous increase in ESG supply upon increasing ESG preferences. For instance, a value $\rho_{Ggr,\delta} = 5$ (10) implies that, following a positive one-standard deviation annual shock to δ_t, the long-run ESG scores of the green asset increases by about 8 (16) percentile points.[1]

In our calibration, when the drift of ESG scores is positively related to ESG demand ($\rho_{G,\delta}, \rho_{Gn,\delta} > 0$), the realized return contemporaneous to the shock of both the green and brown assets are higher than in the base case ($\rho_{G,\delta} = \rho_{Gn,\delta} = 0$). A similar effect is observed on the valuation of the assets following the shock, as the nonpecuniary benefits are higher than in the base case for both assets. As the correlation between the nonpecuniary benefits of the green (brown) asset and the nonpecuniary benefits of the wealth portfolio is higher (lower) than in the base case, the expected return of the green (brown) asset is also higher (lower).

Remarkably, while the values considered for the parameters $\rho_{G,\delta}$ and $\rho_{Gn,\delta}$ imply sizable effects of an increase in ESG demand on ESG scores, the impulse response exercise highlights that the key model implications on expected and realized returns are qualitatively unchanged relative to the baseline specification.

[1]The variation of the long-run ESG score of asset n corresponding to an increase in ESG preferences $\Delta\delta$ is given by $\frac{\rho_{Gn,\delta}\Delta\delta}{1-\rho_{Gn}}$.

Figure A.1: Capitalization-weighted ESG and environmental scores by industry sector.

The figure shows the time series of the capitalization-weighted ESG and environmental scores by industrial sector, as well as of the market portfolio.

(a) ESG scores by industry sector

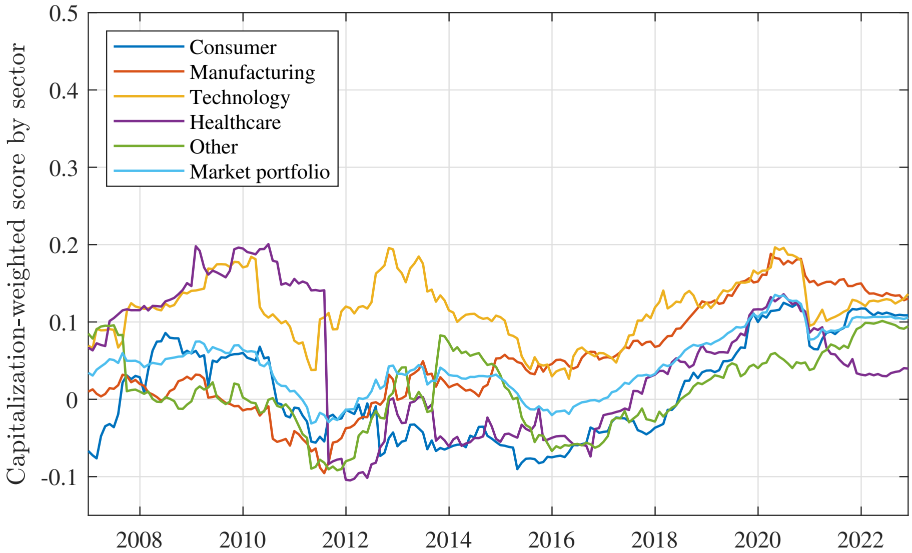

(b) Environmental scores by industry sector

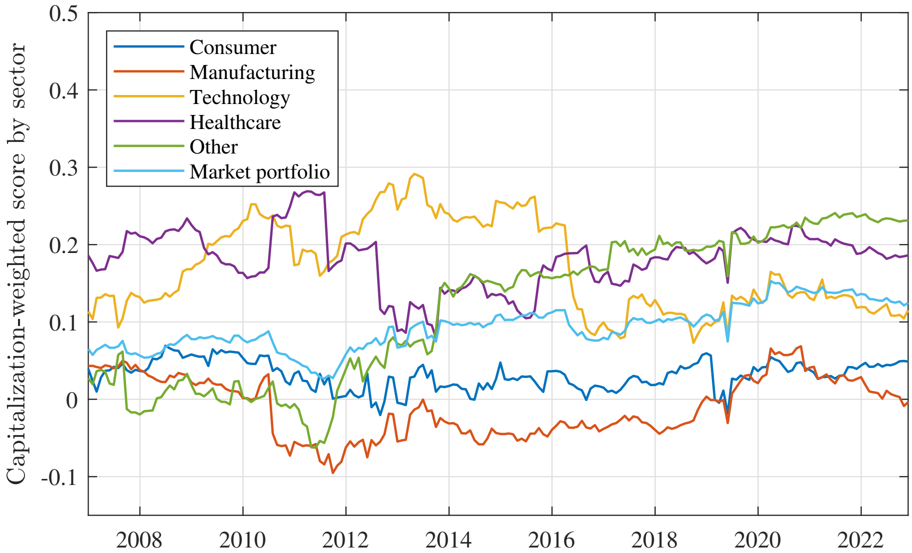

Figure A.2: Relative capitalization and number of stocks in ESG and environmental score-sorted portfolios by industry sector.

The graphs show the time series of the relative capitalization and number of stocks of the five industry sectors within the market and score-sorted portfolios. Panel (a) is based on ESG scores, Panel (b) is based on environmental scores.

(a) Portfolios based on ESG scores

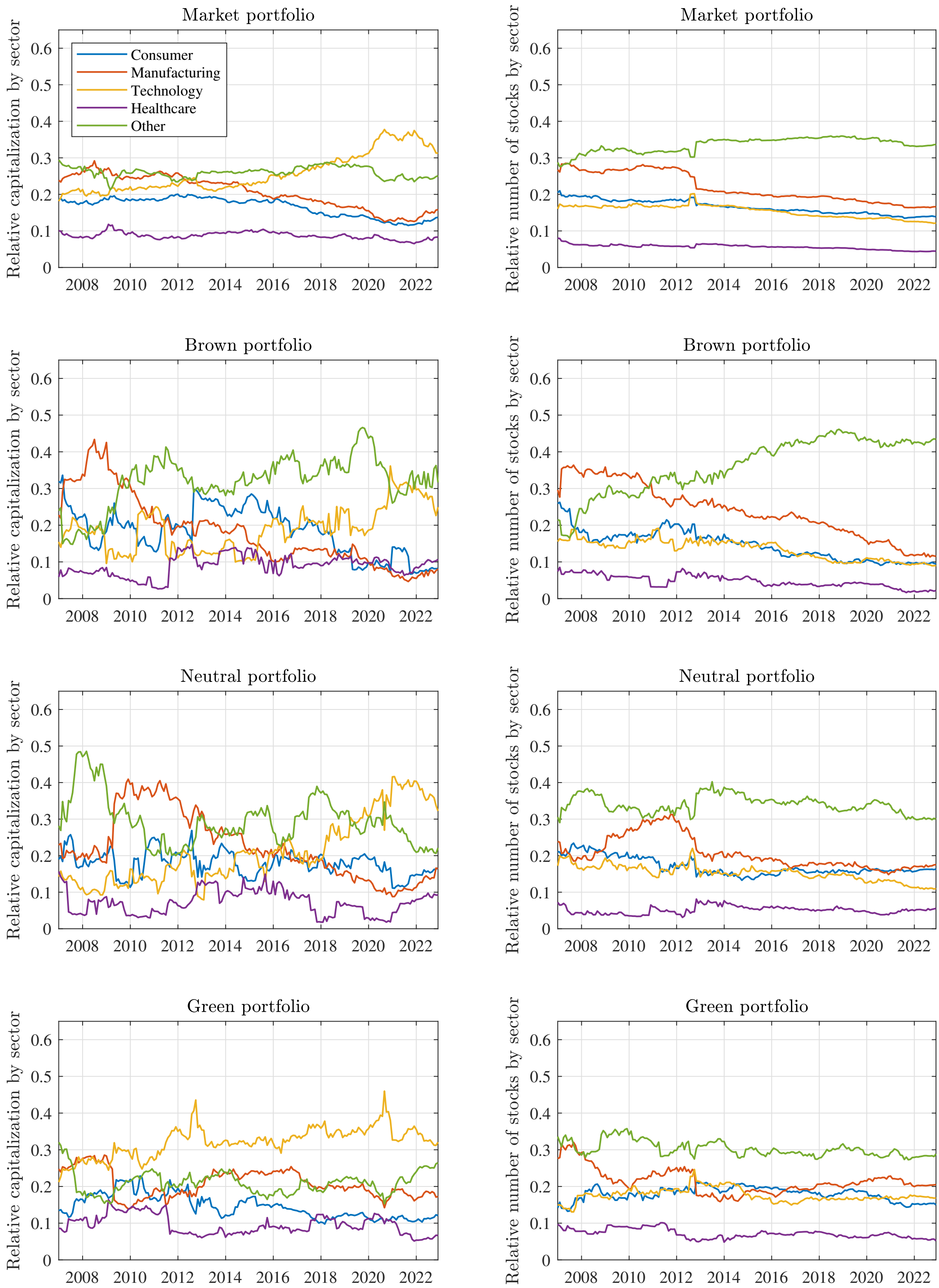

Figure A.2 (continued)

(b) Portfolios based on environmental scores

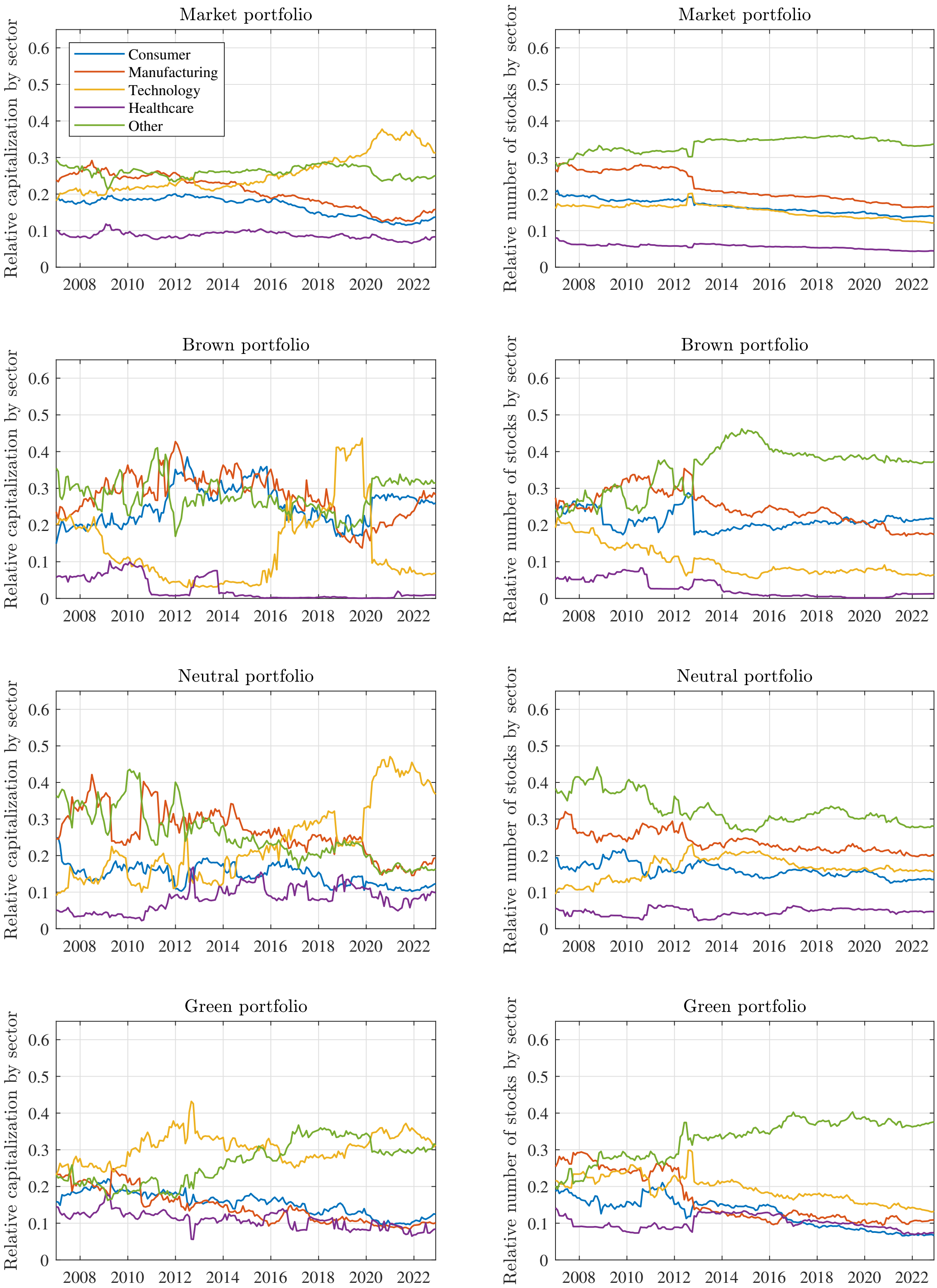

Figure A.3: Time series of expected consumption growth, environmental scores, expected excess returns, and price-to-dividend ratios.

The figure shows the estimated time series of expected consumption growth, environmental scores, expected market and portfolio excess returns, convenience yields from environmental ESG investing, total environmental ESG premia, as well as price-to-annual dividend ratios. All quantities are annualized. The green, neutral, and brown portfolios are obtained sorting stocks by environmental scores. The estimation is performed by maximum likelihood, observing the time series of market and portfolio returns, environmental scores, and consumption growth, as well as average price-to-dividend ratios. The sample runs from January 2007 to December 2022.

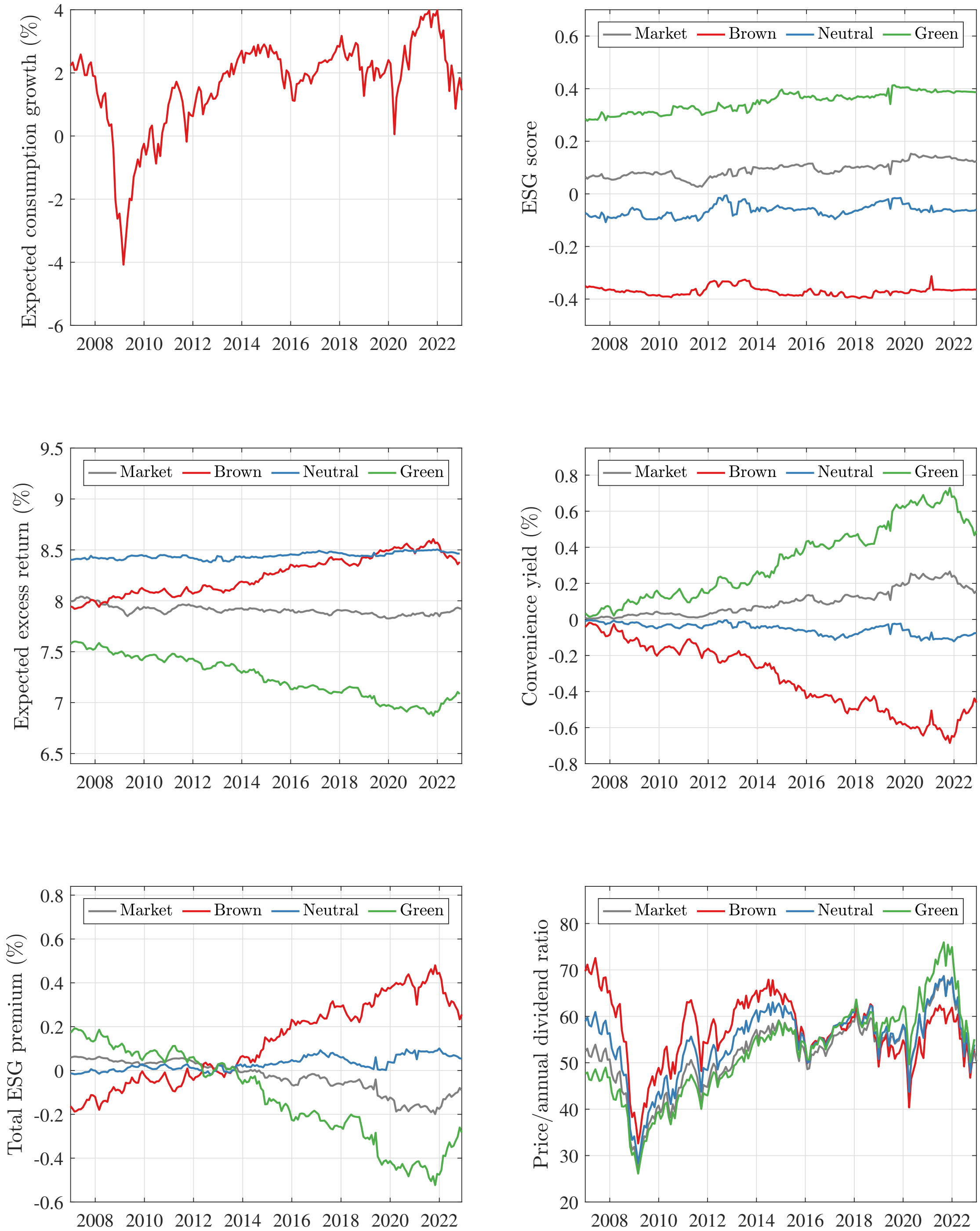

Figure A.4: Time series of aggregate demand and supply for ESG and environmental attributes (excluding stocks in the technology sector).

The figure shows the estimated time series of aggregate ESG demand, δ_t, and supply, $G_{W,t}$. The sample runs from January 2007 to December 2022.

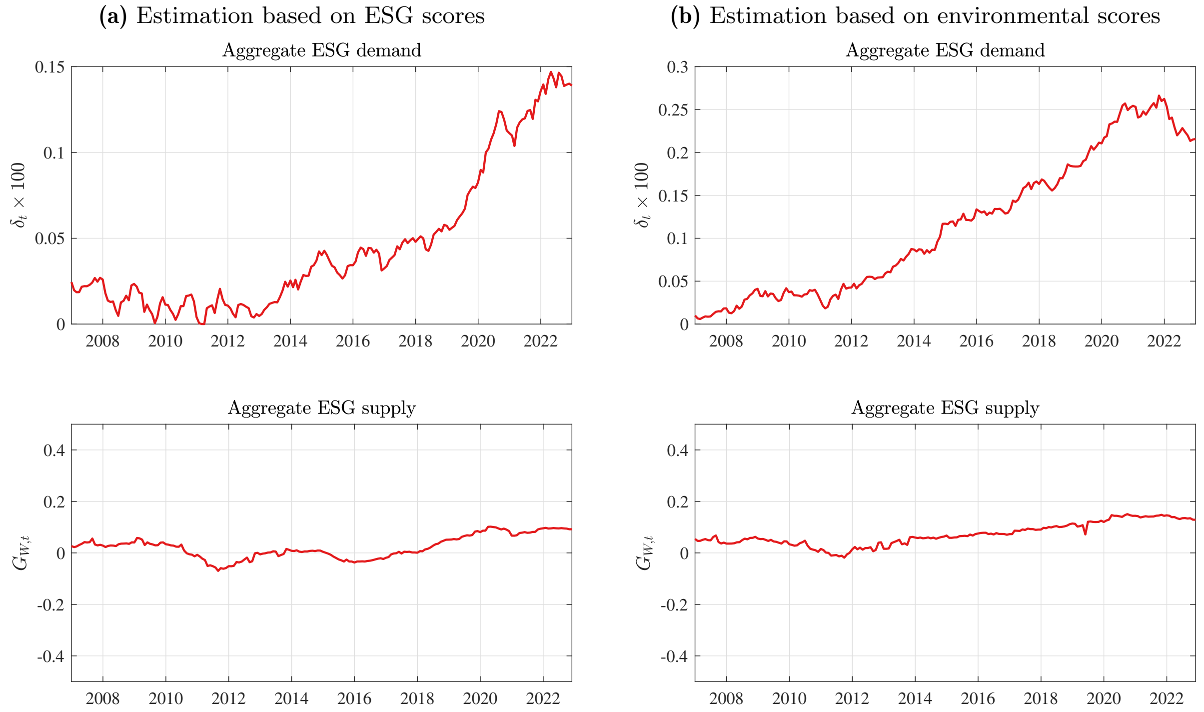

Figure A.5: Time series of expected consumption growth, ESG scores, expected excess returns, and price-to-dividend ratios (excluding stocks in the technology sector).

The figure shows the estimated time series of expected consumption growth, ESG scores, expected market and portfolio excess returns, convenience yields from ESG investing, total ESG premia, as well as price-to-annual dividend ratios. All quantities are annualized. The green, neutral, and brown portfolios are obtained sorting stocks by ESG score. The portfolios are obtained excluding the technology sector and value-weighting stocks sorted by their ESG scores in Panel (a) and environmental scores in Panel (b). The estimation is performed by maximum likelihood, observing the time series of market and portfolio returns, ESG or environmental ratings, and consumption growth, as well as average price-to-dividend ratios. The sample runs from January 2007 to December 2022.

(a) Estimation based on ESG scores

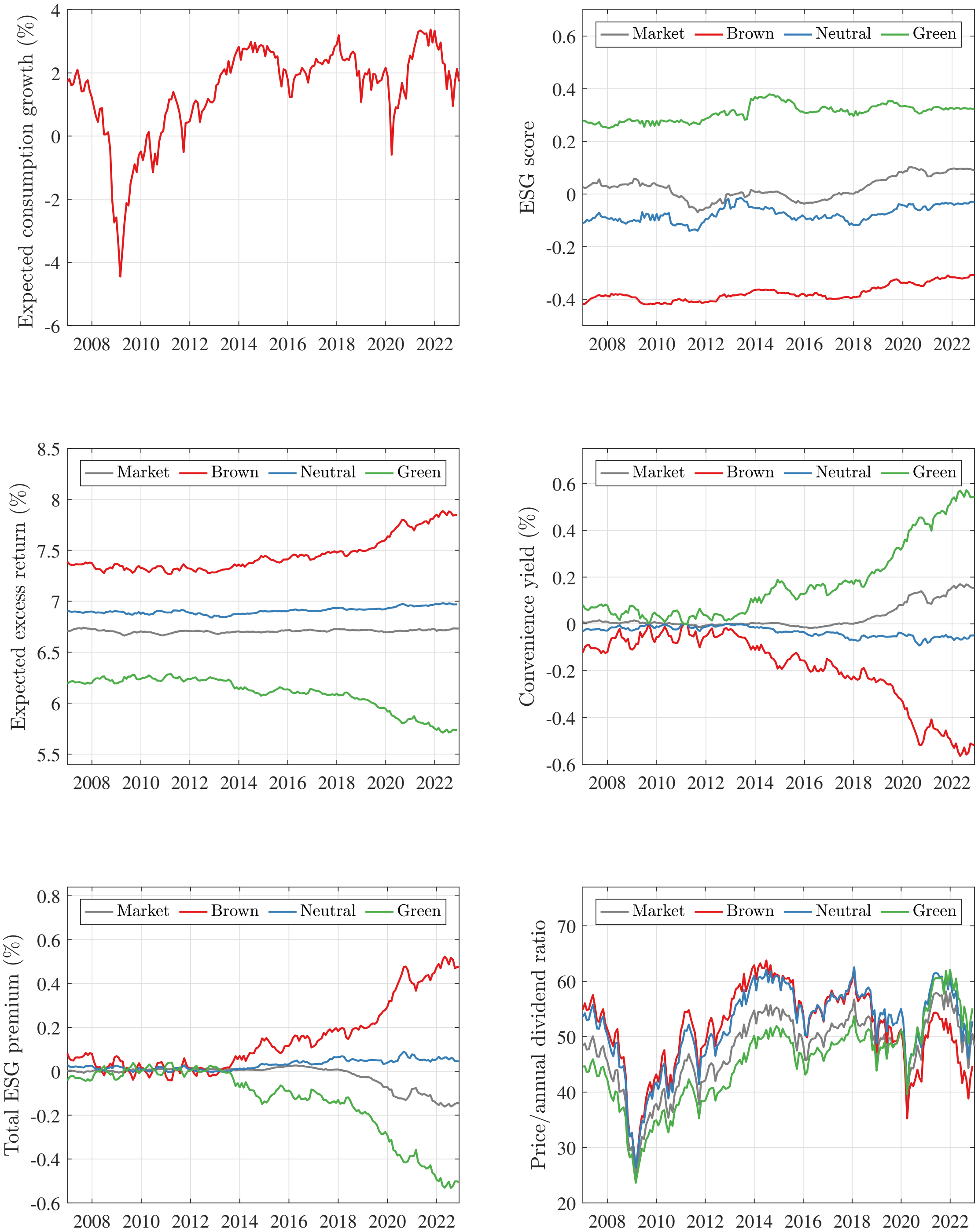

Figure A.5 (continued)

(b) Estimation based on environmental scores

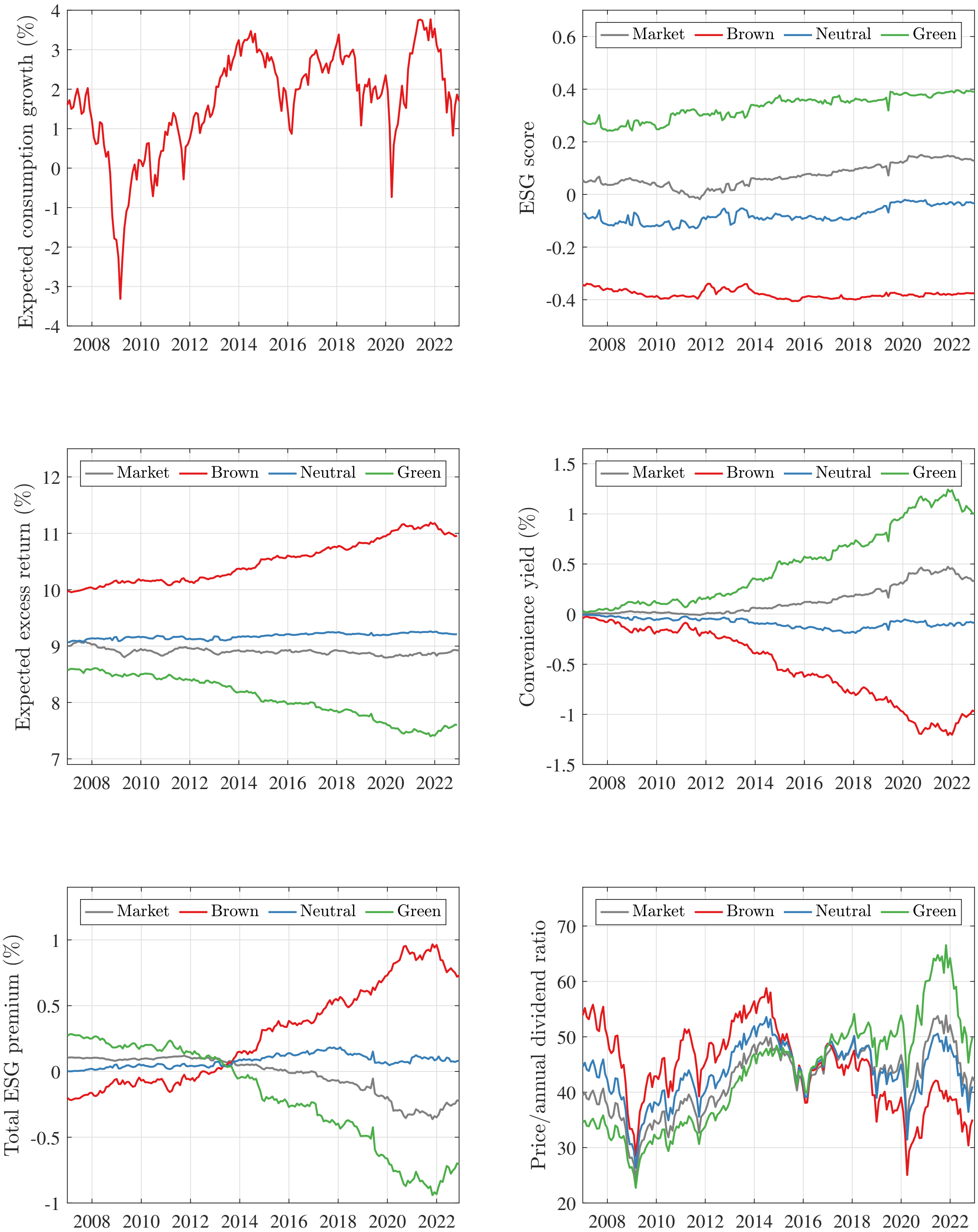

Figure A.6: Returns of green-minus-brown portfolio (excluding stocks in the technology sector).

The left graphs show the realized cumulative logarithmic return of the green-minus-brown portfolio, as well as the model-implied expected return, the unexpected return contribution attributable to ESG demand shocks, and the model-implied expected return augmented by the unexpected return contribution attributable to ESG demand shocks. The right graphs show the 12-month rolling logarithmic return of the same portfolio. The portfolios are obtained excluding the technology sector and value-weighting stocks sorted by their ESG scores in Panel (a) and environmental scores in Panel (b). The estimation is performed by maximum likelihood, observing the time series of market and portfolio returns, ESG or environmental ratings, and consumption growth, as well as average price-to-dividend ratios. The sample runs from January 2007 to December 2022.

(a) Green and brown portfolios based on ESG-scores

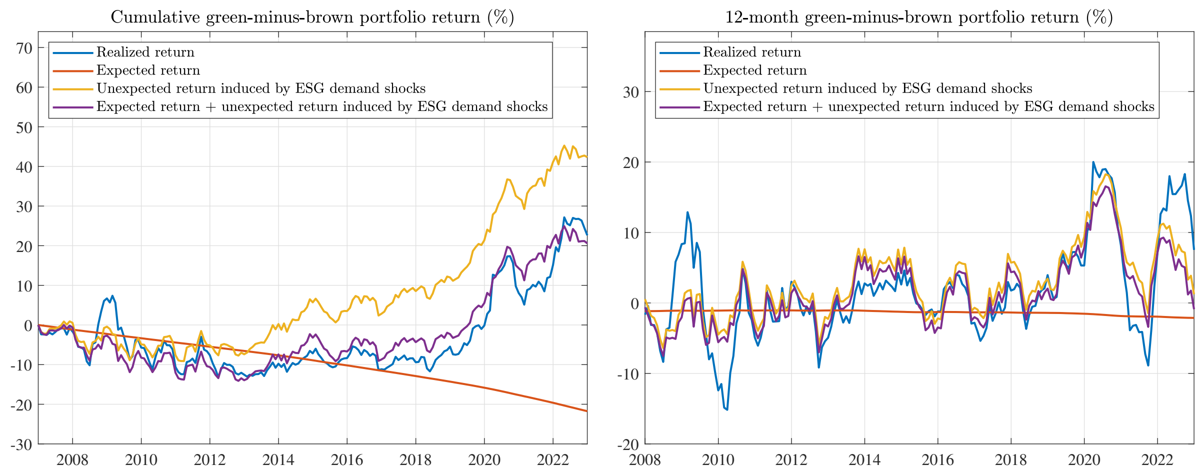

(b) Green and brown portfolios based on environmental scores

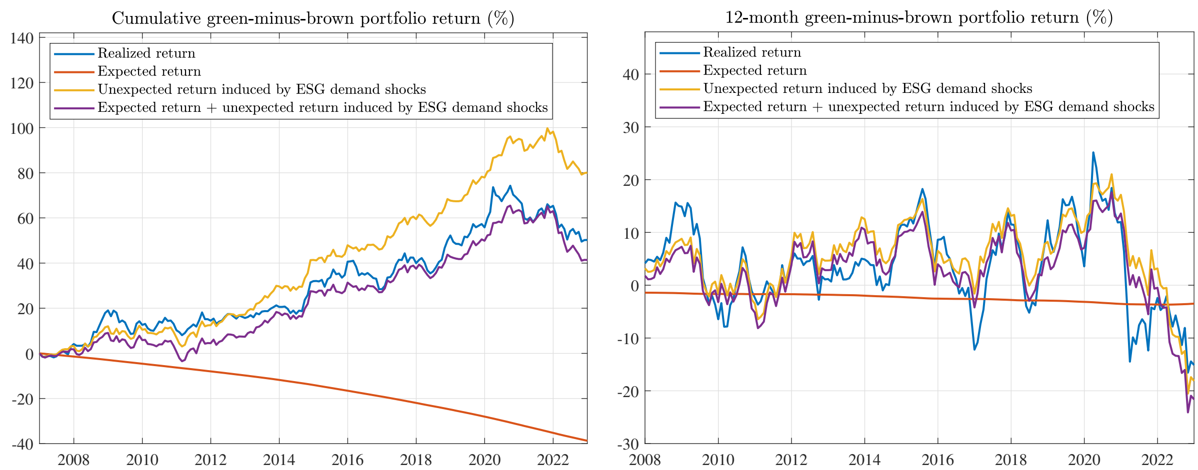

Figure A.7: Impact of cashflows' correlation with ESG demand.

The graphs show responses to a one-standard deviation positive annual shock applied to δ_t. Solid lines correspond to zero correlations, $\mathrm{Corr}_t\left[\Delta d_{gr,t+1}, \delta_{t+1}\right]$ and $\mathrm{Corr}_t\left[\Delta d_{br,t+1}, \delta_{t+1}\right]$, between portfolio dividend growth and δ_t. Dashed lines correspond to a negative (positive) correlation for the green (brown) asset. Dotted lines correspond to a positive (negative) correlation for the green (brown) asset. The expected and realized excess returns of the brown and green portfolios, the cumulative return of the green-minus-brown portfolio, and the price-to-annual dividend ratios of the brown and green portfolios are shown. The state variables are initially set at their average values and the shocks are equally distributed throughout 12 consecutive months. Online Appendix E.1 provides detailed information on the mapping of correlations on the parameter space.

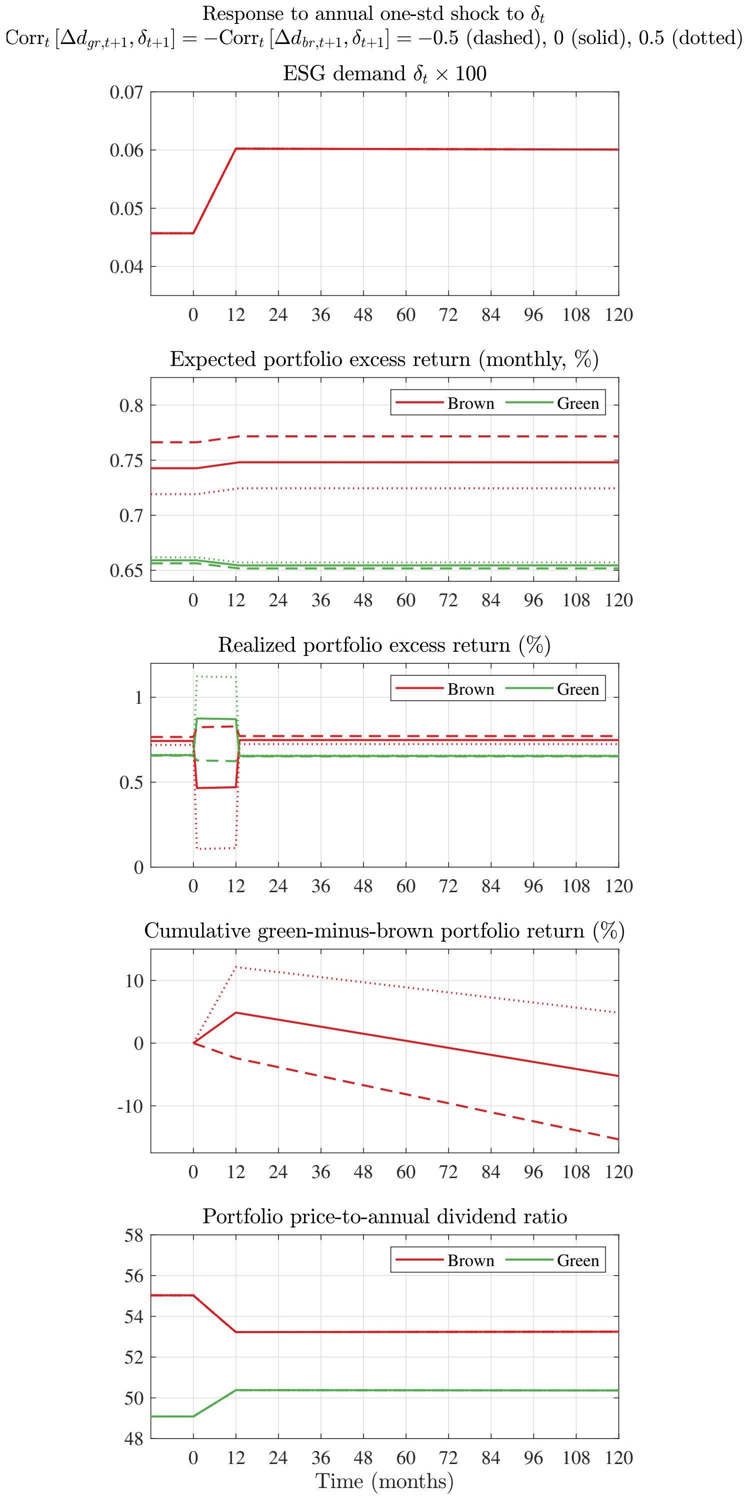

Figure A.8: Impact of cashflows' correlation with ESG score.

The graphs show responses to a +0.1 annual shock to the ESG score of the green portfolio. Solid lines correspond to a zero correlation $\mathrm{Corr}_t\left[\Delta d_{gr,t+1}, G_{gr,t+1}\right]$, dashed (dotted) lines to a negative (positive) correlation. The expected and realized excess returns of the brown and green portfolios, the cumulative return of the green-minus-brown portfolio, and the price-to-annual dividend ratios of the brown and green portfolios are shown. The state variables are initially set at their average values and the shocks are equally distributed throughout 12 consecutive months. Online Appendix E.1 provides detailed information on the mapping of correlations on the parameter space.

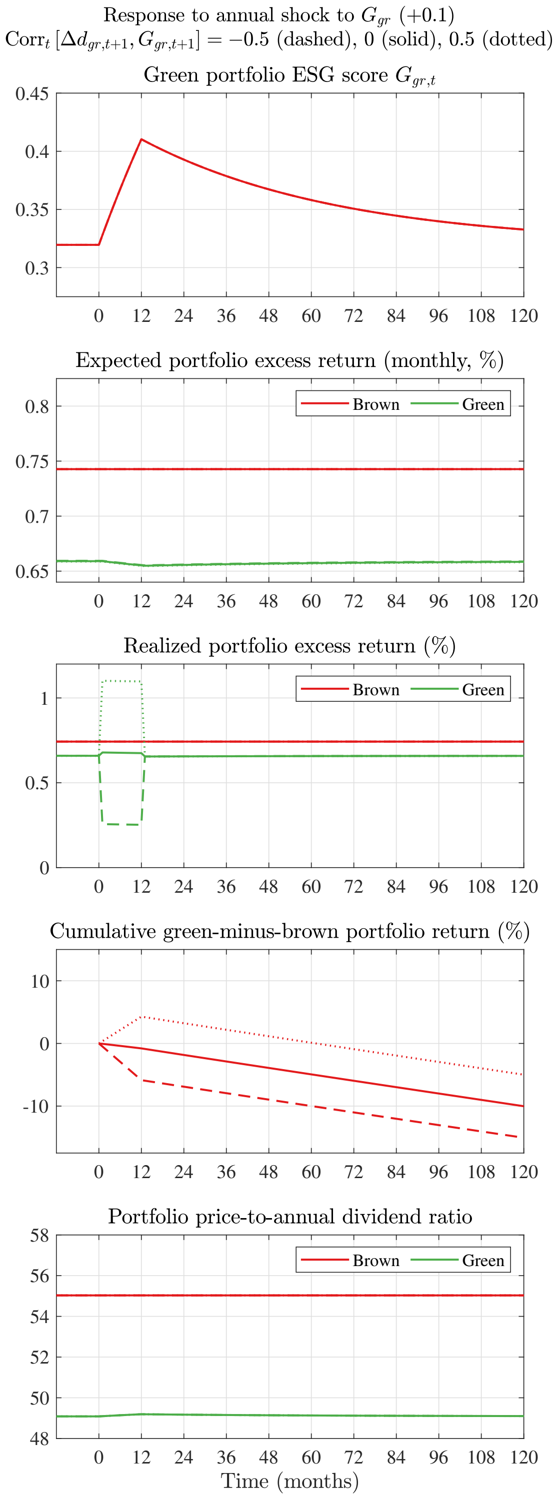

Figure A.9: Impact of dependence of ESG scores over ESG demand.

The graphs show responses to a one-standard deviation positive annual shock applied to δ_t. Solid lines correspond to the baseline specification, where the dynamics of ESG scores in Equations (A.34) and (A.64) is independent of ESG demand ($\rho_{G,\delta} = \rho_{Gn,\delta} = 0$). Dashed and dotted lines correspond to a positive dependence ($\rho_{G,\delta} = \rho_{Gn,\delta} = 5$ and $\rho_{G,\delta} = \rho_{Gn,\delta} = 10$, respectively). The expected and realized excess returns of the brown and green portfolios, the cumulative return of the green-minus-brown portfolio, and the price-to-annual dividend ratios of the brown and green portfolios are shown. The state variables are initially set at their average values and the shocks are equally distributed throughout 12 consecutive months.

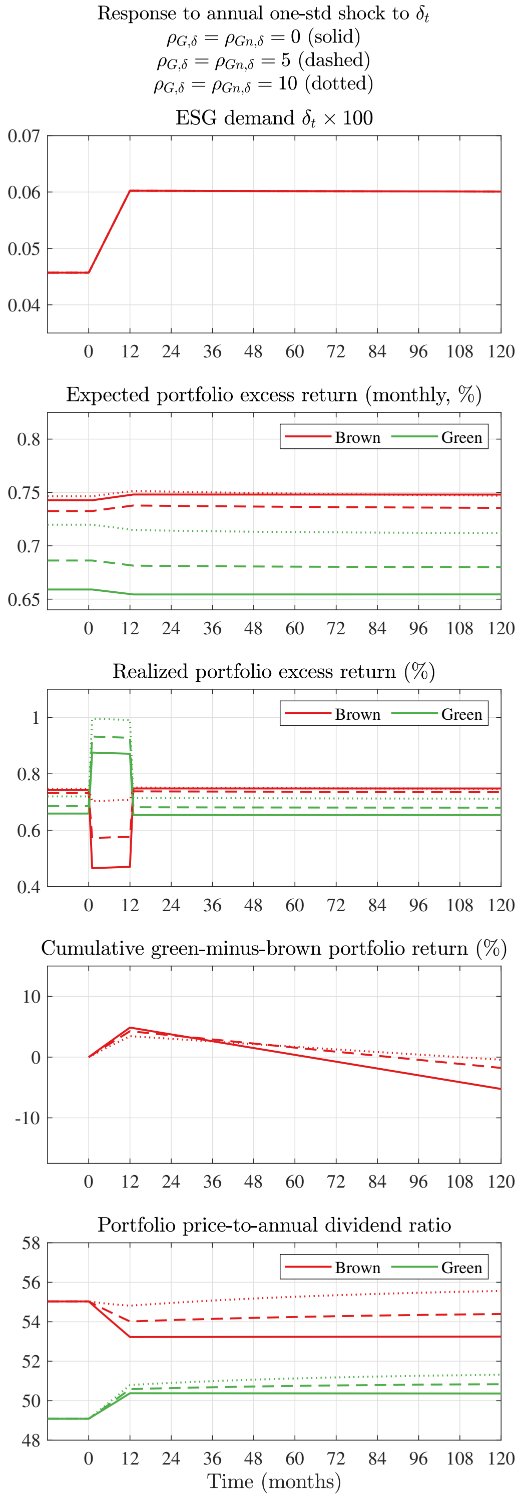

Table A.1: Summary statistics

The table reports the summary statistics of the value-weighted portfolios based on prior ESG and environmental scores. Portfolios in Panel (a) are constructed considering the entire universe of stocks, portfolios in Panel (b) are constructed excluding stocks in the technology sector. The portfolio construction methodology is described in Section 3.

(a) All stocks

	ESG-score portfolios				Environmental-score portfolios			
	Market	Brown	Neutral	Green	Market	Brown	Neutral	Green
Average monthly return (%)	0.84	0.71	0.82	0.88	0.84	0.77	0.85	0.87
Monthly return standard deviation (%)	4.57	5.13	4.69	4.47	4.57	5.13	4.86	4.34
Average score	0.05	-0.37	-0.07	0.32	0.09	-0.37	-0.06	0.35
Score standard deviation	0.04	0.03	0.03	0.03	0.03	0.02	0.02	0.04
Min score	-0.03	-0.41	-0.13	0.25	0.03	-0.40	-0.10	0.28
Max score	0.14	-0.30	0.00	0.37	0.15	-0.33	-0.01	0.41
Average market capitalization (US$ trillion)	20.63	3.99	7.39	9.25	20.63	2.87	7.61	10.15
Average number of stocks	1491	448	596	447	1491	448	596	447

(b) All stocks excluding technology sector

	ESG-score portfolios				Environmental-score portfolios			
	Market	Brown	Neutral	Green	Market	Brown	Neutral	Green
Average monthly return (%)	0.75	0.70	0.76	0.77	0.75	0.62	0.73	0.83
Monthly return standard deviation (%)	4.52	5.19	4.78	4.26	4.52	5.30	4.87	4.24
Average score	0.02	-0.38	-0.08	0.31	0.07	-0.38	-0.08	0.33
Score standard deviation	0.04	0.03	0.03	0.03	0.04	0.02	0.03	0.05
Min score	-0.07	-0.42	-0.14	0.25	-0.02	-0.41	-0.13	0.24
Max score	0.10	-0.31	-0.01	0.38	0.15	-0.34	-0.02	0.40
Average market capitalization (US$ trillion)	14.80	3.11	5.34	6.35	14.80	2.22	5.38	7.20
Average number of stocks	1270	381	508	381	1270	381	508	380

Table A.2: Parameter estimates excluding stocks in the technology sector.

The table reports the estimated parameters for the baseline model specification. The subjective discount rate β is set at 0.998, the intertemporal elasticity of substitution ψ at 1.5, the long-run risk persistence ρ_x at 0.979, its volatility σ_x at 0.00034, and the persistence of ESG demand ρ_δ at 0.9999. The brown, neutral, and green portfolios are obtained by value-weighting stocks sorted by their ESG scores in Panel (a) and environmental scores in Panel (b). The estimation procedure is described in Section 4.1. The sample runs from January 2007 to December 2022.

(a) Estimation based on ESG scores

Economy-wide parameters (Θ_E) and market prices of risk

γ	μ_c	σ_c	x_0	μ_G	ρ_G	σ_G	δ_0	$\bar{\delta}$	σ_δ
10.27107	0.00113	0.01212	0.00031	0.00032	0.98600	0.00942	0.00024	0.00045	0.00004
(2.53918)	(0.00131)	(0.00061)	(0.00365)	(0.00020)	(0.00901)	(0.00047)	(0.00012)	(0.00014)	(0.00000)
λ_c	λ_G	λ_δ	λ_x						
0.12446	0.00384	0.00415	0.14215						
(0.03127)	(0.00126)	(0.00119)	(0.03673)						

Market portfolio parameters (Θ_M)

μ_{dM}	$\rho_{dM,x}$	$\sigma_{dM,c}$	σ_{dM}
0.00498	3.69382	0.00125	0.00291
(0.00130)	(0.69363)	(0.00348)	(0.01047)

Brown portfolio parameters (Θ_{br})

μ_{dbr}	$\rho_{dbr,x}$	$\sigma_{dbr,c}$	$\sigma_{dbr,dM}$	σ_{dbr}	μ_{Gbr}	ρ_{Gbr}	σ_{GbrG}	σ_{Gbr}
0.00574	3.97858	0.00259	0.01145	0.00466	-0.00351	0.99066	-0.01501	0.01701
(0.00156)	(0.79657)	(0.00398)	(0.01456)	(0.00087)	(0.00389)	(0.01035)	(0.00145)	(0.00084)

Neutral portfolio parameters (Θ_{neu})

μ_{dneu}	$\rho_{dneu,x}$	$\sigma_{dneu,c}$	$\sigma_{dneu,dM}$	σ_{dneu}	μ_{Gneu}	ρ_{Gneu}	σ_{GneuG}	σ_{Gneu}
0.00530	3.81903	0.00075	-0.00610	0.00001	-0.00338	0.95578	0.00197	0.00973
(0.00139)	(0.75475)	(0.00368)	(0.01300)	(0.00076)	(0.00184)	(0.02414)	(0.00070)	(0.00049)

Green portfolio parameters (Θ_{gr})

μ_{dgr}	$\rho_{dgr,x}$	$\sigma_{dgr,c}$	$\sigma_{dgr,dM}$	σ_{dgr}	μ_{Ggr}	ρ_{Ggr}	σ_{GgrG}	σ_{Ggr}
0.00439	3.46856	0.00111	0.00653	0.00093	0.00422	0.98635	0.01759	0.01742
(0.00130)	(0.64990)	(0.00327)	(0.01060)	(0.00053)	(0.00278)	(0.00900)	(0.00155)	(0.00084)

(b) Estimation based on environmental scores

Economy-wide parameters (Θ_E) and market prices of risk

γ	μ_c	σ_c	x_0	μ_G	ρ_G	σ_G	δ_0	$\bar{\delta}$	σ_δ
13.23035	0.00224	0.01208	-0.00090	0.00246	0.96554	0.01215	0.00010	0.00114	0.00005
(2.51290)	(0.00136)	(0.00061)	(0.00362)	(0.00078)	(0.01094)	(0.00061)	(0.00013)	(0.00017)	(0.00000)
λ_c	λ_G	λ_δ	λ_x						
0.15978	0.00966	0.02312	0.18772						
(0.03115)	(0.00200)	(0.00661)	(0.03688)						

Market portfolio parameters (Θ_M)

μ_{dM}	$\rho_{dM,x}$	$\sigma_{dM,c}$	σ_{dM}
0.00700	3.58461	0.00114	0.01184
(0.00174)	(0.57199)	(0.00345)	(0.01166)

Brown portfolio parameters (Θ_{br})

μ_{dbr}	$\rho_{dbr,x}$	$\sigma_{dbr,c}$	$\sigma_{dbr,dM}$	σ_{dbr}	μ_{Gbr}	ρ_{Gbr}	σ_{GbrG}	σ_{Gbr}
0.00846	4.08316	0.00138	0.00535	0.00431	-0.05435	0.85650	-0.01971	0.01930
(0.00162)	(0.58987)	(0.00409)	(0.01416)	(0.00168)	(0.01078)	(0.02846)	(0.00173)	(0.00095)

Neutral portfolio parameters (Θ_{neu})

μ_{dneu}	$\rho_{dneu,x}$	$\sigma_{dneu,c}$	$\sigma_{dneu,dM}$	σ_{dneu}	μ_{Gneu}	ρ_{Gneu}	σ_{GneuG}	σ_{Gneu}
0.00731	3.67717	0.00147	0.01888	0.00174	-0.00569	0.92769	0.00136	0.01071
(0.00209)	(0.70049)	(0.00372)	(0.01400)	(0.00098)	(0.00230)	(0.02924)	(0.00077)	(0.00054)

Green portfolio parameters (Θ_{gr})

μ_{dgr}	$\rho_{dgr,x}$	$\sigma_{dgr,c}$	$\sigma_{dgr,dM}$	σ_{dgr}	μ_{Ggr}	ρ_{Ggr}	σ_{GgrG}	σ_{Ggr}
0.00633	3.36876	0.00079	0.00929	0.00006	0.01492	0.95491	0.02564	0.01579
(0.00164)	(0.50490)	(0.00321)	(0.01056)	(0.00046)	(0.00451)	(0.01364)	(0.00174)	(0.00076)

Table A.3: Decomposition of model-implied excess returns and average observed excess returns excluding stocks in the technology sector.

The table reports the observed and model-implied annualized excess returns, as well as the decomposition of model-implied excess returns. The brown, neutral, and green portfolios are obtained by value-weighting stocks sorted by their ESG scores in Panel (a) and environmental scores in Panel (b). The estimation procedure is described in Section 4.1. The sample runs from January 2007 to December 2022.

(a) Estimation based on ESG scores

Portfolio	Market	Brown	Neutral	Green	Green-brown
Model-implied short-run consumption risk premium	0.19%	0.39%	0.11%	0.17%	-0.22%
	(0.55%)	(0.62%)	(0.59%)	(0.51%)	(0.21%)
Model-implied long-run consumption risk premium	7.78%	8.56%	8.15%	7.17%	-1.39%
	(1.66%)	(1.98%)	(1.84%)	(1.58%)	(0.49%)
Model-implied ESG supply risk premium	0.01%	0.00%	0.01%	0.01%	0.01%
	(0.01%)	(0.01%)	(0.01%)	(0.01%)	(0.00%)
Model-implied ESG demand risk premium	0.00%	-0.04%	-0.01%	0.03%	0.08%
	(0.00%)	(0.01%)	(0.00%)	(0.01%)	(0.02%)
Average model-implied convenience yield premium	-0.03%	0.19%	0.03%	-0.17%	-0.36%
	(0.00%)	(0.06%)	(0.01%)	(0.05%)	(0.11%)
Average model-implied expected excess return	6.69%	7.44%	6.90%	6.09%	-1.35%
	(1.64%)	(1.96%)	(1.81%)	(1.60%)	(0.50%)
Average ESG demand shock-induced return (δ-induced return)	0.07%	-1.54%	-0.34%	1.09%	2.63%
	(0.03%)	(0.20%)	(0.04%)	(0.16%)	(0.36%)
Average model-implied expected excess return + δ-induced return	6.76%	5.90%	6.56%	7.18%	1.28%
	(1.63%)	(1.98%)	(1.80%)	(1.57%)	(0.57%)
Average observed excess return	6.97%	5.91%	6.85%	7.33%	1.41%

(b) Estimation based on environmental scores

Portfolio	Market	Brown	Neutral	Green	Green-brown
Model-implied short-run consumption risk premium	0.22%	0.27%	0.28%	0.15%	-0.11%
	(0.64%)	(0.76%)	(0.69%)	(0.60%)	(0.34%)
Model-implied long-run consumption risk premium	9.93%	11.68%	10.27%	9.20%	-2.48%
	(1.90%)	(1.95%)	(2.37%)	(1.68%)	(0.62%)
Model-implied ESG supply risk premium	0.06%	0.05%	0.05%	0.06%	0.01%
	(0.03%)	(0.03%)	(0.03%)	(0.03%)	(0.00%)
Model-implied ESG demand risk premium	0.05%	-0.29%	-0.06%	0.24%	0.54%
	(0.02%)	(0.08%)	(0.02%)	(0.07%)	(0.15%)
Average model-implied convenience yield premium	-0.14%	0.53%	0.08%	-0.49%	-1.02%
	(0.02%)	(0.08%)	(0.02%)	(0.07%)	(0.15%)
Average model-implied expected excess return	8.85%	10.51%	9.15%	8.04%	-2.46%
	(1.84%)	(1.74%)	(2.28%)	(1.69%)	(0.59%)
Average ESG demand shock-induced return (δ-induced return)	0.49%	-2.77%	-0.56%	2.26%	5.04%
	(0.06%)	(0.23%)	(0.05%)	(0.21%)	(0.44%)
Average model-implied expected excess return + δ-induced return	9.34%	7.73%	8.60%	10.31%	2.57%
	(1.81%)	(1.82%)	(2.28%)	(1.60%)	(0.61%)
Average observed excess return	6.97%	4.89%	6.46%	8.03%	3.14%